FUEL FILM DIAGNOSTIC DEVELOPMENT OF A SPARK IGNITED, HOMOGENEOUS CHARGED, FOUR STROKE, AIR-COOLED ENGINE

by

forrest auchmuty jehlik

A thesis submitted in partial fulfillment of the
requirements for the degree of

Master of Science
(Mechanical Engineering)

at the

UNIVERSITY OF WISCONSIN-MADISON

2000

1

INTRODUCTION

1.1 Motivation For Transient Fueling Research

Fuel mixture preparation is essential to the operation and reliability of an engine. Prior to stringent emission legislation in the early 1970's, it was well known that air fuel mixtures rich in fuel produced more power while significantly reducing misfires in engines. This was not only favorable to the buying consumer, but easy to produce for manufacturers as well. Although lean fuel mixtures increased fuel economy, rough engine operation and cheap fuel costs did not dictate advancement in fuel mixture preparation technology.

With the overall growing concern of the adverse effect internal combustion engine emissions have on human health and the environment, the small engine manufacturers find themselves much in the same position as the automotive industry in the 1970's. This position requires vast reductions in engine emissions. This trend is clearly visible in legislation being proposed to regulate small engines. Current and proposed EPA emissions regulations for both NO_x + HC and CO may be seen in Tables 1.1 and 1.2. CARB's proposed emission regulations may be seen in Table 1.3.

	Model year	Model year	Model year	Model year	Model year
Engine class	2001	2002	2003	2004	2005
Class I	25	25	25	25	25
Class II	18	16.6	15	13.6	12.1[2]

Class I	non-hand held, less than 225cc displacement
Class II	non-hand held, greater or equal to 225cc displacement
Class III	hand held, less than 20cc displacement
Class IV	hand held, 20cc to less than 50cc
Class V	hand held, greater or equal to 50cc

Table 1.1 Proposed EPA HC+NOx ULGE emission regulations in g/kW-hr. Adapted from [30]. The 12.1 g/kW-hr Class II standard assumes a phase-in from 50 percent in model year 2001 to 100 percent in model year 2005 of OHV or comparably clean and durable technology.

Engine Class	I	II	III	IV	V
CO Standard (g/kW-hr)	610	610	805	805	603

Table 1.2 Proposed EPA CO ULGE emission regulations in g/kW-hr. Adapted from [30].

Year	Engine class	HC+NOx (g/kW-hr)	HC (g/kW-hr)	NOx (g/kW-hr)	CO (g/kW-hr)
1995	Class I	16.1	-	-	402.3
	Class II	13.4	-	-	402.3
1999	Class I	4.3	-	-	134.1
	Class II	4.3	-	-	134.1

Table 1.3 Proposed CARB HC+NO_x/CO emission regulations in g/kW-hr. Adapted from [18].

The emission reduction trends displayed in Tables 1.1-1.3 indicate the regulated emission reductions that will take place both on the Federal (EPA) and State (CARB) level. California has for a number of years lead the country in aggressive air pollution reduction legislation. This trend continues with small utility engines, and is important to the small engine manufacturer since the state of California currently has the world's 7th largest economy. Since the small engine manufacturers are interested in producing economical engines, the addition of pollution control devices (i.e. fuel injection systems,

computer controlled management, catalytic converters) are not necessarily viable. The added cost of such systems could potentially price such producers out of market.

It has been found that transient operation of engines leads to air fuel (A/F) ratio excursions, which can increase engine emissions. These excursions have been attributed to the formation of fuel films in the intake port, which are caused by a portion of the intake fuel impinging and adhering on the relatively cool port surface. These films act as a source or sink which cause the AF variations depending upon the transient condition. Gaining a fundamental understanding of the nature and quantity of such films may assist in future fuel mixture preparation designs that could aid in emission reductions, yet would not require overly expensive nor complicated systems. Currently, the most commonly used fuel delivery device for small engines is the carburetor for numerous reasons: they are inexpensive to manufacture, relatively simple in design, and highly reliable. A fundamental understanding of fuel film behavior may allow manufacturers to continue to use the carburetor.

1.2 Research Objectives

The main objective of this research has been to develop techniques for qualifying and quantifying fuel film development in the intake port of a small air-cooled four-stroke utility engine. These techniques should be able to quantify the total mass of fuel film in the intake port under various operating conditions. Such techniques would determine operating conditions that lead to the formation of fuel films, yielding information into fuel film behavior and possible means of reducing such effects.

To achieve the above-mentioned objectives, five methods were used to assess fuel films under various operating conditions. The five methods used to assess fuel films were

1. Indolene- and propane-fueled impulsive fueling transients using a heated universal exhaust gas oxygen (UEGO) sensor as a diagnostic.
2. Indolene- and propane-fueled impulsive throttle transients using a UEGO sensor as a diagnostic.
3. Capacitance fuel film measurements.
4. Skip-injection with fast flame ionization detector (FFID) exhaust hydrocarbon sampling.
5. Stop-injection with FFID exhaust hydrocarbon sampling.

The thesis is presented as follows. Chapter 2 consists of a literature review of various other research work conducted on fuel film behavior. In Chapter 3, the laboratory setup and equipment used for this experiment is presented such that the experiment could be independently repeated. Chapter 4 consists of characterizing the response time of the UEGO sensor that is used for both the impulsive fuel and impulsive throttle transient tests listed as 1 and 2 above. Statistical tests are also presented that verify the validity of the tests. In Chapter 5, the techniques and results of the indolene-fueled impulsive transients are presented. In Chapter 6, the techniques and results to indolene and propane impulsive throttle transients are presented. In Chapter 7, a localized capacitance technique of measuring film thickness is presented. Two methods of calibrating the sensors are presented, as well as the results of using such gages on a

motored engine. In Chapter 8, results of skip-injection and stop-injection tests with FFID exhaust sampling techniques and are presented. The thesis concludes with Chapter 9, which summarizes the work and recommendations for future research on fuel film behavior involving small air-cooled utility engines.

2

2 BACKGROUND AND LITERATURE REVIEW

2.1 Fuel Mixture Preparation: An Introduction

A fundamental requirement for smooth and reliable engine operation is fuel mixture preparation. The main function of an engine induction system is to mix and deliver fuel with air in an appropriate ratio over an engine's entire operating range. Ideal fuel mixture preparation minimizes fuel consumption and misfires while maintaining thermal durability. This applies not only to small Utility and Lawn and Garden Equipment (ULGE) engines, but larger engines as well. Although minimizing fuel consumption by running the engine in leaner air-fuel (A/F) regimes is possible, both lean misfire limits and regulated NO_x emission constraints greatly complicate the matter. Also, engine durability issues arise for certain A/F regimes.

2.1.1 Fuel Mixture Preparation And Emissions

The relationship between the three federal regulated emissions (HC, CO, NO_x) and A/F ratio is well documented. As an engine operates slightly lean of stoichiometric, NO_x emissions reach a maximum while HC and CO emissions decrease. Conversely, as the engine operates in a rich A/F regime, NO_x emissions are reduced while HC and CO emissions increase. This relationship may be seen in Figure 2.1.

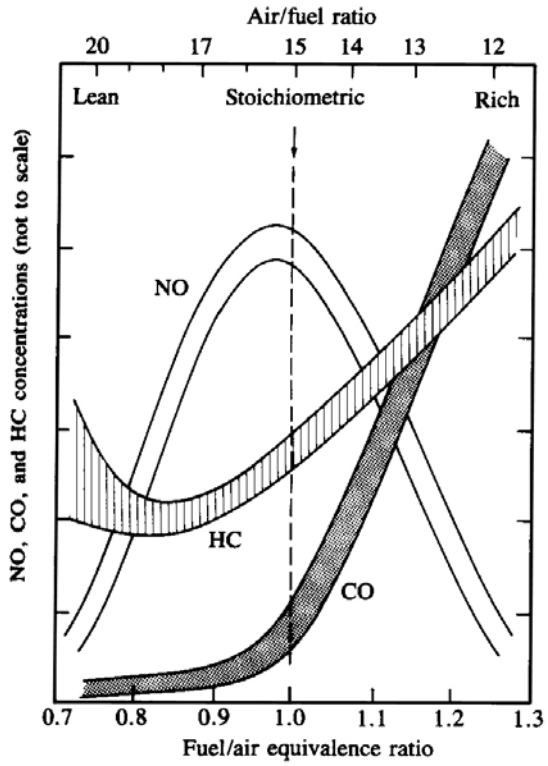

Figure 2.1 Typical variation of regulated emissions as a function of air fuel ratio, taken from [1].

Since peak power is found at an equivalence ratio slightly rich of stoichiometric, small engine manufacturers often supply the A/F mixture in this regime thereby maximizing power density. This reduces NO_x emissions at the cost of an increase in both HC and CO emissions, as well as a decrease in fuel economy. Running in this regime also has the advantage of reducing thermal fatigue. However, with the implementation of small engine emission regulations that require reductions in CO and HC, using lean fueling strategies becomes complicated due to an increase in NO_x emissions. Although an engine can be run lean enough as to abate this increase in NO_x emissions in the lean region, misfires and flammability limits of the fuel become increasingly complicated engineering issues to address.

2.1.2 Fuel Mixture Preparation And Thermal Issues

It has been found that peak heat fluxes in the combustion chamber walls can reach as high as 10MW/m^2 [1]. High heat fluxes can lead to thermal stresses which need to be minimized to avoid thermal fatigue. Work conducted by both Boyce [6] and Strucel [8] on a small four-stroke air-cooled utility engine determined the functional relationship between air fuel ratio and in-cylinder heat flux. In these studies, an array of heat flux sensors were located in the cylinder head [6] and in the cylinder liner [8] to determine the spatial distribution of the steady state engine heat flux. By locating a series of thermocouples in a pre-determined 3-dimensional array, instantaneous 3-dimensional heat flux vectors were obtained. An example of the average peak heat flux obtained by Boyce may be seen in Figure 2.2.

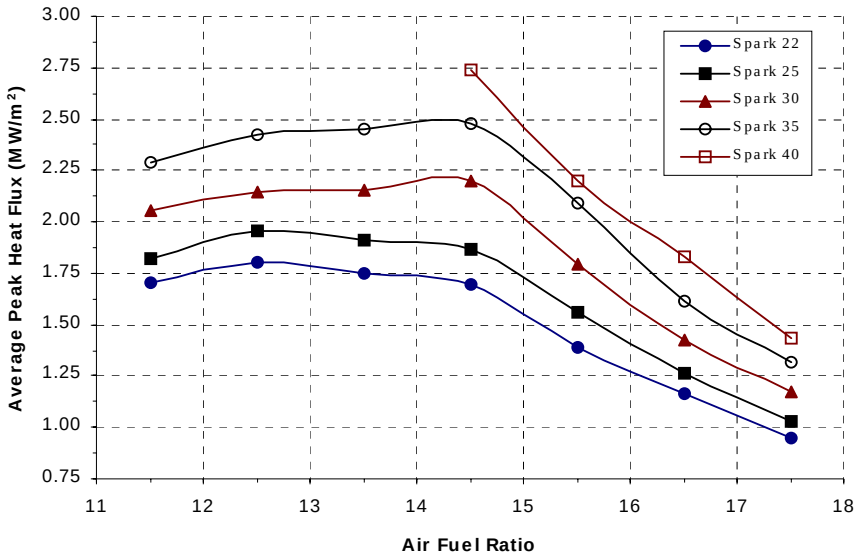

Figure 2.2 Average peak heat flux per cycle for various air fuel ratio and ignition timing advance.
Used with permission, taken from Boyce, B.P. [6]

In both studies, a maximum in-cylinder heat flux was found to occur slightly rich of the stoichiometric equivalence ratio over a wide range of spark timings, with this value

diminishing rapidly for increasing A/F ratios past the maximum flux. Heat flux was also found to reduce for decreasing A/F ratios from the maximum flux point. From this it was determined that various AF ratios could be used to minimize the peak thermal stresses.

2.2 Fuel Mixture Preparation And Combustion Quality

Although both heat flux and regulated CO/HC emissions are reduced by running in lean A/F regimes, misfires become a significant issue. The three contributing factors for misfires are [1]:

1. Variation of in-cylinder gas motion due cycle-by-cycle flow dynamics
2. Variation in intake mixture of fuel, air, recycled exhaust gas supplied to the combustion chamber on a cycle-by-cycle basis
3. Variation of in-cylinder composition caused by variations in air-fuel mixing, recycled exhaust gas, and residual combustion gases

Work conducted by Itano *et al*. [5] qualitatively showed the effect of three carburetor designs on fuel mixture preparation for a small air-cooled four-stroke utility engine. This research addressed the variations in A/F mixing using three carburetor designs by visualizing the formation of intake port fuel films. The three carburetors, one with a fixed venturi and fixed-jet butterfly, the second with a slide valve, and the third a constant velocity carburetor, were mounted to an optically accessible extended port. High-speed movie images were then taken as the engine was motored. It was found that the stock carburetor exhibited substantially more wall fuel film compared to the other carburetor designs. This was partially attributed to the throttle plate directing the fuel mixture into the wall. This work suggested a variation found in the quality of mixture

preparation using different carburetor designs, and the effect that the throttle plate has on fuel film formation.

In a set of companion studies, Bonneau [2] and Cunningham [4] directly demonstrated the effect that fuel mixture preparation has on combustion performance. These studies were conducted using the same small utility engine as was used in Itano's work. A homogeneous mixture system was developed that pre-conditioned the A/F intake charge. This was accomplished by injecting the fuel far upstream of the intake port into a heated and conditioned air stream. The mixture then passed into a surge tank prior to entering the intake manifold. By ensuring that the fuel was homogeneously mixed and pre-heated prior to entering the combustion chamber, fuel film and non-homogeneity effects were eliminated. Results showed that the lean burn limit was extended, and that both HC and CO emissions were reduced. Maximum power output increased 0.2 BHP over the stock carbureted engine. NO_x emissions increased during various load cases as well due to increased peak combustion temperatures as a result of more complete combustion.

2.3 Carburetors

Carburetors are the most widely utilized method of preparing and delivering A/F mixtures to an engine [1]. Their simplicity of design and ease of manufacturing make them attractive to manufacturers. Although not used in the modern automobile, carburetors are still extensively used in lawn and garden equipment, power generators, recreational vehicles, and numerous other small engine applications.

2.3.1 Carburetor Fundamentals

A carburetor meters an appropriate amount of fuel and air by utilizing a converging-diverging nozzle known as a venturi. Air is drawn through the converging-diverging nozzle by the downward motion of the piston(s). As the air is drawn through the converging portion of the nozzle, the increased air velocity creates a pressure drop which is a maximum at the venturi throat. Fuel stored at atmospheric pressure is drawn through the venturi nozzle due to this pressure drop, and is entrained into the air stream. Fuel metering is kept proportional to the mass air flow by metering the air mass flow with a throttle plate. This enables the carburetor to meter an proportionate amount of fuel over an engine's full load range.

2.3.2 Carburetor Components

In Figure 2.3, a basic schematic of the essential components of a carburetor may be seen.

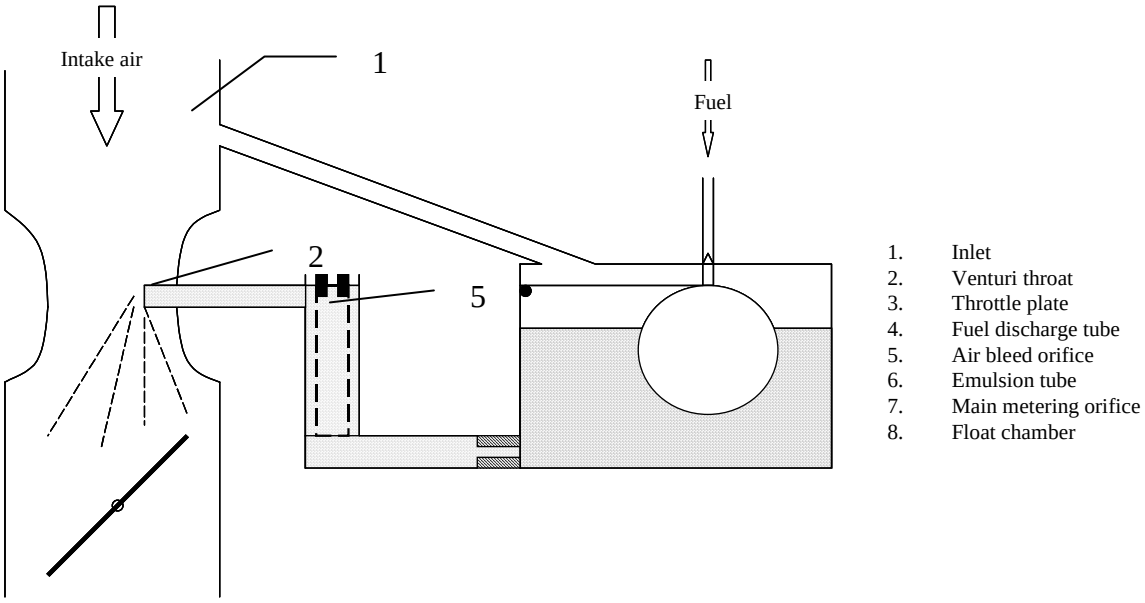

Figure 2.3 Elementary carburetor schematic.

Air at atmospheric pressure enters the intake portion of the carburetor (1) where its velocity increases in the venturi (2). Due to this increase in velocity of the airflow, a reduction in pressure of the incoming airflow occurs. The mass flow of air through the carburetor venturi is given by Equation 2.1

$$\dot{m}_a = \frac{C_{D_T} A_T P_0}{\sqrt{RT_0}} \left(\frac{P_T}{P_0}\right)^{1/\gamma} \left\{ \frac{2\gamma}{\gamma - 1} \left[1 - \left(\frac{P_T}{P_0}\right)^{(\gamma-1)/\gamma} \right] \right\}^{1/2} \tag{2.1}$$

where C_{DT} is the venturi orifice discharge coefficient, A_T is the throats cross sectional area, R is the universal gas constant, γ is the ratio of specific heats, P is pressure and T is temperature, where the subscripts *0* refers to inlet conditions and T corresponds to throat conditions. Due to the decreased pressure at the venturi throat, fuel stored at atmospheric pressure in the carburetor float chamber (8) flows through the main metered orifice known as a jet (7) into the venturi fuel discharge tube, (4). Since fuel can be considered incompressible, the fuel mass flow rate is given by Equation 2.2

$$\dot{m}_f = C_{D_0} A_0 \left(2\rho_f \Delta P_f\right)^{1/2} \tag{2.2}$$

where C_{D0} is the jet orifice discharge coefficient, A_0 is the orifice cross sectional area, ρ_f is the fuel density, ΔP_f pressure drop across the orifice. The fuel then mixes with the low-pressure airflow assisting in atomizing the fuel and passes the throttle (3) where a portion of the pressure drop is recovered.

2.3.3 Carburetor Compensation Systems

Although simple in principle, modern carburetors contain fairly complex compensation systems to overcome inherent shortcomings. Due to variations in C_{D_T}, C_{D_0}, $\dot{m}_f$, and $\dot{m}_a$ as a function of pressure drop in the venturi, the delivered equivalance ratio does not remain constant over an engines entire operating range. The variations in carburetion over a dynamic operating regime may be summarized by the following [1]:

1. Leaner mixtures occur at low loads
2. Near stoichiometric equivalence ratios occur at intermediate loads
3. Near stoichiometric equivalence ratios occur at WOT, however enrichment is required for maximum power
4. Intake manifold transient gas dynamics require carburetion compensation: fuel flow rate increases more rapidly to pressure drops resulting in rich mixtures
5. Altitude effects on intake air density need to be accounted for

In order to deal with these shortcomings, compensation systems have been implemented. The following systems are used to compensate carburetors for inherent deficiencies that may have an effect on intake port fuel film dynamics. Other compensation systems exist that do not directly involve intake port fuel films. They are omitted for sake of this study.

Main Metering Compensation System

This system increases the effective vacuum pressure applied to the fuel from the venturi fuel discharge nozzle by introducing extraneous air into the fuel stream prior to the venturi nozzle through an emulsion tube (6) (see Figure 2.3). As the vacuum increases in the venturi throat, excess air is bled into the tube. The addition of air into the tube alters

the density of the fuel and air mixture. As a result the velocity of the mixture to the nozzle orifice increases. This assists in breaking up and vaporizing the fuel droplets by introducing high velocity air with the fuel stream. Also, the increased velocity assists in a greater pressure drop across the main orifice assisting in partial load enrichment.

Enrichment System

When the throttle of a carburetor opens rapidly, the AF mixture leans out temporarily due to a portion of the fuel impacting the intake manifold wall and forming a fuel film [10]. This fuel film is responsible for a time delay in fuel transport. The most common means of load enrichment during these lean excursions is an accelerator pump. A separate reservoir connected to the main fuel bowl via a check valve and a small orifice stores a small amount of additional fuel. The pressure in this separate reservoir is controlled via a diaphragm connected to the throttle plate through a linkage. As the throttle tips suddenly, the diaphragm increases the pressure on the fuel in the reservoir. This relatively high-pressure fuel is then introduced through the accelerator pump discharge nozzle(s) into the air stream.

2.4 Fuel Injection

With the advent of stricter emission and fuel economy regulations, the need for precision fuel metering became apparent. The advent of fuel injectors offered such precision fuel metering. The advantages of fuel injection over carburetion are numerous: increased power, more uniform cylinder-to-cylinder fuel distribution, increased vaporization of fuel, individual cylinder and cycle-to-cycle fuel metering, and rapid engine response to

throttle changes [1]. However, fuel injection systems are inherently more costly to manufacture and not practical for all applications.

2.4.1 Fuel Injection Fundamentals

Fuel injectors are electromagnetically (solenoid) actuated valves. A cross section of a typical fuel injector may be seen in Figure 2.4.

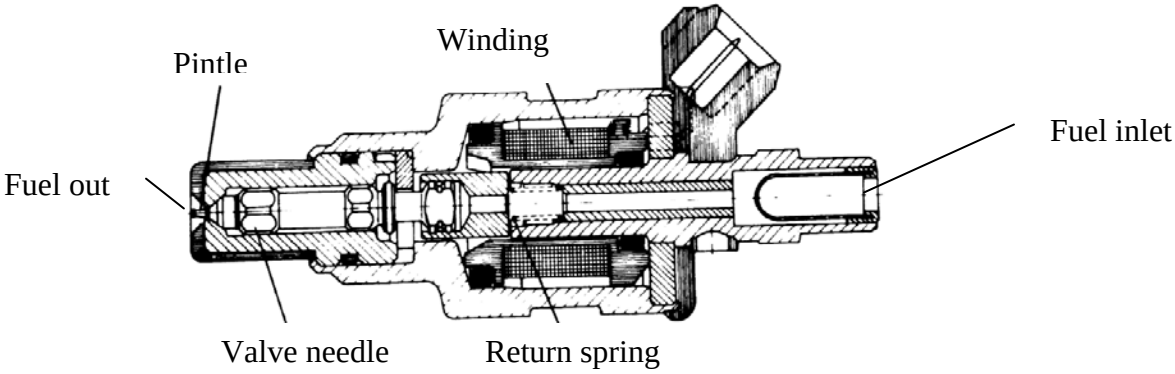

Figure 2.4 Cross section of a typical fuel injector

When the solenoid is not actuated, the pintle is forced against its seat by the return spring. When current from the fuel injector driver actuates the solenoid, the induced magnetic field pulls the pintle off the seat against the pressure of the return spring. Typical pintle lifting distances are on the order of 0.15 mm. The mass of fuel introduced per injection is controlled by the duration the coil is excited. Typical injection durations are between 1.5-10ms [1].

Fuel injection systems commonly operate at a fuel injection pressure between 205-240 kPa. A specially designed atomizing pintle with a ground tip assists in

atomizing the fuel, and fuel injector spray patterns are often designed to produce a narrow spray cone. This assists in reducing the amount wall films that adversely effect combustion for both steady and transient engine operation [1, 10, 12].

2.4.2 Fuel Injection Control Strategy

The most commonly used fuel injection control strategy is referred to as a speed-density system. The mass of fuel injected in a speed-density system is determined by the engine speed, manifold pressure or a direct air-stream mass flow measurement, and intake manifold temperature. The mass of fuel injected can be correlated to the mass of intake airflow with the desired operating AF ratio. When using manifold absolute pressure (MAP) measurements over direct mass airflow measurements, a predetermined map of pressure versus airflow is stored in the ECU. The temperature measurement is then used as a density correction. The mass of air introduced to the engine is given by

$$m_a = \frac{\eta_\upsilon V_d \, p_i}{R_a T_i} \tag{2.3}$$

where η_υ is the volumetric efficiency, V_d is the cylinder displaced volume, p_i is the intake charge pressure, T_i is the intake charge temperature, and R_a is the universal gas constant. The volumetric efficiency of an engine is not constant for any specific engine design or speed, however experimental data may be fit and the value determined with the following correlation [10]

$$\eta_v = E\frac{\gamma - 1}{\gamma} + \frac{r_c - \left(P_{exh}/P\right)}{\gamma\left(r_c - 1\right)} \tag{2.4}$$

where E is a constant chosen to fit data, γ is the ratio of specific heats, r_c is the engine compression ratio, P_{exh} is the exhaust gas pressure, and P is the absolute manifold pressure. The mass of fuel injected is then proportional to the mass of air introduced and is prescribed by

$$m_{f,injected} = m_{air,induced}\left(\frac{1}{A/F}\right) \qquad (2.5)$$

where $m_{air,induced}$ is the mass of intake charge induced per cycle, and A/F is the desired A/F ratio. Advantages of using direct airflow measurements over MAP sensors are: (1) compensation for changes in mass airflow due to combustion chamber deposits, valve wear, and valve adjustments, (2) compensation for exhaust gas pressure on volumetric efficiency, (3) reduced acceleration fuel enrichment due to mass airflow signal preceding filling of cylinders, (4) improved idle stability, and (5) lack of system sensitivity due to the airflow sensor preceding addition of EGR [1].

2.5 Fuel Film Research

It has long since been understood that the presence of fuel films in the intake manifold and ports of SI engines have an adverse effect on transient operation and emissions [11, 12]. These adverse effects have been investigated and quantified using various diagnostic techniques. The following sections describe prior research work that has been completed on the behavior of fuel films. The majority of diagnostic work, however, has

been conducted using liquid cooled fuel injection engine platforms with the emphasis placed on automotive manufacturers meeting emission criteria.

2.5.1 Early Transient Fuel Film Research

Some of the earliest investigations into fuel film behavior began with qualifying the presence of fuel films in multi-cylinder carbureted SI engines. In 1978, Kay [9] found the presence of substantial fuel films under a variety of operating conditions in a 2.3 liter multi-cylinder engine. Tests were conducted by inserting clear viewing ports within the intake manifold, and the engine was run through a series of speed/load conditions. This allowed for visual qualifications to be made to the extent of fuel film formation under various throttle settings. Also, heaters in the base of the intake manifold were installed to investigate the effect of manifold temperature on fuel vaporization. Results showed that by heating the manifold floor the fuel film could be virtually eliminated. However, by collecting A/F measurements on a cylinder-to-cylinder basis for both the heated and non-heated case, it was found that the A/F distribution was unaffected under steady state conditions regardless of the presence of fuel films. This suggested that the fuel films did not affect steady state fueling control. However, the question of transient effects had not been addressed

In 1981 Aquino [10] *et al*. investigated the transient operation of a five-liter central injection throttle body engine. A series of fixed engine speed, varied intake manifold temperature, one second step throttle transient tests were conducted in order to introduce a step transient to the incoming airflow. By accurately measuring fuel metering and the exhaust stream A/F ratio, the magnitude of the excursions was quantified. It was

found that overly rich excursions occurred during throttle closing, and that overly lean excursions occurred during throttle opening. Research also showed that increasing manifold temperature resulted in a reduction of these excursions. These excursions were attributed to the formation of a port wall fuel film that acted as a temporary reservoir to the incoming fuel.

From these results a two parameter phenomenological model was developed to predict the fraction of injected fuel that impacts the manifold wall, and the rate at which this fraction of fuel vaporizes. A diagram of the model may be seen in Figure 2.5.

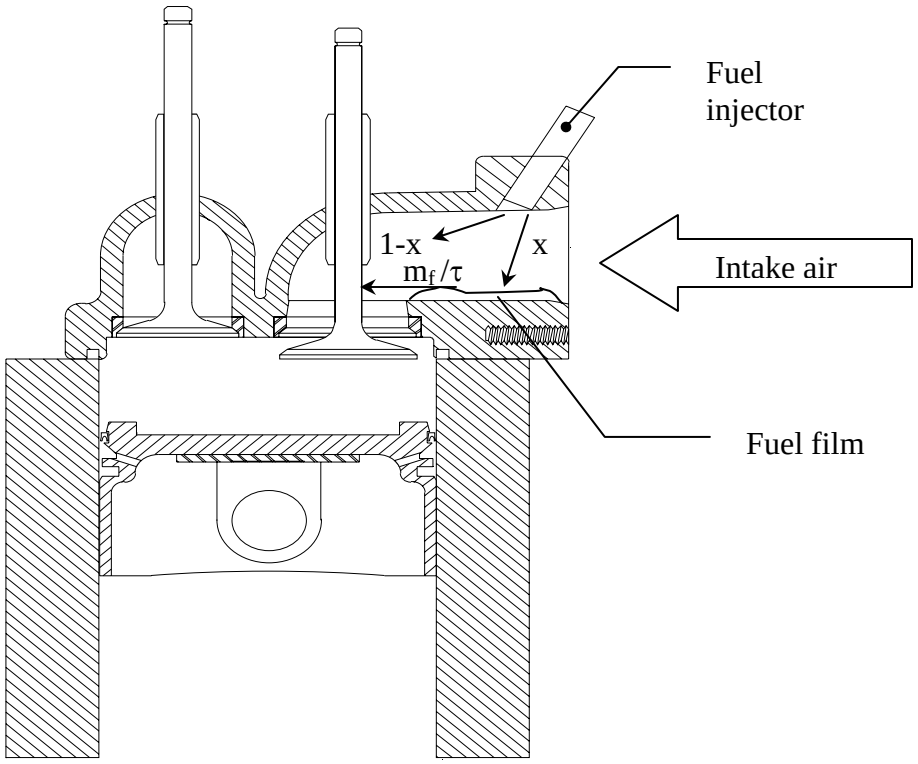

Figure 2.5 Tau-x model representation, adapted from Patrie, used with permission.

From Figure 2.5 it may be seen that a fraction, *x*, of fuel directly impacts the wall. The remaining fraction of fuel (1-*x*) is entrained in the intake stream. The rate of film

depletion is directly dependent upon the film mass, and inversely with a time constant, τ, which is effectively a combined vaporization and mass transfer coefficient that encompasses the physics of fuel film depletion. The total fuel mass entering the combustion chamber is given by the sum of the fuel directly entrained, and the mass evaporated from the fuel film. By applying the conservation of mass to the system in Figure 2.5, the model is prescribed by the following governing equations

$$\dot{m}_{induced} = (1-x)\dot{m}_{inj} + \frac{m_f}{\tau} \tag{2.5}$$

$$\dot{m}_f = x\dot{m}_{inj} - \frac{m_f}{\tau} \tag{2.6}$$

where $\dot{m}_{induced}$ is the total amount of fuel inducted into the cylinder both from the injector and from the evaporating fuel film, $\dot{m}_f$ is the rate of change of the fuel film mass, and m_f is the mass of intake port film. Thus it may be seen from the model that rate of change of the wall fuel film is directly proportional to the fraction, x, of fuel that impacts the port wall, and indirectly proportional to the combined vaporization/mass transfer coefficient, τ. Using this model the authors concluded that manifold wall wetting was the most significant contributor to A/F excursions. Also, wall wetting of the throttle body had a significant effect on A/F excursions, with heating of either the manifold or throttle body reducing these effects.

Further application of the tau-x model led to determining and compensating for fuel transport characteristics of multiport fuel injection spark-ignition engines. Shayler *et al.* [20] investigated both step fueling and step throttle transients of a 5.0 liter port fuel-

injected engine. These transients were conducted over a range of engine temperatures starting at –30^{o}C and lasted until the thermostat opened. Research showed that load effects were insignificant on the formation of fuel films, and engine temperature and speed were found to have greatest effect on fuel film formation. The effects of step throttle transients were shown to have markedly greater excursions than for the step fueling transients, indicating that liquid fuel films respond slower than the gas phase flows.

2.5.2 Spectroscopic And Optical Fuel Film Techniques

Since the early discovery of fuel films and their adverse effects on transient engine operation, numerous techniques have been implemented in quantifying and qualifying their presence. One method has been the use of various spectroscopic and optical techniques.

Work conducted by Bourke and Evers [17 used optical probes to measure relative film thickness. These probes were inserted into the intake port of a production 1.9 liter four cylinder engine. These probes consisted of both receiving and transmitting fiber bundles. The transmitting bundle would direct red-laser light to a clear epoxy reflector at a specific angle. A portion of the light was then refracted through the film, and the amount collected in the receiving bundle would vary due to the index of refraction of the fuel film and its thickness. Results showed that the relative magnitude of the film decreased as coolant temperature increased. Also, it was found that fuel injection patterns produced by various injectors had a significant effect on the amount of fuel film produced.

Similar work conducted by Almkvist [22] *et al*. utilized laser-induced fluorescence within an intake port of a single-cylinder fuel-injected research engine to quantify fuel film thickness. A 487cm^3 single cylinder engine was outfitted such that a beam of a Nd:YAG laser was used to detect the fuel along a line on the wall. The signal was detected with an intensified diode-array camera. Results showed that there was a significant reduction in fuel film during open valve injection. It was speculated that increasing shear stress was the significant factor in this reduction. Closed valve injection resulted in an increase of the fuel film, which suggested that evaporation was not as significant in reducing the film as increased shear stress. Contrary to the work of Shayler, Almkvist showed that the fuel film was dependent upon engine load, with increased load reducing fuel films. Temperature was also shown to have a significant effect with increased temperature resulting in reduced fuel film mass.

Hentschel [29] *et al*. used a spectroscopic technique to determine the fuel film thickness in a 1.05 liter four-cylinder multipoint fuel-injected SI engine. An array of bifurcated fiber optic probes were developed that transmitted Argon laser light at 457.9 nm through a transmitting fiber bundle. The receiving fiber bundle then collected the fluorescent light, the amount depending upon the thickness of the fuel, and was transmitted through a series of signal conditioning stages to produce a voltage output. These probes were located in the intake port opposite the fuel injector and were used to gain temporal resolution of the fuel film during the engine cycle under various load conditions. Research showed that both the engine speed and load drastically influenced the development of the wall film. Increased engine speed was found to decrease the film

thickness. It was speculated that increased shear stress of the air stream reduced the film thickness, whereas increased temperature assisted in fuel vaporization.

2.5.3 Thermal Fuel Film Techniques

Another technique used to investigate intake port fuel film thickness has been to use experimental and analytical thermal techniques. The use of thermal measurements has been conducted since evaporation of the fuel results in lower localized temperatures. Also, modeling analysis of the intake port liquid and gas-phase intake charge has been conducted to better understand the physics of fuel film behavior.

Bauer [31] *et al*. mounted a series of thin film thermopile heat flux probes in the intake port of a single-cylinder fuel-injected research engine. Each probe consisted of 20 thermocouple pairs that allow for resolved heat flux measurements. These probes were located on both the top and bottom of the intake port, as well as on the back of the intake valve. After conducting tests using propane, indolene, and iso-octane, research showed a spray targeted region in which fuel film was present. This region was located across and downstream from the fuel injector. It was shown that a fuel film was present regardless of open or closed valve injection timing, with open valve injection timing reducing the overall mass. This was determined from a reduction in the intake valve temperature, caused by greater impingement from the injected fuel. By compensating the heat flux measurements with the results found using propane, research also showed that under high wall temperature conditions the fuel film is sheared off of the sensors, rather than totally vaporized.

Thermal modeling to the fuel film issue was addressed by Chen *et al*. [25] by applying a one-dimensional, unsteady, multi-component, multi-phase flow model to the intake port. This model included the effects of fuel vaporization and the wall fuel film effects. The system may be seen in Figure 2.6.

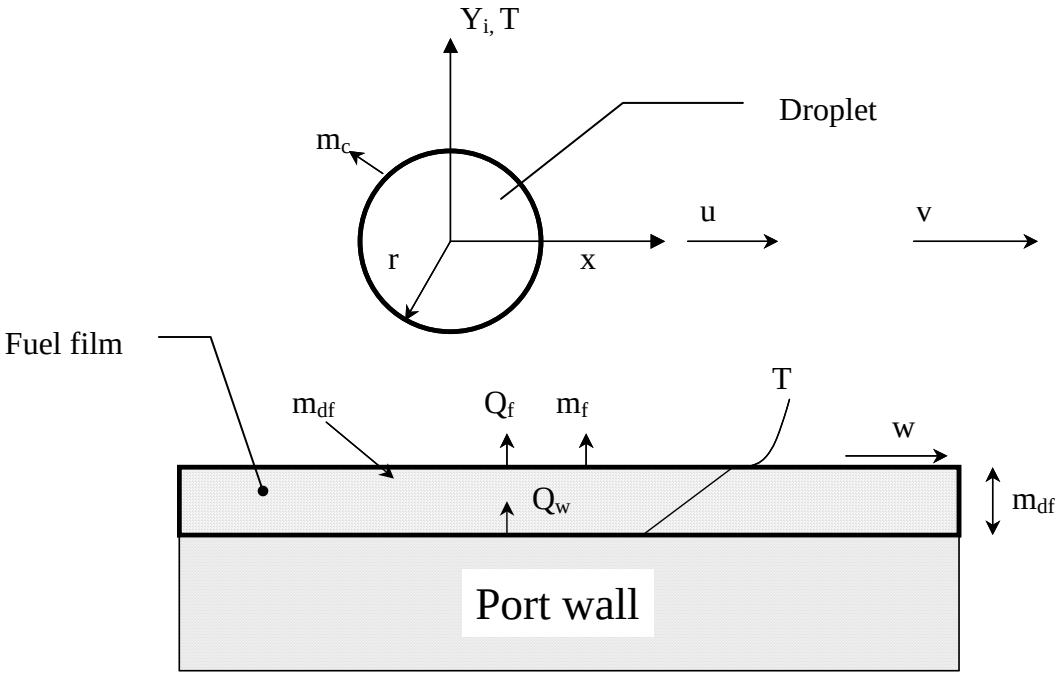

Figure 2.6 One-dimensional fuel flow physical model.

In order to model droplet vaporization, a multi-component model was used which considered both species and thermal diffusion within the droplet. Similar considerations were taken into account for the port wall fuel film. However, it was assumed that the fuel film thickness was insignificant compared to the port diameter allowing the fuel film model to be assumed one-dimensional.

Results of the model showed that heating of the intake air charge had little effect on the reduction of fuel films. It was also found that relatively small temperature

differences between the injected fuel and air resulted in a compromised heat transfer potential. Increased port temperature had a significant effect on fuel film reduction, as was shown in other studies. The model suggested that initial fuel temperature had a significant impact on fuel film mass, with higher initial fuel temperatures resulting in a potential reduction of film mass. This was attributed with the heated injected droplets ability to store potential energy that assists in vaporizing the droplet.

2.5.4. Stop-Injection Hydrocarbon Sampling Techniques

Fuel shut-off transients have been used to determine intake port fuel film mass. This technique allows for determining a cumulative fuel film mass by measuring the in-cylinder, or exhaust stream, hydrocarbon concentration from the onset of shutting off the fuel until no more fuel is present. Although the global contribution can be found, this technique does not allow for localized fuel film mass contributions to be determined.

Work conducted by Ladommatos *et al*. [23] used in-cylinder fast FID measurements of the hydrocarbon concentration during fuel shut-off transients in a 1.6 liter multi-point fuel-injected spark-ignition engine. Under steady-state conditions, the number one fuel injector was disabled and the total hydrocarbon mass integrated over approximately 15 engine cycles. Research showed that the hydrocarbon concentration decayed rapidly, and within approximately 10 engine cycles almost none existed. There was no direct calibration done during this experiment to determine the integrated film mass.

Skippon *et al*. [26] utilized differential infra-red absorption within the combustion chamber of a single-cylinder research engine to determine the mass of fuel inducted using

various fuels with different vaporization characteristics. A narrow infra-red beam traversed the cylinder under the head and the attenuation was integrated over the beams area to determine the total mass of film introduced after a fuel shut-off transient occurred. Standard gasoline was compared with three single component fuels (iso-pentane, iso-octane, and xylene) in order to compare a wide range of volatilites. Research showed that little fuel film existed when lighter components were used, whereas a significant fuel film was present for heavier end components. Comparing results to gasoline, it was determined that non-equilibrium vaporization occurred in the fuel film resulting in the heavier end components forming the majority of the fuel film. For gasoline, research showed that an appreciable mass still existed after 80 engine cycles following fuel shut-off, and that the mass was still decaying. It was also shown that open valve injection contributed to less fuel film formation than closed valve injection.

2.6 Description of Capacitance Technique

Aside from the global mass measuring techniques used to measure fuel film thickness, localized techniques have been developed as well. One such method is the use of capacitive measurements. Although different sensor designs have been implemented, the basic idea of capacitance film measurements remains the same.

The typical capacitance sensor is composed of a central conductive electrode, which is insulated from a shield that surrounds the electrode. Both the shield and the center electrode are driven at the same AC potential by a specialized circuit, which effectively eliminates any capacitance formed between the shield and the electrode. This electrode then forms a capacitance to the ground. When the sensor is brought into close

proximity of a grounded surface, the capacitance changes as a function of the dielectric formed between the sensor and the ground. The film thickness can then extracted from this measured capacitance.

Originally, the capacitive technique of measuring films was applied to applications other than internal combustion engine intake port fuel films. Some of the other applications will be described here, concluding with capacitance techniques applied to a production engine.

2.6.1 Capacitance Based Film Measurements For Non-IC Engine Applications

Graham *et al*. [33] developed a scanning technique for measuring thin dielectric films through the use of a spherical probe. In this technique, a stainless steel sphere ranging from 1 to 5 mm was insulated from a grounded shield via shrink tubing. The sphere was then connected to a lead. Both the lead and shield were then driven at the same AC potential. The probe was then used to measure thin dielectric stationary films located above a grounded surface.

It was found using a 1 mm center electrode with this technique that films on the order of ~200 μm to within an accuracy of ~ 0.2 μm could be measured. Since this method was used to measure stationary films under fixed conditions, it would not be suitable for dynamic fluid film measurements in an internal combustion engine.

Stiyer *et* al. [30] utilized a parallel plate capacitive technique for calibrating LIF oil film thickness measurements in a motored single-cylinder research engine. A thin wire of known diameter was located flush with the engine bore, and was insulated from the surface substrate. The wire was then driven by a sinusoidal voltage of known

amplitude and frequency. When the conducting target, or in this case the piston ring, approached the face of the wire, a capacitance was formed between the wire and the grounded piston ring. Since the oil acted as a dielectric medium, the thickness could be determined from the parallel plate formula

$$d = \frac{\varepsilon A}{C} \tag{2.7}$$

where d is the distance from the capacitor to ground, ε is the dielectric constant, A is the wire cross sectional area, and C is the measured capacitance. Thus distance could be correlated from knowledge of the capacitance and sensor geometry.

2.6.2 Capacitance Based Film Measurements For IC Engine Applications

Simon [34] developed a capacitive technique to measure, locally, fuel film thickness in the intake port of a production central throttle body fuel injected 1.81 liter engine. The capacitive sensors were located at 10mm intervals on thin flexible polyimide sheets with the back side of the sensors shielded. This allowed for a non-intrusive means of characterizing fuel film thickness. An array of sensors were located in the intake manifold ports and on the intake manifold floor. By locating an array of sensors in the manifold, spatial fuel film thickness distributions were determined. Wall films were measured for both cold and hot engine operation under various load conditions.

It was found that gravity had little effect of pooling the fuel film on the intake manifold floor, and that the films were distributed evenly along the port periphery, indicating that flow effects were dominant. Increased engine speed was shown to significantly reduce the fuel film mass due to increased shear stress. Heating the manifold was also shown to significantly reduce fuel film mass, and under hot engine

conditions, the mass was shown to reduce 77%. Overall fuel film mass was shown to increase significantly 800 ms after the onset of the transient, settling into a new steady state condition 3000 ms after the transients conclusion. Results were indicative of the increased response rate of the air flow over that of the fuel film.

3

ENGINE & LABORATORY EQUIPMENT

3.1 Engine Description

The engine used in this study was a Briggs & Stratton, model number 977 Europa engine. The engine falls into the under 25 horsepower non-handheld class of mobile utility engines and is rated at 5 hp. It is an air-cooled, four-stroke, vertical shaft, overhead valve, fixed timing, single-cylinder engine. The stock spark timing is fixed at 22 ^{o}BTDC and is controlled by a magneto. The engine specifications are listed in Table 3.1.

Bore	64.5 mm	2.56 in
Stroke	44.2 mm	1.74 in
Connecting Rod Length	76.2 mm	3.00 in
Displacement	147 cm^3	8.99 in^3
Compression Ratio	8.5:1	
Stock Spark Timing	22 ^{o}BTDC	
Intake Valve Opens (IVO)	320 ^{o}ATDC	
Intake Valve Closes (IVC)	104 ^{o}BTDC	
Exhaust Valve Opens	96 ^{o}ATDC	
Exhaust Valve Closes	328 ^{o}BTDC	

Table 3.1 Briggs and Stratton model 977 Europa engine specifications.

All of the liquid fuel tests were performed with indolene motor fuel HOIII supplied by the Amoco Oil Company. The gaseous fuel tests were conducted with 99.0% pure CP grade propane. Engine lubrication was supplied by Shell Rotella T, SAE30 non-detergent grade oil. The fuel properties are listed in Table 3.2.

FUEL/LUBRICATION	PROPERTY	VALUE
Indolene	Stoichiometric A/F Ratio	14.58
	Specific Gravity	0.74
	Octane Number (RON+MON)/2	92.1
	Net Heating Value(LHV) MJ/kg	42.95
Propane (99.0% pure)	Stoichiometric A/F Ratio	15.67
	Specific Gravity	0.51
	Octane Number (RON+MON)/2	97
	Net Heating Value(LHV) MJ/kg	46.4

Table 3.2 Indolene and propane fuel specifications.

3.2 Dynamometer And Torque Measurements

The engine was mounted on a vertical shaft, 10 hp DC motor/generator dynamometer that was manufactured by Cox Instrument Division and supplied by the Briggs and Stratton Corporation. A custom hybrid Mooreflex/Dodge coupling was used at the interface between the dynamometer and the engine. The dynamometer was used to run the engine at constant speed and was capable of both motoring and firing tests. Speed was regulated to within +/- 5 RPM during motored tests, and to within +/- 10 RPM during steady state firing tests.

A load cell manufactured by Interface Corporation was integrated with the dynamometer and was used to measure engine torque. This cell is capable of measuring torque to 339 Nm. The load cell torque arm measured 0.3 m.

3.3 Liquid Fuel Injection System

In order to gain fueling control for step transient testing, a fuel injection system using the stock carburetor body was devised [7]. This system allows for controlled step fueling transients that could not be obtained using a stock carburetor. The float bowl, float, float

needle valve, and spring retaining system of the stock carburetor were removed. A Bosch fuel injector was mounted in its place with a retaining bracket. The fuel injector is a four hole automotive-type rated at 8.62 kg/hr at 241 kPa fuel pressure. The bracket served both to hold the fuel injector in place and to feed fuel from the fuel injector orifice to the throttle body via a siphon tube approximately 20 mm in length and containing a residence volume of 38 mm^3. The siphon tube replaced the carburetor fuel discharge tube; and it was the intention to mimic carburetor fuel delivery with this system using the metered flow capabilities of a fuel injector. All emulsion and air-assist holes in the carburetor were then sealed with high temperature epoxy. The siphon tube fuel injection system may be seen in Figure 3.1.

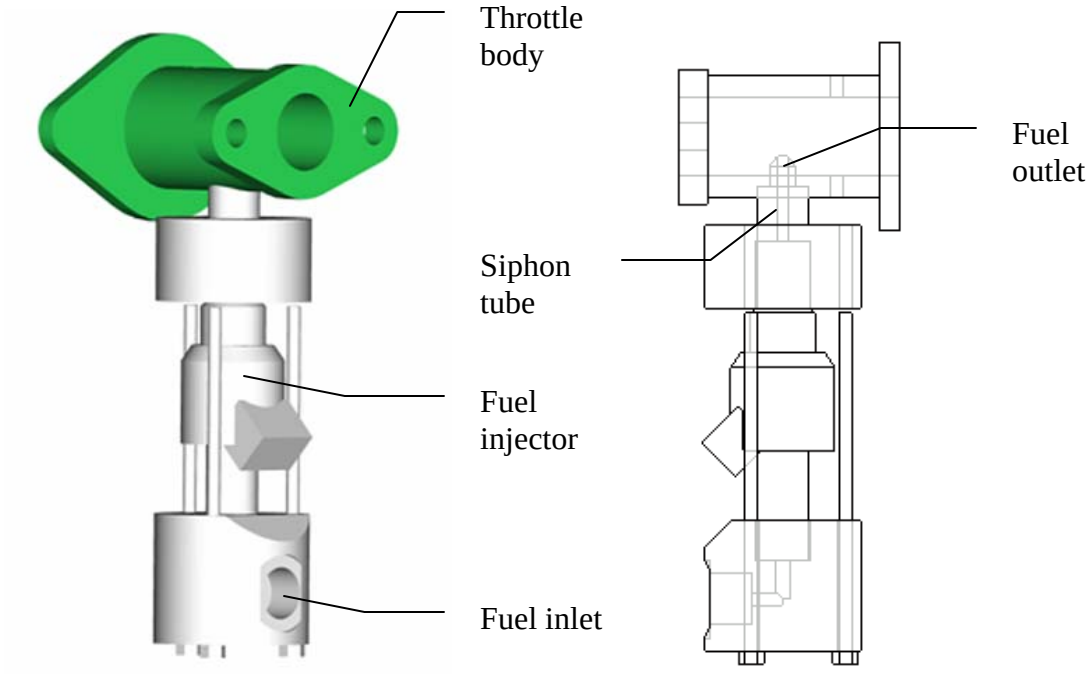

Figure 3.1 Siphon tube fuel injection system.

By mounting the fuel injector to the throttle body of the carburetor via a siphon tube, fuel delivery similar to the stock carburetor has been observed [7]. Tests were

performed using typical short duration fuel injection pulses under high fuel injection pressure, and with longer duration fuel injection pulses under low fuel injection pressure. By using low pressure, long duration fuel injection through the siphon tube during the intake stroke it was felt that exit flow characteristics from the tube would more closely resemble venturi tube exit flow characteristics. Typical pressures for low pressure operation were 13.8 kPa (gage), and for high pressure 345 kPa (gage).

3.4 Propane Fuel Injection System

In the effort of separating fuel film from combustion and breathing effects, a propane fuel injection system was developed. A Servojet gaseous fuel injector model number SP-021, manufactured by Clean Air Partners, was used. This fuel injector is of bottom-fed design, and contains a ball and seat type of configuration to seal against high pressures or vacuums. The effective flow area is 1.4 mm^2, and maximum rated operation pressure 5100 kPa. An aluminum injector rail was machined locating the injector on the top of the intake port. The injector sealed against the adaptor rail with two o-rings. The first o-ring separated and sealed the inlet and outlet ports of the injector, and the second sealed the injector from the atmosphere. A stainless steel delivery tube was connected to the intake port and fuel injector rail by epoxy, and the rail was welded to the intake port. The Servojet fuel injector may be seen in Figure 3.2. A cutaway view of the propane fuel injector rail may be seen in Figure 3.3.

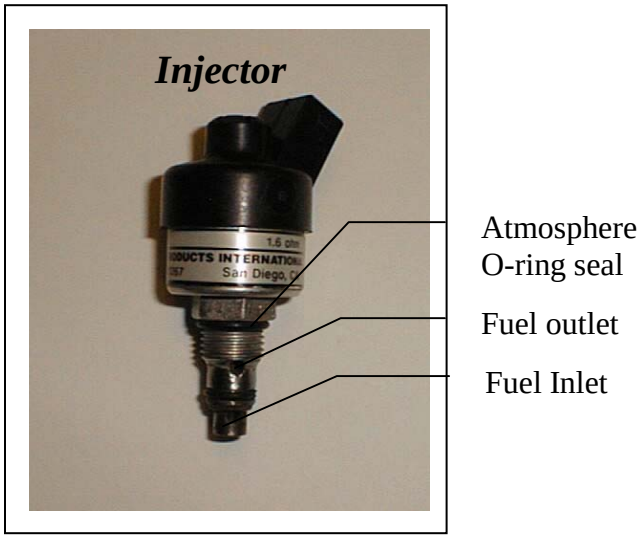

Figure 3.2 Servojet fuel injector.

The 2.46mm diameter delivery tube was located approximately 36mm from the back face of the intake valve. The residence volume of the tube is 0.24 cm^3, which is sufficiently less than the volume of propane required per cycle under stoichiometric, ambient conditions (see Appendix B-2 for calculations). By minimizing the residence volume of the injector rail and delivery tube, excess propane was ensured not to reside in the crevice volume after closure of the fuel injector. This allowed step transient control without residual crevice volume propane affecting transient. The propane fuel injection system may be seen in Figure 3.3.

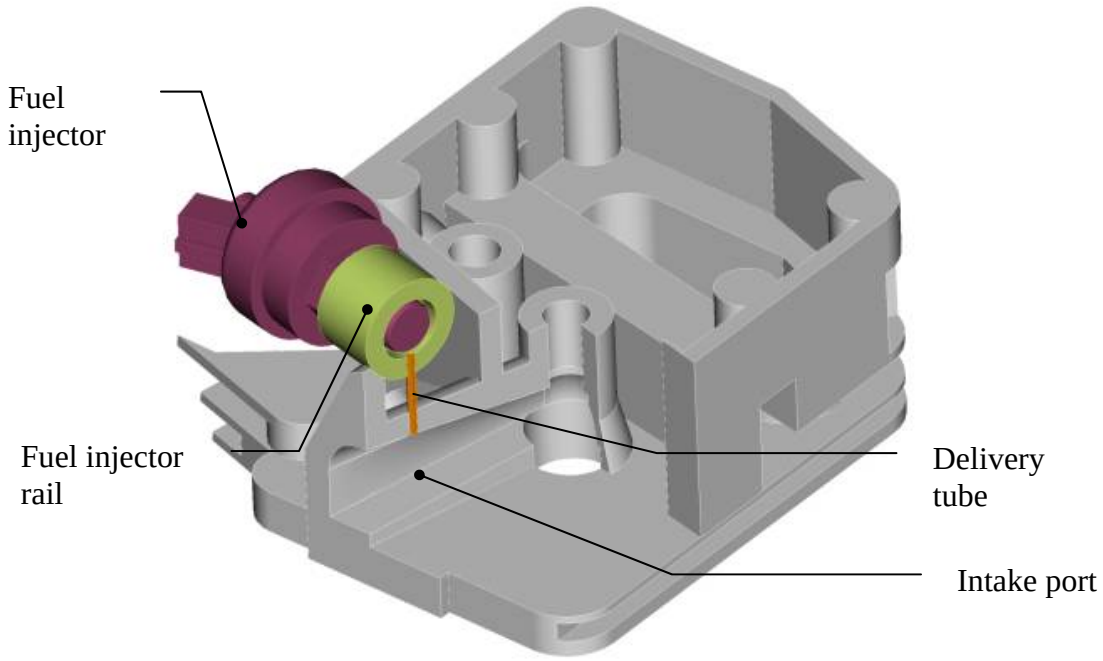

Figure 3.3 Propane fuel injection system.

The propane was regulated through a Matheson model #3284-580 two-stage regulator. The two-stage regulator was used to reduce regulator creep during engine operation.

3.5 Fuel Injection Control System

A program was written in LabView that interfaced with a computer counter card in order to gain dynamic control over fuel injection transients for both propane and liquid fuel. The system consists of a SD-1 Clean Air Partners Solenoid Driver, 233 MHz Pentium computer, National Instruments PC10-TIO counter card, 12 volt power supply, crankshaft timing encoder, timing optical interrupter, and a crankshaft encoder buffer box. The system may be seen in Figure 3.4.

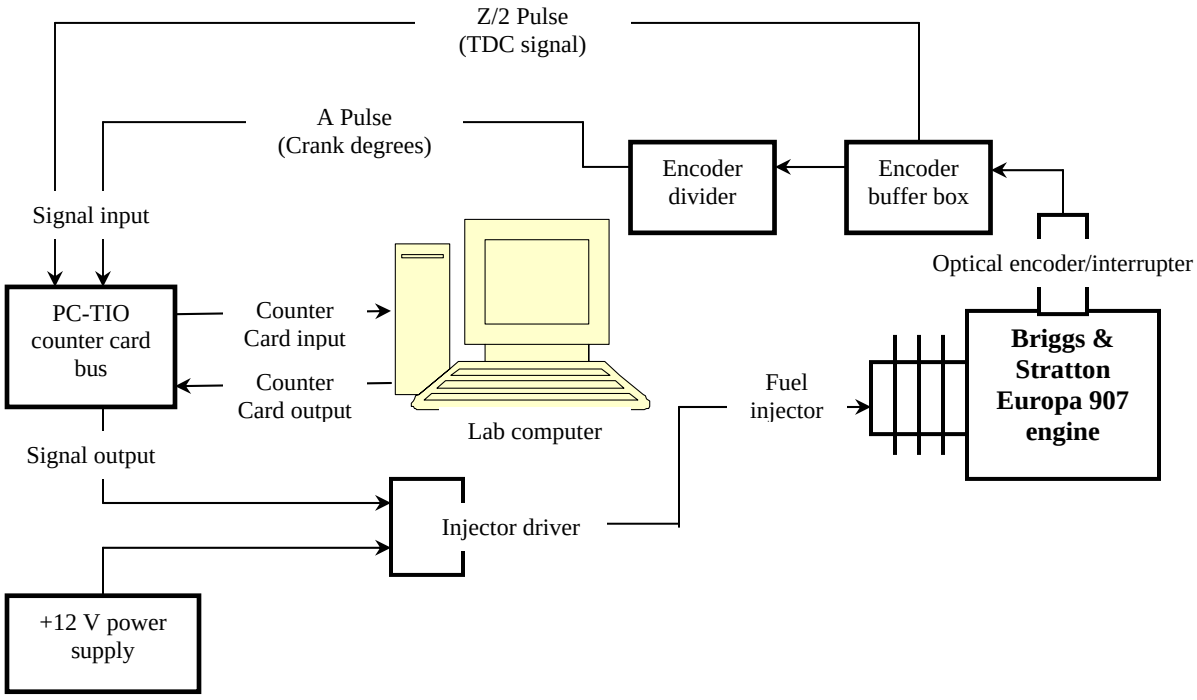

Figure 3.4 Fuel injection system.

The shaft encoder output was routed from the engine crankshaft to a buffer box. The counter buffer box conditions the shaft encoder signal and outputs both a TDC Transistor-Transistor-Logic (TTL) logic digital signal during either the intake or exhaust stroke (Z/2-pulse), and 2 pulses for every crankshaft degree (A-pulse). TDC pulse timing was set by an optical interrupter that turned at half the engine speed. This was done via a 2:1 gear and belt system connecting the interrupter to the engine crankshaft and allowed identification of the TDC intake and TDC compression stroke. Both the A and Z/2 signals were routed to the PC-TIO-10 counter card bus, which directed the signals into the computer counter card. The program logically gated the injector signal to the TDC signal (Z/2 pulse) and paused a specified number of crank degrees (A pulse) before

sending out the fuel injection TTL signal to the injector driver. The program provided the ability to change the injection pulsewidth in one cycle after a specified number of cycles had been completed.

3.6 Transient Throttle System

In order to control throttle transients under constant fueling conditions, a transient throttle system was developed [7]. This system allowed for throttle control while maintaining constant fueling (either liquid or gaseous fuel) creating intake air transients. This allowed for separation of combustion and transient intake air-flow effects.

This system consisted of a stepper motor, stepper motor system controller, RS-232 port connection between the stepper motor system controller and the computer, Labview programmable interface, and the carburetor-to-stepper motor connector bracket. All stepper motor motion was programmable and was controlled by the LabView interface. Motion between the stepper motor and carburetor throttle shaft was transmitted through a 2:1 belt drive. The throttle transient system may be seen in Figure 3.5.

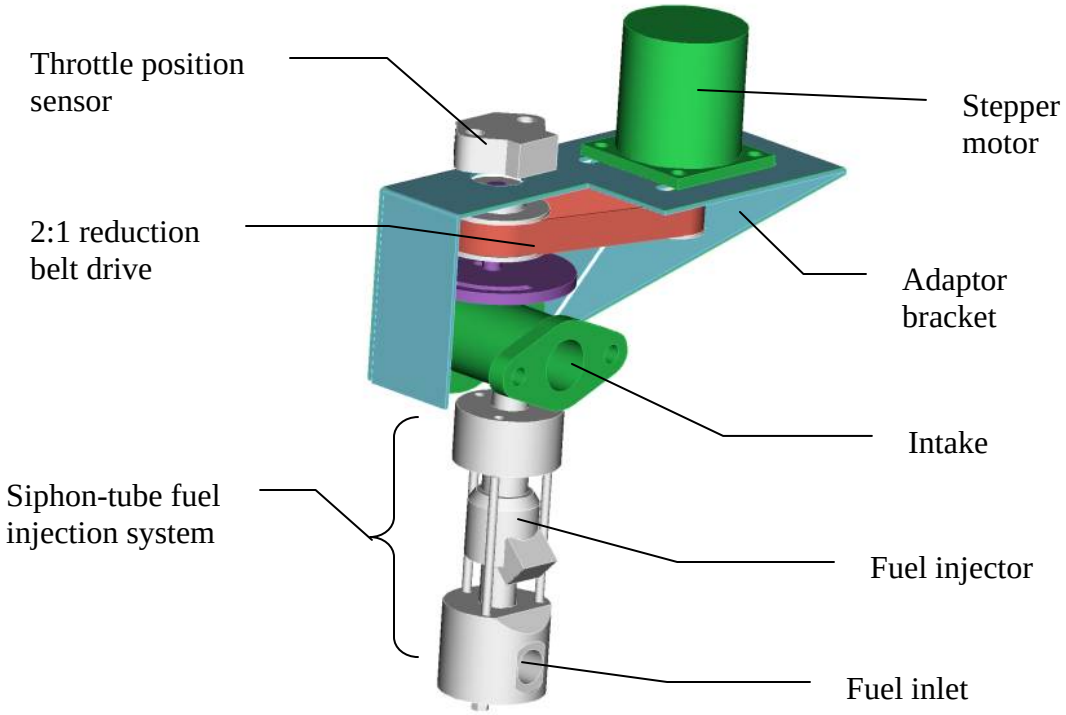

Figure 3.5 Transient throttle system.

The carburetor throttle shaft is driven by the quad step stepper motor with a resolution of 0.225 degrees per step. The stepper motor controller allows for an adjustable stepper motor rate. Stepper motor control was obtained by an interface between the stepper motor system controller and a LabView program. The program controlled steady state fuel injection and sent directions into the stepper motor controller EPROM. Due to stepper motor programming limitations, throttle motion rate and relative motion was controlled on a time and not crank angle basis. However, it was found that repeatability was sufficient with this configuration

3.7 Exhaust Fast-FID Hydrocarbon Sampling System

An exhaust sampling diagnostic technique was devised to quantitatively investigate the presence of fuel films in the intake port. This system allowed for exhaust stream hydrocarbon sampling during the entire engine cycle utilizing a FFID. During a skip-injection engine cycle, the majority of exhaust stream hydrocarbons present were speculated to originate from intake port fuel films. Although research has shown that a portion of exhaust hydrocarbons may originate from crevice volumes, re-entrainment from cylinder wall oil films, or oil from ring-pack blow-by, this contribution is considered to be minor relative to the HC associated with an unburned AF mixture [20]. By skipping injection events or ceasing fuel injection altogether, the exhaust stream HC concentration could be measured and the intake port fuel film contribution determined.

This system consists of a Cambustion fast FID, data acquisition capable of crank degree resolved resolution, triggered signal generator, TTL counting circuit that disabled a specified number of injector signals after a given number of engine cycles, and the siphon-tube fuel injection system. The TDC pulse from the encoder was directed into the signal generator and acted as a trigger for fuel injection. Once triggered at TDC of the intake stroke, the TTL pulse was directed to the TTL counting circuit and counted. After 30 counts, the TTL signal would go low for either 1 or 3 engine cycles, disabling fuel injection, where the number of skipped injections depended upon the test. The exhaust stream HC concentration was sampled during the entire engine cycle using the fast FID. The system may be seen in Figure 3.6.

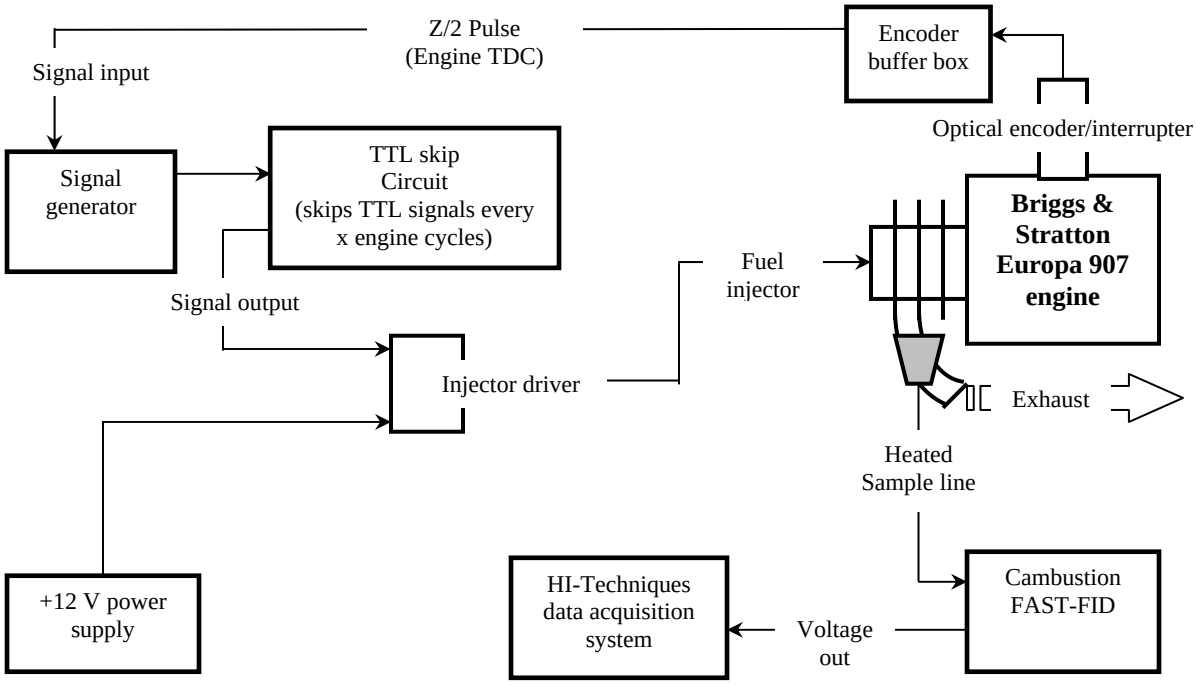

Figure 3.6 Fast-FID exhaust sampling system.

3.8 Fast-FID

Crankangle-resolved hydrocarbon concentration measurements were collected using a Cambustion HFR-500 FFID. This system measures HC concentrations with high temporal resolution. The probe response time is cited at 0.9 ms, and the transit delay cited at 5 ms. By offsetting for this delay, cycle-resolved hydrocarbon concentrations may be determined.

The FFID detects hydrocarbons using an ionization detection sensor. The sample gas is collected through a small 0.6 mm capillary tube, and is carried to the detection unit located 0.3 m away. The sample gas is then burned in a 40-60% helium-hydrogen flame. The combustion of hydrocarbon fuels produces a significant number of ions. The number of ions are nearly proportional to the number of carbon atoms allowing the hydrocarbon

concentration of the sample to be determined. All tests were conducted after calibrating the FFID using 6280 ppm propane span gas. It was not necessary to offset the FFID data for the time delay for either the skip-injection or stop-injection tests. Correlating the FFID data with either the injector signal or cylinder pressure indicated the onset of the transient, and the FFID data was integrated on a cycle-to-cycle basis.

In order to obtain accurate FFID hydrocarbon measurements, the location of the sample probe is important. Mixing downstream of the exhaust valve has been shown to drastically affect the hydrocarbon concentration measurements. To obtain accurate hydrocarbon measurements, the probe should be located as close to the exhaust port as possible. For this study, the probe was centrally located in the exhaust port 4.4 cm from the back of the exhaust valve. Physical constraints did not allow for closer placement of the probe to the valve face.

3.9 Pressure Transducer

Pressure measurements for this study were collected using a liquid cooled piezo-electric Kistler model 6061 pressure transducer. In order to protect the pressure transducer from thermal strain, the face of the transducer was coated with a 1.5 mm thick silicone sheet. The silicon was manufactured devoid of bubbles. The presence of bubbles has been shown to cause a rapid degradation of the silicon coating. The silicon sheet was cut to match the face of the transducer and was fixed with a thin film of high temperature silicon. The sensor was then placed in a drying oven at 50^{o}C for a 24 hour period and allowed to dry. Calibration of the transducer was conducted, the results of which may be seen in Appendix A-4.

3.9 Exhaust Air/Fuel Ration Measurements

All exhaust air fuel measurements were conducted using a Horiba KX-721030F heated universal exhaust gas oxygen (UEGO) sensor in conjunction with a Horiba MEXA-110λ air fuel analyzer. The sensor was located in the exhaust manifold approximately 23 cm from the exhaust valve seat. Accuracy of the system over a range of operating air to fuel ratios may be seen in Table 3.3 [34].

Accuracy	Air-Fuel Ratio
± 0.3	12.5
± 0.1	14.7
± 0.5	23.0

Table 3.3 UEGO sensor accuracy.

3.10 Capacitance Sensor Fuel Film Measurement System

To further investigate the effects of intake port wall fuel films, a system was devised to measure fuel film thickness. The system consists of small capacitance probes and a first-order, amplitude modulated, capacitance measurement circuit. The probes were inserted at strategic points in the intake port and measurements performed to determine fuel film thickness during engine operation. The probes were connected to an amplitude modulation circuit that is used to convert small changes in capacitance to an output voltage. The details of the capacitance circuit are given in the following sections, and details of the capacitance gage are provided in Chapter 7.

3.10.1 First Order Amplitude Modulated Capacitance Circuit

The circuit used to measure film thickness is a first-order amplitude-modulated preamp circuit. The device is designed to convert small changes in capacitance to a DC output voltage that represents the distance between the probe and a grounded surface. Although the change in capacitance may be associated with the probe proximity to a grounded surface, a change in dielectric medium would result in change as well. The circuit provides a sine wave that drives the probe. When a change in capacitance occurs, the sine wave amplitude will change proportionally. This amplitude modulation signal is then demodulated by passing it through a low pass filter and a broadband RMS to DC converter.

The system consists of seven subsystems; amplitude modulator, shield driver, AM sine wave gain stage, AM signal detector, DC servo with integrator, output gain stage and the output shift lever. Six of the seven systems will be briefly discussed here (the DC servo loop is used for static capacitance calibration and was not utilized. Therefore it will not be covered).

3.10.1.1 Amplitude Modulator

The amplitude modulator is a first order RC circuit connected in series. The variable capacitance of the probe and the ground form the capacitor. The amplitude modulator works by forming a voltage divider between the probe and a resistor. When the probe is brought to within close proximity of the surface ground, or as the dielectric changes, the voltage drop of the probe varies. This effectively links a change in capacitance to a change in wave amplitude.

The transfer function of the system may be prescribed as follows

$$\frac{V_{probe}}{V_0} = \frac{1}{\sqrt{4\pi^2 R^2 f^2 C^2 + 1}} \tag{3.1}$$

This system behaves as a low pass filter system, and has a corner frequency described by

$$f_c = \frac{1}{2\pi RC} \tag{3.2}$$

As the sine wave frequency supplied to the circuit is twice that of the corner frequency, the system behaves linearly and may be more simply described as follows

$$\frac{V_{probe}}{V_0} = \frac{1}{2\pi RfC} \tag{3.3}$$

3.10.1.2 Shield Driver

Since a capacitance forms between two objects held at a voltage potential separated by some distance, the shield driver eliminates the capacitance between the coaxial cable shield (braid) and the center coaxial wire. This is essential since stray capacitances may mask the small capacitance trying to be measured by the probe. Shielding is achieved by driving the outer conductive coaxial shield with the same potential as the center electrode of the probe. By driving the probe and the shield at the same potential, the electric field strength is zero resulting in no capacitance.

3.10.1.3 Sine Wave Gain Stage

This stage of the circuit is used to amplify the small amplitude modulated signal from the probe to a required 20V peak-to-peak wave. This is done through a variable gain non-inverting amplifier.

3.10.1.4 Signal Detector

The signal detector converts the sinusoidal amplitude-modulated probe signal into a DC form. This is done through a wide band RMS to DC converter, and the output of the signal is the RMS value of the input sine wave.

3.10.1.5 Output Gain Stage

The output gain stage is an inverting amplifier used to increase output gain. This is achieved via a jumper, the maximum allowable gain being 20.2 times the input. It used to increase the gage output voltage.

3.10.1.6 Output Level Shifter

This last portion of the circuit allows for DC offset adjustment of the output signal. This is done to adjust for various oscilloscopes or data acquisition systems that may be used in conjunction with this circuit.

3.11 Data Acquisition System

The data acquisition system used during this project was a Hi-Techniques HT-600 data acquisition and analysis instrument. This system consists of a mainframe unit that contains all necessary power supplies, high speed mother board, digitizer short bus, and all required BNC connections. There are a total of 8 channels of data that may be collected simultaneously. Triggering of data through this system was accomplished with an on board gate and counter, which were connected to the TDC and crank degree counting pulses from the shaft encoder. All data channels had independent calibration

coefficients, which allowed the input voltage to be converted to respective engine parameters.

Included with the data acquisition system was REVelation combustion analyzer packaged software. This software is specific to engine combustion analysis. This software allows for cycle resolved determination of IMEP, heat release, peak pressure, burned mass fraction, coefficient of expansion, as well as other pertinent engine data. By averaging between 10 and 500 cycles of engine data, indicative engine trends could be determined.

Two programs were used to post process test data. For the step fueling and step throttle transient tests, two programs in Visual Basic were written. Both programs aligned five runs of data to a digital high signal that occurred at the onset of the transient. The data was then truncated and reduced. Details to the programs may be seen in Appendix C-1 and C-2. Igor Pro was used to calculate the hydrocarbon mass for the skip-injection and stop-injection tests. Details to these programs may be seen in Appendix D-1 and D-2.

4

UEGO SENSOR RESPONSE DETERMINATION

4.1 Transient Operation Statistical Analysis

Exhaust gas lambda sensors are a useful diagnostic for in-cylinder processes. However, these sensors have a limited bandwidth. In order to assess the sensor's characteristics, the close-coupled propane fuel injection system was utilized and step-fueling perturbations were performed at constant throttle position and nominal engine speed.

During step fueling, step load, or step throttle transients, engines undergo dynamic speed excursions. Due to cycle-to-cycle variability and dynamic speed excursions that occur during transient operation, a series of tests were performed to determine the number of transient tests required to be indicative of a step transient. Statistical analysis was conducted on a series of 20 fueling transients to assess how many tests would be necessary to accurately characterize the UEGO sensor data. The transient A/F results of these tests were progressively averaged together in increments of five runs: the first five A/F transient tests were averaged over their full 400 engine cycles, then the first ten, then fifteen, and finally all twenty. The results of these four averaged sets of data were then compared to determine the number of tests required to collect a statistically representative sample for future experiments.

The transient fueling tests consisted of step perturbations from approximately 16.0:1 to 10.5:1, then back to 16.0:1. Indolene was selected as the fuel, and the fuel injection pressure for the siphon-tube fuel injection system was regulated to 345 kPa.

The initial injection pulse width was 3.36 ms, and the transient injection pulse width was 5.6 ms. The engine was run at a constant speed of 3060 RPM under constant throttle position, and the engine oil temperature reached a steady value of 114^{o}C. The engine was allowed to fire approximately half an hour prior to any transient data sampling to ensure steady state operation. At the conclusion of a transient test, the fuel injection program was reset, at which point the engine momentarily ceased firing (under 5 seconds). After resetting the fuel injection program, the engine was allowed to stabilize for 1850 engine cycles prior to collecting the next set of data to again ensure steady state operation. This was observed to be sufficient in maintaining steady state conditions.

After collecting the data, the fuel injection TTL signal was used to determine the onset of the transient. The data were shifted so that there were 75 engine cycles prior to the step transient. The fueling transient lasted 200 engine cycles, and a total of 400 engine cycles of data were collected. The results of the tests may be seen in Figure 4.1.

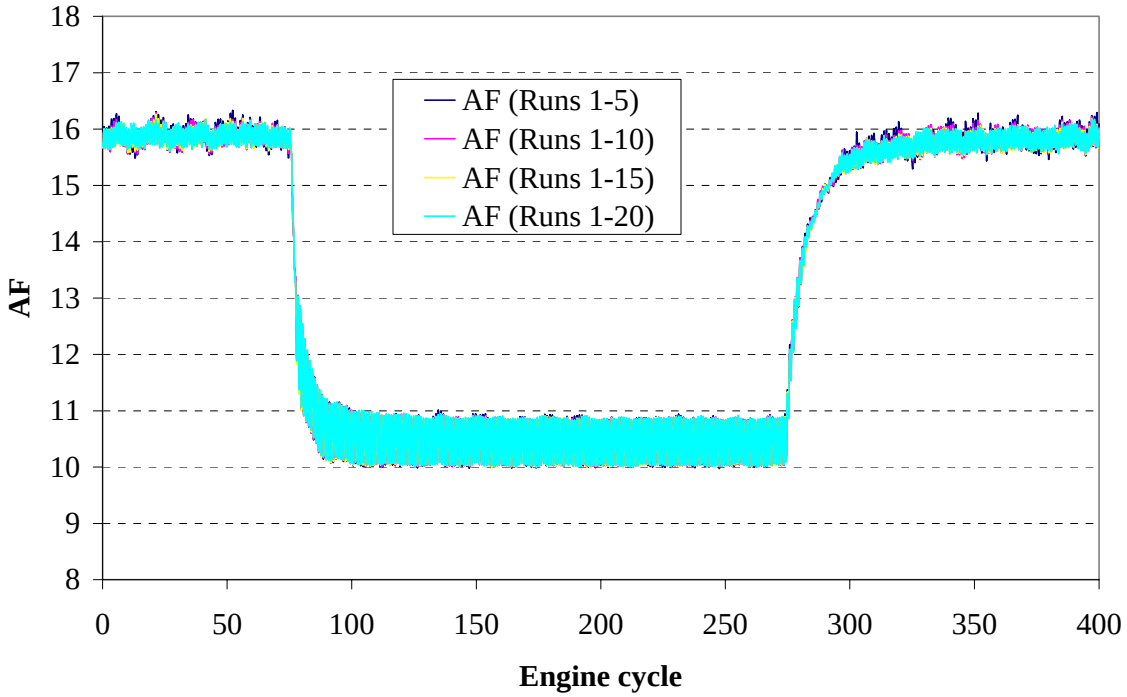

Figure 4.1 Combined averaged indolene fuel transient runs.

Due to the scale of Figure 4.1, it is difficult to assess the amount of variability occurring between the progressively five-run averaged sets of data. To determine the differences between the average of the four sets of data, the deviation of each of the averaged data sets from the 20 run averaged set was calculated. Since the 20 run averaged set contains the largest data population, it is considered the datum from which the other data sets are compared. The results of these deviations may be seen in Figures 4.2 through 4.4.

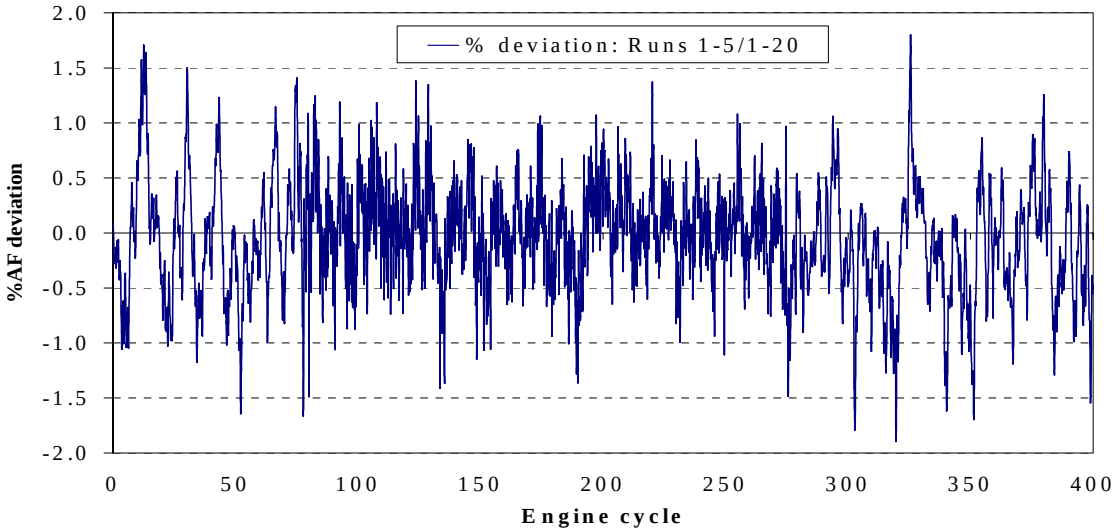

Figure 4.2 Runs 1-5/1-20 combined average deviation– indolene fuel transient runs.

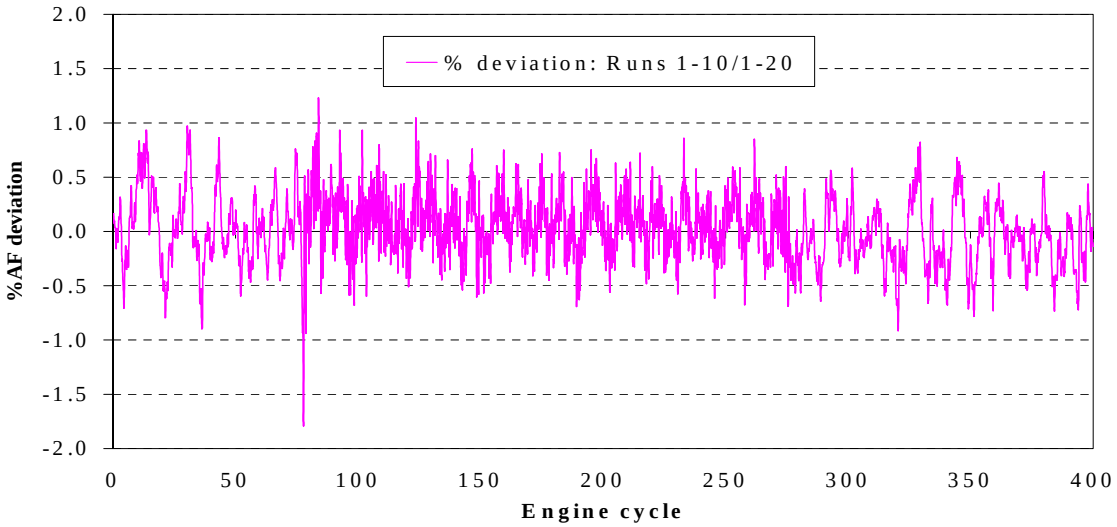

Figure 4.3 Runs 1-10/1-20 combined average deviation– indolene fuel transient runs.

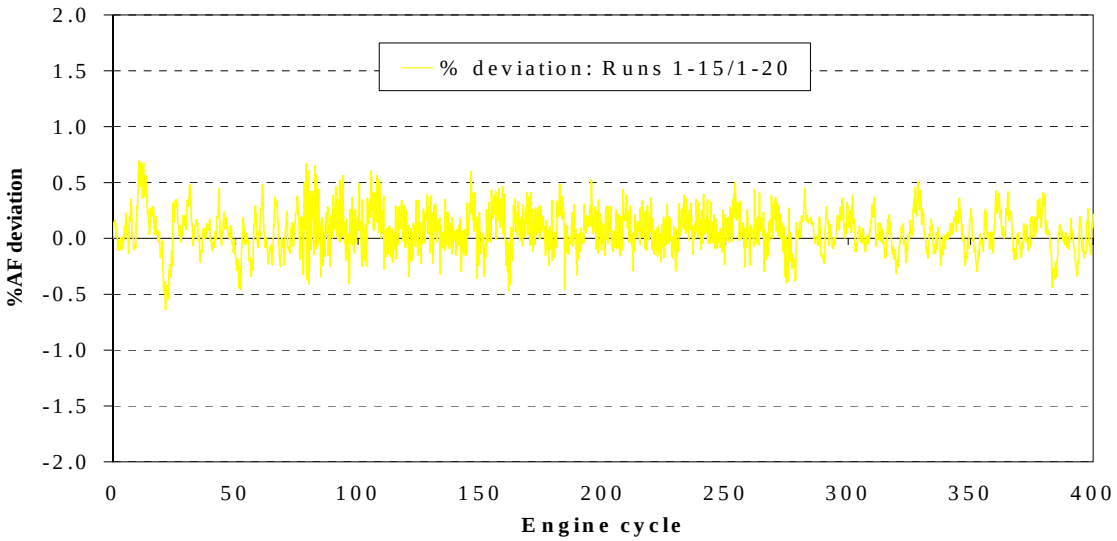

Figure 4.4 Runs 1-15/1-20 combined average deviation– indolene fuel transient runs.

From Figures 4.2 through 4.4 one finds the maximum deviation occurs in the 5 run averaged data set, approximately 0.3 A/F units from the 20 run averaged base case, or approximately 1.9% deviation. From this information it was determined that 5 runs were sufficient in gathering a statistically representative transient data set.

4.2 UEGO Sensor Response Determination: An Introduction

There are two time delays associated with oxygen sensors. The first delay is associated with the time for in-cylinder combustion gas to reach the sensor located in the exhaust manifold downstream of the exhaust valve, and for the sensor to begin responding to the change in exhaust stream composition. This time delay is referred to as τ_1, and is a function of the sensor's distance from the exhaust valve. The second delay is associated with the amount of time required for the electrolytic UEGO sensor to fully respond to a change in exhaust gas oxygen concentration. This delay is referred to as τ_2, and may be modeled by a first order time response. Prior to investigating fuel film effects in the

intake manifold, the time delay (τ_1) and sensor response time (τ_2) of the heated UEGO sensor were determined by a series of propane fueled step transient tests. Propane does not form fuel films in the intake port that may result in lengthened response times.

4.3 UEGO Sensor Response Testing Conditions

All sensor response tests consisted of a series of propane-fueled transients. The transient tests consisted of running the engine at different loads and fuel injection timing, and impulsively varying the fuel injection pulse width. All tests were conducted with the propane pressure set to 620 kPa. Steady state operation was ensured by running the engine approximately one half hour prior to any transient tests. After that time, engine oil temperature reached a steady value ranging from 101 to 115^{o}C, depending upon the engine load. Engine speed was set at 3060 RPM. Exhaust pressure was set at a constant 1.87 mm Hg vacuum. The step fuel perturbation event for all tests lasted for 200 engine cycles. At the conclusion of a transient test, the fuel injection program was reset, at which point the engine momentarily ceased firing (under 5 seconds). After resetting the fuel injection program, the engine was allowed to stabilize for 1850 engine cycles prior to collecting the next set of data to again ensure steady state operation. Five transient tests were averaged together for each parameter change since it was determined that five runs are statistically sufficient (section 4.1).

To calculate the time response delay (τ_1) and first order response time (τ_2) of the sensor, a program was written in EES. The program calculated the time delay response and the sensor first order response by minimizing the squared deviation between the

actual A/F signal and a first order response curve by varying τ_1 and τ_2. This equation is of the form

$$r = AF_2 + (AF_1 - AF_2)\exp\left(-\frac{t-\tau_1}{\tau_2}\right) \qquad (4.1)$$

where *r* is the sensor response, AF_1 is the pre-transient A/F ratio, AF_2 is the transient A/F ratio, *t* is the time from which the transient begins, τ_1 is the sensor delay time and τ_2 is the sensor response time. The actual program may be seen in Appendix B-1. Approximately 75 engine cycles of A/F data was averaged to determine pre-transient and transient A/F ratio. These values were used as AF_1 and AF_2 in equation 4.1. To determine the starting point to calculate the value for τ_1 in equation 4.1, the data collected was offset according to a digital signal that was outputted when the fuel injection pulse width increased, or decreased, indicating the start of the transient. An additional offset was then required to account for the delay between the time of fuel injection and the time that the exhaust valve opened (exhaust valve opening is the actual time in which the UEGO sensor might first expect to see a change in exhaust stream composition). This offset was determined knowing the fuel injection timing with respect to TDC intake, and the engine speed. The exhaust valve opening offset was included for all tests.

4.3.1 Fuel Injection Timing Effect On UEGO Sensor Response

Tests were conducted to determine the effect fuel injection timing has on UEGO sensor response time. This was done to determine if early or late mixing of the gaseous fuel with intake air would alter sensor response. The initial fuel injection duration for all

three tests was set to 2.85 ms, and the transient injection duration was set to 4.65 ms. These fuel injection durations resulted in A/F ratios of approximately 15.5:1 prior to the transient, and 11:1 during the transient. The fuel injection timings investigated were:180 degrees BTDC intake stroke, TDC intake stroke, and 180 degrees ATDC intake stroke. The averaged A/F ratio ensemble for the step transient tests for the three fuel injection timings may be seen in Figure 4.5.

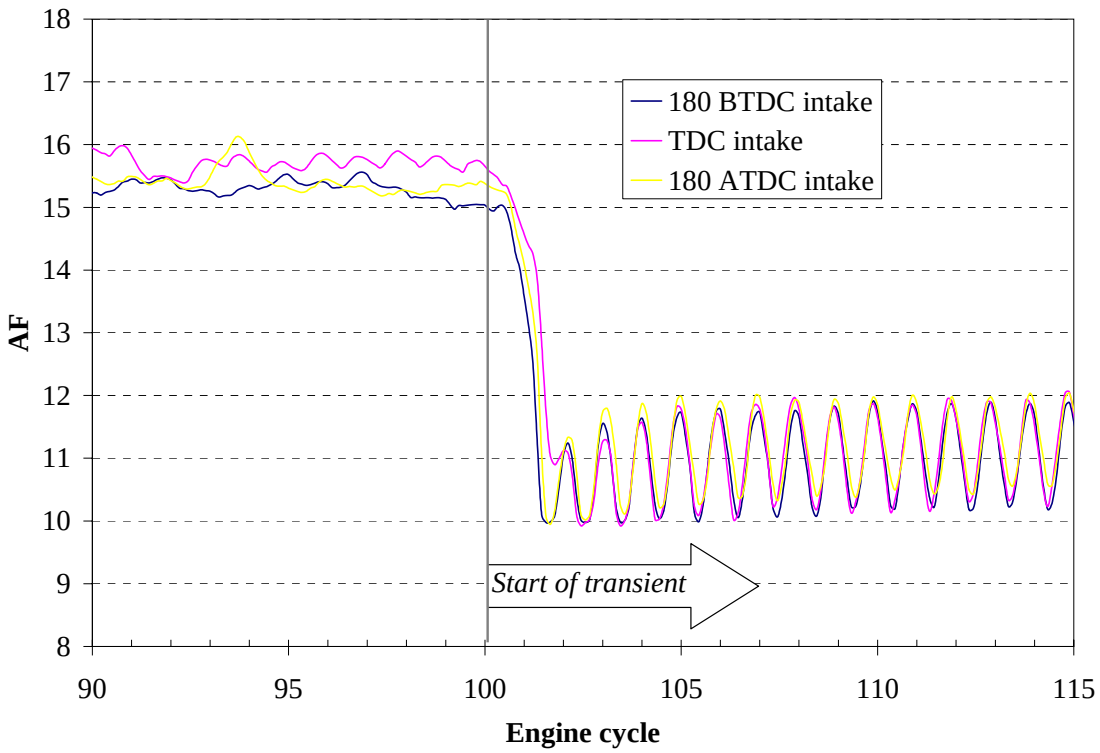

Figure 4.5 Propane fueled step transient tests, varied fuel injection timing, 5 tests averaged.

From Figure 4.5 one notes that there exists discernable cycle-to-cycle A/F oscillations. These oscillations are in phase with the engine, and are more pronounced following the transient. Since the data are five runs averages, it is clear that there exists some phenomenon with the UEGO sensor reacting to the combustion gas that causes such oscillations.

Although the line indicating the start of the transient for Figure 4.5 starts at the 100^{th} engine cycle (the arbitrary engine cycle in which the injector pulse width changed) this is not considered the start of the fueling transient for which τ_1 is determined. The earliest time at which the UEGO sensor is expected to see the step change in A/F ratio does not occur until the exhaust valve opens after the first combusted cycle with the increased injection pulse width. Therefore a delay time must be subtracted from the time arrived at by the fitting technique. The actual response times are roughly noted (for visual reference only) by the τ_1 and τ_2 markers on the figures presented below. The exhaust valve is closed any time preceding τ_1. All sensor response tests have been corrected for this delay. These corrections were determined knowing the engine speed and the exhaust valve profile (the valve profile may be seen in Appendix E-1). The best-fit response curves determined by equation 4.1 may be seen in Figures 4.6– 4.8.

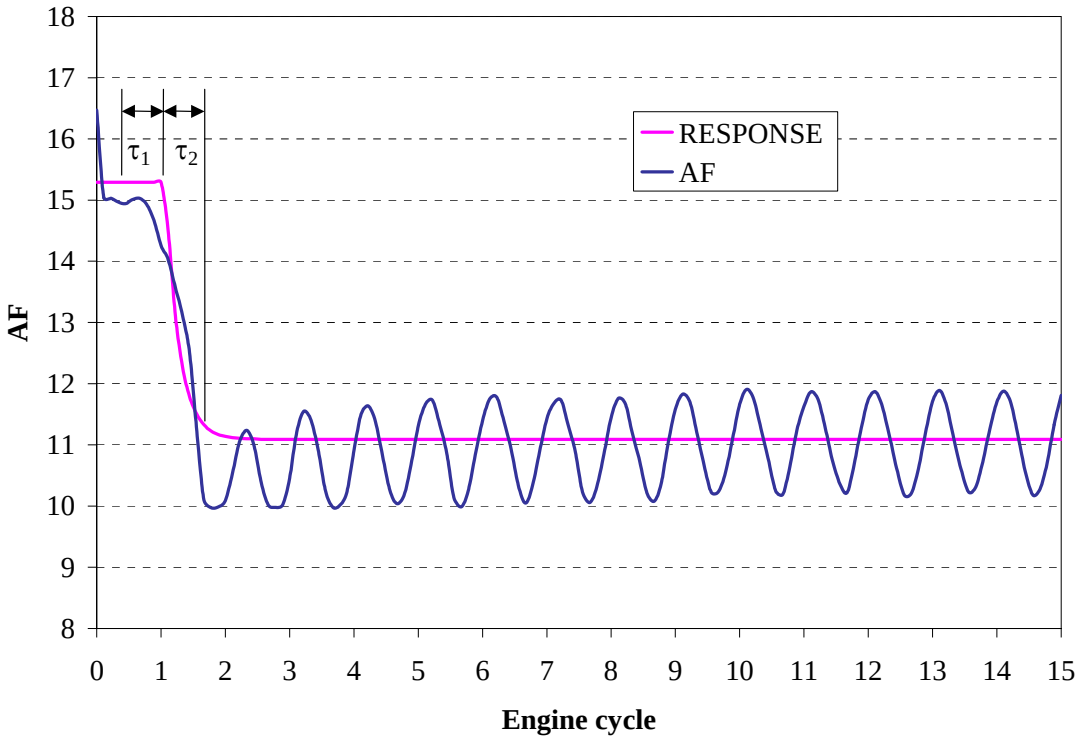

Figure 4.6 UEGO sensor response time curve fit, injection timing 180 degrees BTDC intake stroke.

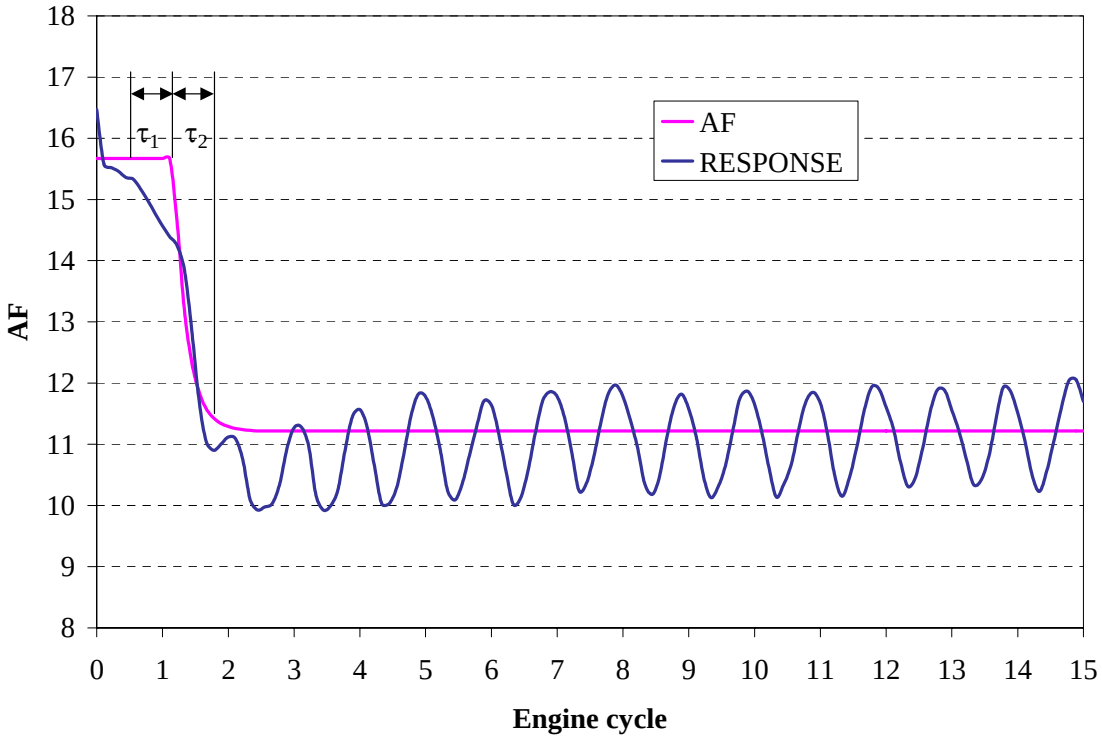

Figure 4.7 UEGO sensor response time curve fit, injection timing TDC intake stroke.

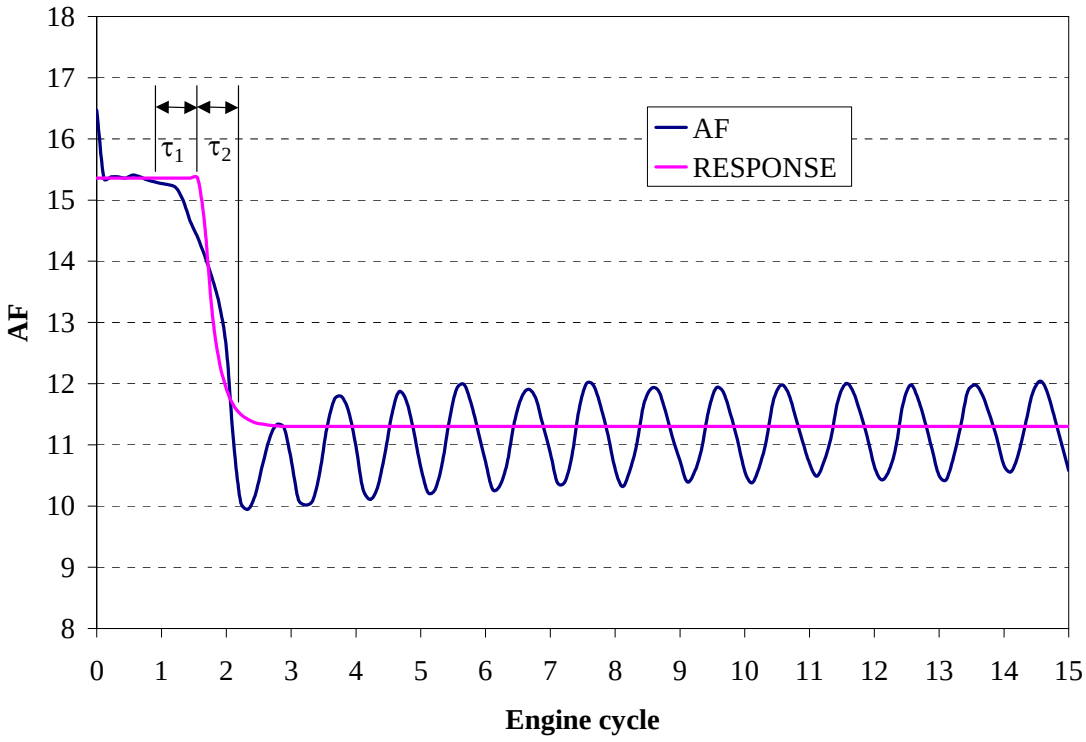

Figure 4.8 UEGO sensor response time curve fit, injection timing 180 degrees ATDC intake stroke.

After correcting for the closed exhaust window, the results of the fuel injection timing test on UEGO sensor response may be seen in Figure 4.9.

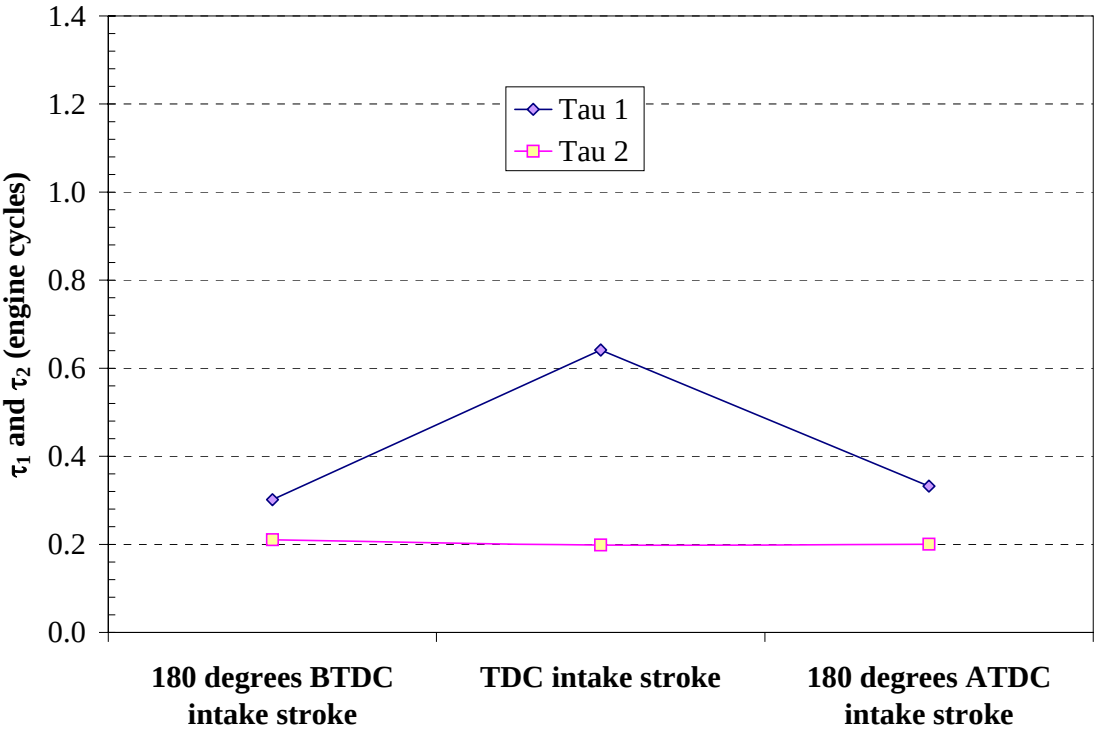

Figure 4.9 UEGO sensor τ_1 and τ_2 time determination: propane fueled step transient tests, varied fuel injection timing

The response time delay (τ_1) varies from approximately 0.3 to 0.6 engine cycles after the step transient occurs, and the first order response time (τ_2) of the sensor takes approximately 0.2 of an engine cycle. Fuel injection timing appears to have no effect on τ_2. However, during the TDC injection timing case, τ_1 approximately doubles. The only logical factor affecting the results for the TDC case would be mixing time. In investigating Figure 4.5, one finds that the A/F trace for the TDC case does not dip as far as the other two cases following the transient. This may be indicative of a less homogenous mixture resulting in incomplete combustion in the first cycle of the transient event.

4.3.2 UEGO Sensor Testing Validation

To validate the τ_1 and τ_2 results, all the conditions for the TDC fuel injection timing test were matched and the test repeated one week after the initial data collection.

This was done to test the repeatability of the transient fueling system with respect to determining the values for τ_1 and τ_2. The overlay of the response curve fit for both the original TDC test and the validation test may be seen in Figure 4.10.

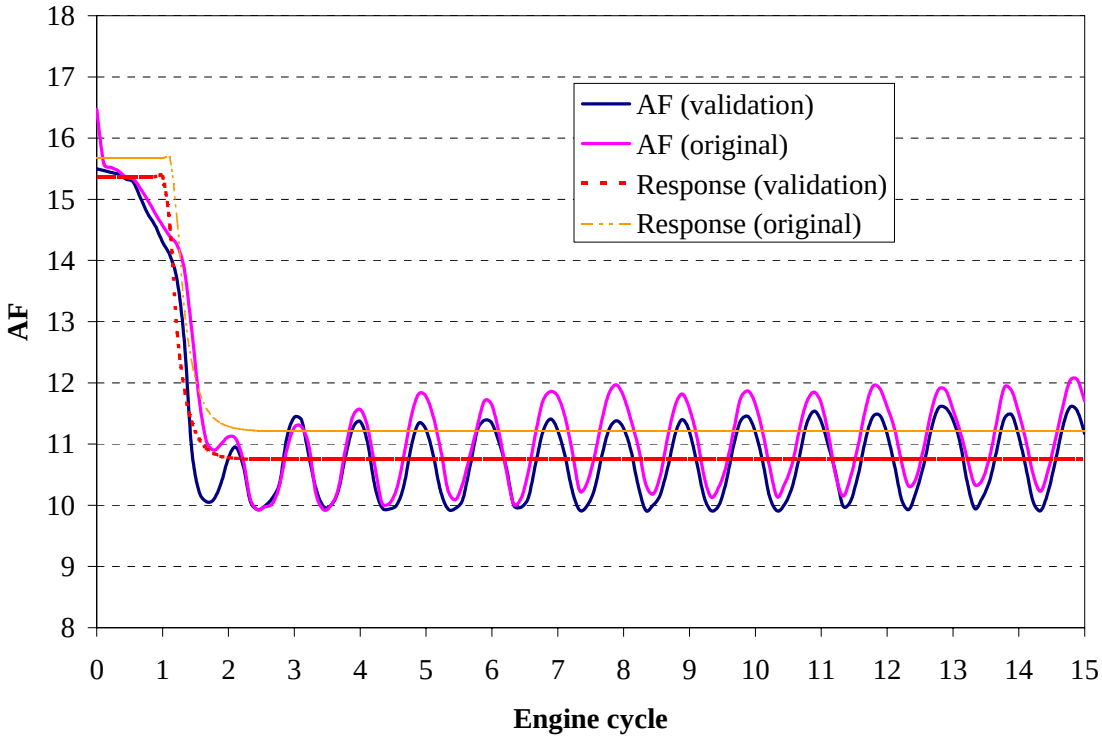

Figure 4.10 System repeatability validation tests: original UEGO sensor response time curve fit, injection timing TDC intake stroke.

The same method of determining τ_1 and τ_2 were applied to the validation tests, and the values calculated. The results of determining τ_1 and τ_2 for the validation tests may be seen presented with the values determined in the original tests in Table 4.1.

	TDC intake stroke, Validation run	TDC intake stroke, Original run	% Difference
τ_1	0.55	0.61	11.0
τ_2	0.18	0.20	7.8

Table 4.1 Validation tests τ_1 and τ_2 determination.

It was found that the validation values for τ_1 and τ_2 deviated approximately 11% and 8%, respectively, from the original runs. Slight deviations in τ_2 are attributed to the small variation in initial and transient A/F ratio between the runs caused by a variation in fuel pressure. Since the pressure regulator was hand adjusted with an analogue gage with an accuracy of +/- 6.9 kPa, slight variations occurred. Variations in fuel pressure affect the engine A/F ratio, which in turn change oxygen gas concentration in the exhaust stream. The slight variation in A/F ratio may be seen in Figure 4.10. This affects the sensor response time due to a limited mass transfer potential across the ceramic substrate. Since the validation run is slightly richer than the original run, there is a greater potential across the substrate. However, these deviations were minor and repeatability of the system was deemed sufficient.

4.3.3 Load Effect On UEGO Sensor Response

To further characterize UEGO sensor response times, the effect of engine load on sensor response time was investigated. The tests consisted of step-fueled transients under various load conditions. Three loads were investigated: 55%, 75%, and 100%. For 55% load, the initial fuel injection duration was set to 2.32 ms and the transient fuel injection duration was set to 3.02 ms. For 75% load, initial fuel injection duration was set to 2.51 ms and transient fuel injection duration was set to 3.50 ms. For 100% load, initial fuel

injection duration was set to 2.85 ms and transient fuel injection duration was set to 4.65 ms. Fuel injection timing was set to 180 BTDC intake for all tests. Since earlier tests showed injection timing to have little effect on transients, this timing was selected arbitrarily. The τ_1 and τ_2 results may be seen in Figure 4.11.

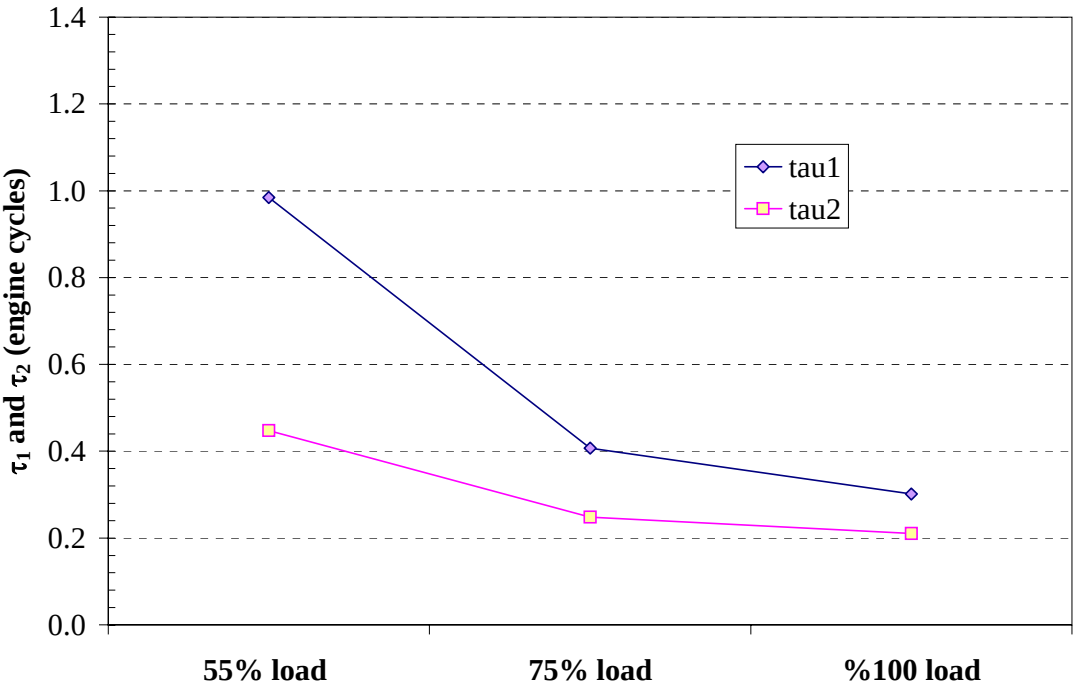

Figure 4.11 Load effect on UEGO sensor response time.

From Figure 4.11 it may be seen that τ_1 ranges from approximately 0.3 to 1.0 engine cycles and that τ_2 ranges from approximately 0.3 to 0.5 engine cycles. The increase in τ_1 and τ_2 for the 55% and 75% load cases may be attributable to the low exhaust temperatures. As the load decreases, the exhaust temperatures are reduced significantly. Varied temperature has been shown to affect O_2 sensor response output voltage [12].

4.3.4 Excursion Magnitude Effect On UEGO Sensor Response

Since the UEGO sensor output voltage is related to the concentration potential between exhaust stream and ambient oxygen, a step fueled transient test was conducted in which the relative fuel perturbation was reduced. This was done to determine if sensor response was sensitive to the magnitude of A/F excursion. The test consisted of step fuel perturbations from approximately 15.0:1 to 13.0:1 (most other tests contained excursions ranging from 15.5:1 to 11.0:1). Initial fuel injection duration was set to 2.88 ms and transient duration set to 3.54 ms. Fuel injection timing was set to 180^{o} BTDC. The results of the response curve may be seen in Figure 4.12.

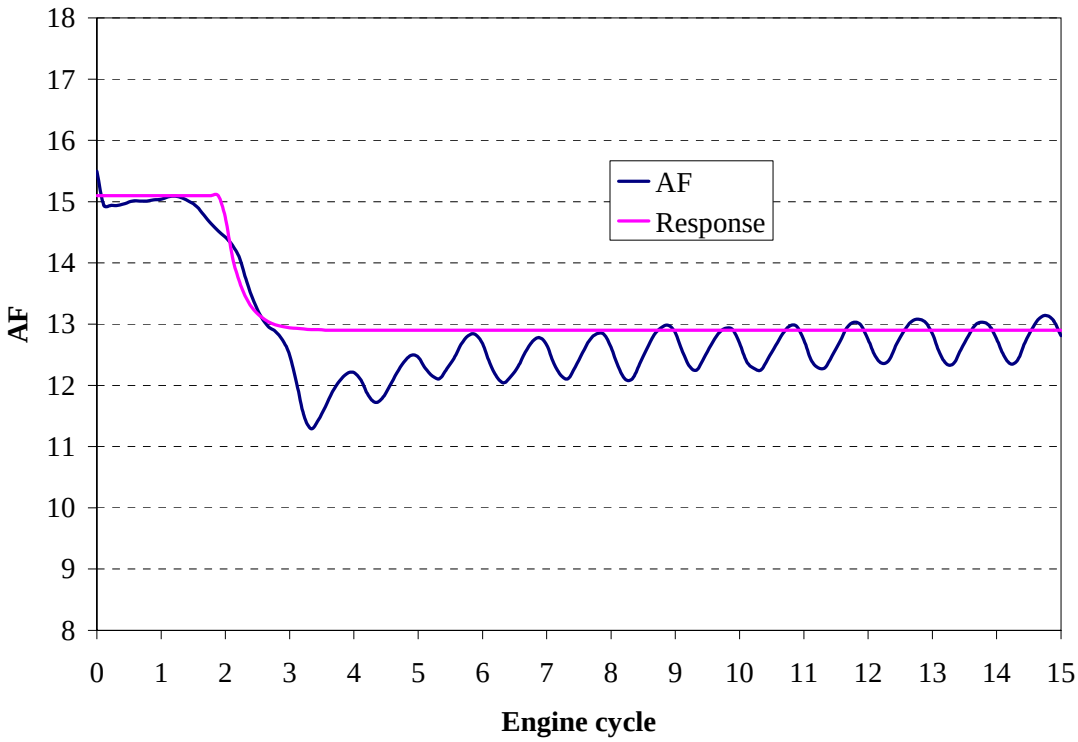

Figure 4.12 Slight A/F excursion modeled sensor response.

From these results, the values for τ_1 and τ_2 were determined to be 1.19 and 0.26 engine cycles, respectively. The value for τ_1 is elevated from the altered injection timing and load tests conducted earlier, but the magnitude for τ_2 is approximately the same.

4.3.5 Low-High Transient A/F Effect On UEGO Sensor Response

The last effect investigated on UEGO sensor response time was the direction of the A/F fueling excursion. This was investigated to determine if UEGO transport across the sensor ceramic substrate from an opposite concentration potential has a significant effect on response. A step-fueled transient from a rich steady state operating condition to a lean operating condition was conducted. The initial fuel injection pulse width was set to 3.85 ms, and the transient injector pulse width 2.73 ms. Fuel injection timing was set to 180 degrees BTDC intake. The sensor response is shown in Figure 4.13.

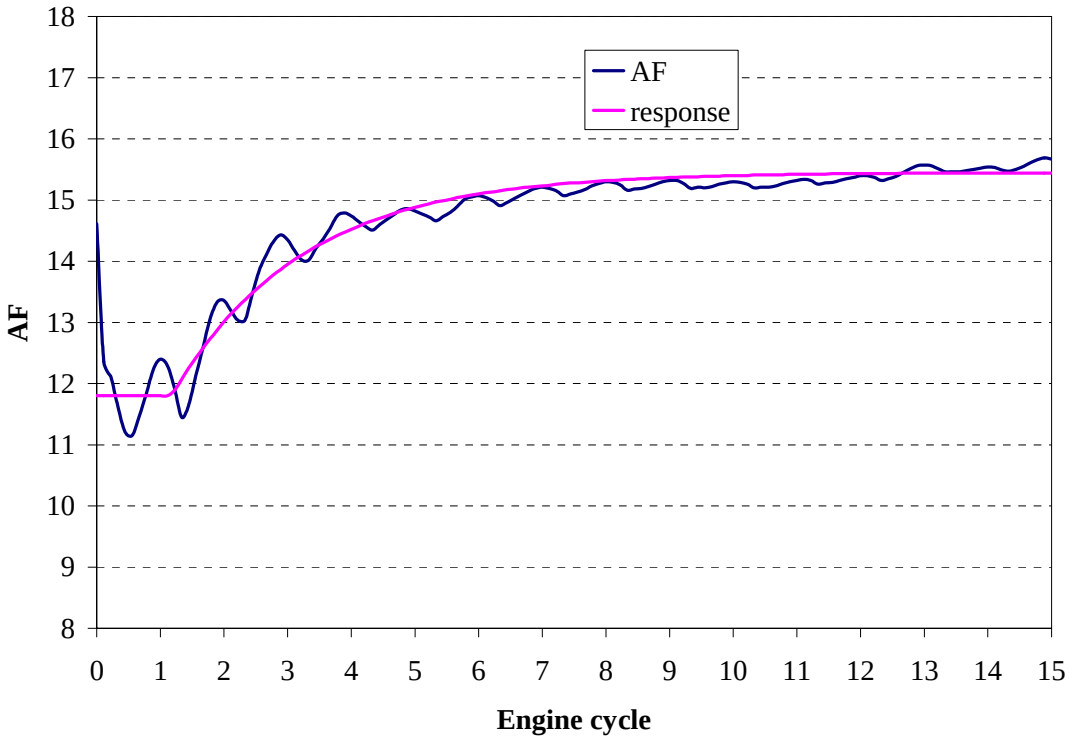

Figure 4.13 Low to high A/F excursion modeled sensor response.

From Figure 4.13, τ_1 and τ_2 were determined to be 0.40 and 2.06 engine cycles, respectively. The value for τ_1 is approximately the same value found in other tests.

However, τ_2 differs significantly, requiring approximately 2 engine cycles for the sensor to respond to the step perturbation as opposed to the 0.3 engine cycles determined earlier.

Typical UEGO sensor response on the lean side has been shown to have the following sensor output dependencies [12]

$$I_p = \frac{4FDS}{RTL}\left(P_{O\,exh} - P_{O\,cav}\right) \tag{4.1}$$

where I_p is the sensor output, F is the Faraday constant, D is the diffusion coefficient of O_2, R is the gas law constant, T is the temperature, S is the cross section of gas diffusion path, L is the length of the diffusion path, P_{Oexh} is the exhaust stream partial pressure and P_{Ocav} is the detecting cavity partial pressure. However, if the exhaust stream is rich, the sensor response is dependent upon the diffusion coefficients of H_2, CO, and C_xH_y across the substrate, which are temperature dependent. This relationship is given by [12]

$$I_p = \frac{2FS}{RTL}\left(D_{H\,2}P_{H\,2\,exh} + D_{CO}P_{CO\,exh} + D_{CxHy}P_{CxHy\,exh}\right) \tag{4.2}$$

where D_{H2} is the hydrogen diffusion coefficient, P_{H2exh} is the exhaust stream hydrogen partial pressure, D_{CO} is the carbon monoxide diffusion coefficient, P_{COexh} is the exhaust stream carbon monoxide partial pressure, D_{CxHy} is the hydrocarbon diffusion coefficient, and $P_{CxHyexh}$ is the exhaust stream hydrocarbon partial pressure. Therefore, the sensor output depends upon different diffusion coefficients when detecting lean or rich exhaust compositions. In turn these diffusion coefficients are temperature dependent. It is likely

that the difference in the rate of the sensor output as a function of the direction of the change in A/F is due to the difference in diffusion coefficients and their unique temperature dependencies.

4.4 Summary

After completing various propane fueled transient tests, the UEGO sensor response time was determined. At a given speed and load transition, the *minimum* response of τ_1 and τ_2 defines the sensor response time. Any response for a given set of engine conditions above the minimum response of τ_1 and τ_2 may be associated with propane mixing effects. The results of determining the sensor response time may be seen in Table 4.2.

Load	A/F Transition	τ_1	τ_2
100%	15.5:1 - 11.0:1	0.30	0.21
100%	11.0:1 - 15.5:1	0.41	2.06
100%	15.0:1 - 13.0:1	1.19	0.26
75%	15.5:1 - 11.0:1	0.41	0.25
55%	15.5:1 - 11.0:1	0.98	0.45

Table 4.2 τ_1 and τ_2 response time summary.

It was determined that the sensor responds within approximately one-half of and engine cycle under full load conditions with an lean to rich A/F transient from approximately 15.5:1-11.0:1. The sensor response is approximately five times slower under identical conditions for a rich to lean transient. This response delay is thought to be associated with the change in exhaust stream gas temperature. It was found that the sensor response time increases with decreasing load, and that this effect is also

considered to be associated with temperature. The sensor response time is slower for small magnitude excursions, responding within 1.5 engine cycles.

5

GASOLINE-FUELED STEP TRANSIENTS

5.1 Introduction

By matching testing conditions with liquid indolene to those for the propane tests presented in Chapter 4, step fueling transient tests were performed and compared to the propane case in which no film exists. Tests consisted of running the engine steady state and impulsively changing fuel injection mass flow for a specific number of engine cycles. The effects of fuel injection timing and engine load were investigated.

5.2 Indolene-Fueled Step Transient Testing Conditions

All indolene-fueled transient tests consisted of running the engine at full load and impulsively varying the fuel injection pulse width. All tests were conducted with the fuel pressure set to 345 kPa. Steady state operation was ensured by running the engine approximately one half hour prior to any transient tests. After that time, engine oil temperature reached a steady value ranging from 112 to 115 ^{o}C, depending upon engine load. Engine speed was set at 3060 RPM. Exhaust pressure was set at a constant 1.87 mm Hg vacuum. At the conclusion of a transient test, the fuel injection program was reset, at which point the engine momentarily ceased firing (under 5 seconds). After resetting the fuel injection program, the engine was allowed to stabilize for 1850 engine cycles prior to collecting the next set of data to again ensure steady state operation. Five transient tests were averaged together for each parameter change since it was determined that five runs are statistically sufficient (section 4.1). After collecting the transient data,

response times for the transient tests were determined in the same manner as outlined in section 4.3.

5.3 Fuel Injection Timing Effect On Indolene Fueled Transients

The effects of fuel injection timing on liquid-fueled transients were investigated. By injecting early, fuel has longer contact time with the intake port surface allowing for more potential fuel vaporization. A competing effect with the intake port contact time is the increasing shear stress on the fuel when injected during the intake stroke. If fuel is injected prior to the opening of the intake valve, the lack of airflow does not assist in atomizing the fuel. As the injection occurs while the intake valve is open, the increasing airflow assists in atomizing the fuel. By varying the injection timing, insight into these competing factors can be determined.

Three fuel injection timings were selected for these tests: 180 BTDC intake stroke, TDC intake stroke, and 90 ATDC intake stroke. This range of fuel injection timings was selected to investigate the potential effects of open and closed intake valve injection timing on A/F excurions. Initial fuel injection duration was set to 3.6 ms, and the transient duration set to 5.6 ms. Results of the modeled response times for the various injection timings may be seen in Figure 5.1.

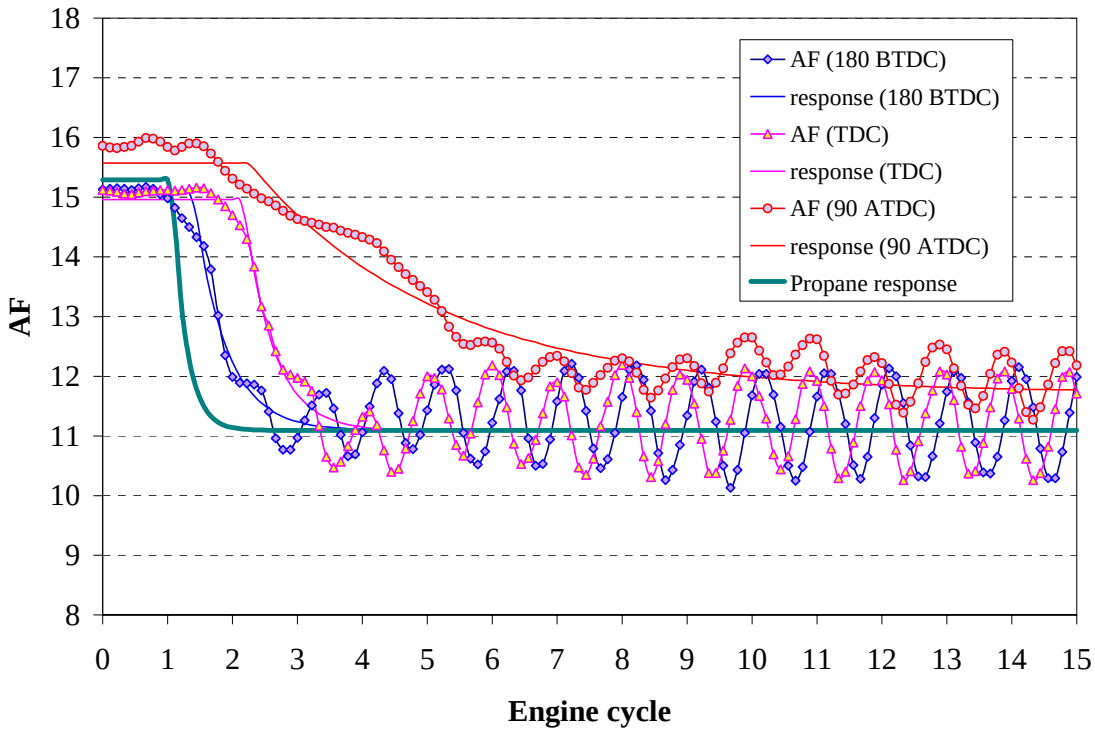

Figure 5.1 Indolene fueled transient response times for varied fuel injection timing, 5 tests averaged.

From Figure 5.1 it may be seen that the UEGO sensor overall response time increases as injection timing is delayed. In comparing the response times to that of propane (also shown in Figure 5.1), one finds that indolene fueled transient response for all injection timings is slightly slower. This small increase for the 180° BTDC and TDC injection timings relative to propane is suggestive of small fuel film contributions during the step-fueling transients. The actual values of τ_1 and τ_2 for indolene under the various fuel injection timings may be seen in Figure 5.2.

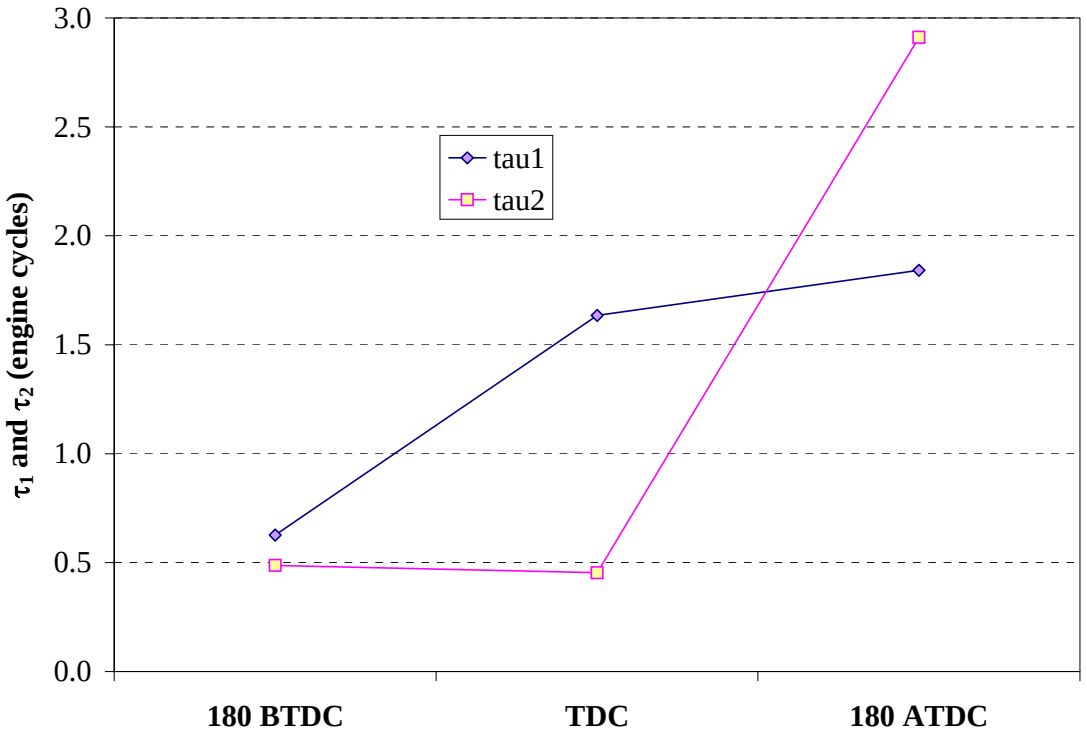

Figure 5.2 UEGO sensor τ_1 and τ_2 time determination: indolene fueled step transient tests, varied fuel injection timing, 100% load, 5 tests averaged.

Figure 5.2 shows that the engine A/F responds within approximately one engine cycle for 180^o BTDC, but requires over four engine cycles for injection timing set to 90^o ATDC. The TDC injection timing requires approximately two engine cycles. In section 4.4 it was determined that the minimum sensor response under similar conditions was approximately half of an engine cycle. Thus it is found that there is an increase in sensor response time for liquid fueling. This increased delay is suggestive of fuel film formation in the intake port, which may act as a reservoir for the fuel during the transient fueling event. The slight increase in sensor response times for the other injection times does not indicate significant fuel film effects during the step fueling change.

The UEGO sensor response delay increases as the injection timing is delayed, the longest delay time occurring close to when the piston is traveling at maximum velocity

(90^{o}ATDC injection timing). At maximum piston velocity, the air stream would impart greater shear stress to the fuel assisting in fuel atomization. Since late injection does not allow the fuel to contact port walls as long and vaporize, this suggests that heat transfer to a fuel film on the intake port may be the dominant factor over the atomizing effects of the incoming intake charge. At 180^{o} BTDC the sensor response is delayed four-tenths of an engine cycle from the similar propane transient tests. This slight deviation suggests that the fuel is fairly well vaporized due to intake port wall temperature and that response is not overly compromised. During late injection (90^{o} ATDC) sensor response is approximately seven times slower than propane step transients under similar conditions. This may be attributed to the lack of time in which the fuel film has to contact and vaporize along the port wall.

A second factor affecting the airstream's ability to vaporize the fuel is fuel impingement. The siphon-tube injection system injects fuel out of the stock venturi location in much the same manner as the carburetor, although for these tests the pressure of injection is substantially greater than that of the stock carburetor. The higher injection pressure might assist in forming a fuel film on the top-side of the carburetor venturi.

5.3 Engine Load Effect On Indolene Fueled Transients

By varying engine load for indolene fueled transients, the effects of fuel impingement on the throttle plate, and to an extent intake port temperature, were investigated. Three loads were selected for these tests: 55%, 75% and 100% load. These loads were obtained by altering the throttle position and changing the initial and transient injection pulse width in the siphon tube injection system. For the 55% load case, initial and transient pulse

widths were set to 2.68 and 3.93 ms, for the 75% load case, initial and transient pulse widths were set to 3.12 and 4.72 ms, and for the 100% load case, initial and transient pulse widths were set to 3.6 and 5.6 ms, respectively. These fueling durations resulted in similar initial and transient equivalence ratios. Fuel injection timing for all tests were set to 90^{o} ATDC. This timing was chosen to better represent carburetor venturi behavior by metering the fuel during the intake stroke only. It was shown in section 5.2.1 that early introduction of the fuel results in reduced response times most likely due to vaporization of the fuel on the intake port caused by high intake port wall temperature.

Since the throttle plate is located downstream of the siphon-tube, various plate angles may play a significant role on fueling transients due to fuel impingement. Also the engine oil temperature is, on an average, 16^{o}C cooler at 55% load than at 100% load. This decrease in temperature may also have a competing effect on the intake port fuel film vaporization. The results for modeling the response times of the three various loads may be seen in Figure 5.3.

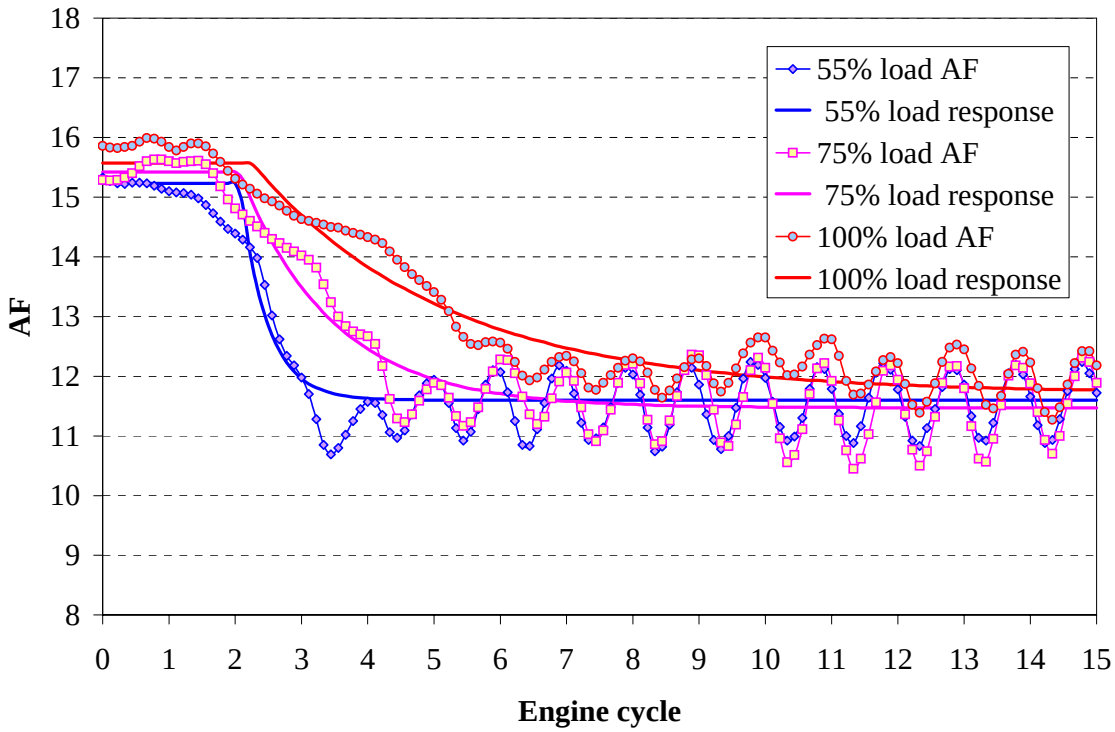

Figure 5.3 Indolene fueled transient response times for various loads, 5 tests averaged.

From Figure 5.3 it may be seen that the UEGO sensor overall response time increases as the engine load increases. The actual values for determining τ_1 and τ_2 may be seen in Figure 5.4.

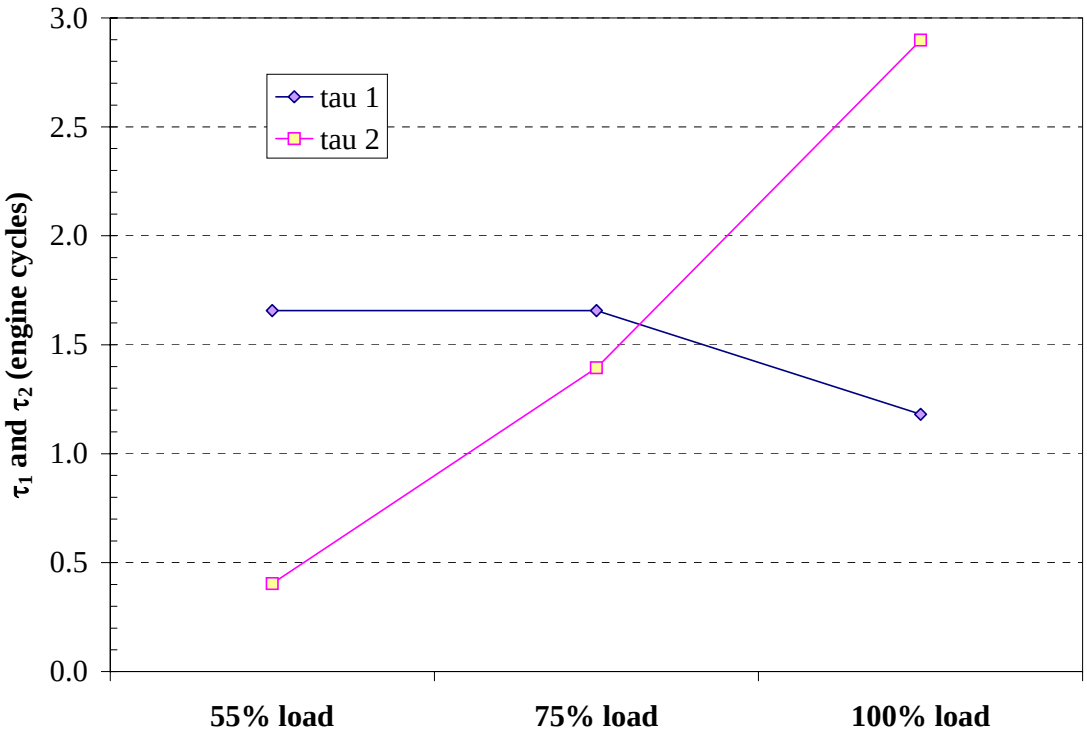

Figure 5.4 UEGO sensor τ_1 and τ_2 time determination: indolene fueled step transient tests, varied engine load, 90° ATDC injection timing, 5 tests averaged.

From Figure 5.4 it can be seen that the overall sensor response to an indolene-fueled transient is approximately two engine cycles at 55% load to over four engine cycles at 100% load. In section 4.4 it was determined that propane-fueled transients under similar load conditions responds within 0.8 engine cycles, with the 55% case being slightly elevated. This increase in delay time is also suggestive of the presence of fuel films in the intake port.

Deviation in τ_1 and τ_2 for the various loads may again be due to the variation in exhaust stream temperature. At lower loads the exhaust temperature is lower than for higher load cases, and it is thought that the exhaust temperature affects the sensor diffusion coefficients thus resulting in altered response times. This temperature dependency was discussed in section 4.3.5.

5.3 Summary

After conducting a series of indolene-fueled step transient tests, comparison of the results found for propane-fueled tests indicated the presence of fuel films. This was determined by the delayed UEGO sensor response relative to the propane tests presented in Chapter 4. However, the relative difference was not too significant; approximately twice the response time for indolene was found compared to propane. This suggests that impulsive fuel transients do not disturb the fuel film to a great extent. The sensor response time for 90^{o} ATDC injection timing was the slowest. Since late fuel injection does not allow the fuel to contact the relatively hot intake port wall for as long as early injection, this suggests that heat transfer to the fuel film may be a dominant effect in fuel film vaporization.

6

GASOLINE & PROPANE FUELED STEP THROTTLE TRANSIENTS

6.1 Introduction

In chapter five, behavior indicative of the presence of an intake port fuel film was found. Changing the fuel mass flow rate under fixed throttle conditions disturbed these fuel films and behavior indicative of their presence was observed. Another method of introducing a perturbation is by changing the engine air mass flow rate while holding the fueling rate constant. By holding the fueling rate constant and impulsively changing the fuel mass flow rate via the throttle plate, fuel flow and air flow effects may be decoupled. Insight into the behavior of the air flow and its effects on intake port fuel film may be determined by the decoupling of these effects

A series of transient tests were conducted in which the fueling rate was held constant while the throttle went through step perturbations. Testing conditions were matched using both indolene and propane in order to decouple fuel film effects from combustion and sensor effects.

6.2 Throttle Transient Testing Conditions

All throttle transient tests consisted of running the engine under constant fuel mass flow rate and step changing the throttle position. These tests consisted of impulsively changing the throttle from either 100% load to 55% load (high-low transient), or impulsively changing the throttle from 55% to 100% load (low-high transient). The

throttle transient took 120 ms, or approximately 3 full engine cycles. Two fuels were investigated: propane and indolene. For all propane fueled tests, fuel pressure set to 620 kPa (gage), and fuel injection duration was set to 2.9 ms. For indolene fueled tests, two fuel injection pressures were selected: 13.8 kPa and 345 kPa (gage). Both low and high pressure fuel injection were investigated using the siphon-tube fuel injection system to determine whether or not high pressure, short duration fuel injection would have an effect on transient response as opposed to low pressure, long duration fuel injection. For high pressure indolene injection, fuel injection duration was set to 3.6 ms. For low pressure, fuel injection duration was 16 ms. Fuel injection timing for both propane and indolene tests was set to TDC of the intake stroke. Since carburetors release fuel during downward motion of the piston, this timing was chosen to better mimic carburetor behavior.

Steady state operation was ensured by running the engine approximately one half hour prior to any transient tests. After that time, engine oil temperature reached a steady value ranging from 98 to 115 ^{o}C, depending upon the load. Engine speed was set at 3060 RPM. Exhaust pressure was set at a constant 1.87 mm Hg vacuum. Full throttle motion required approximately 4 engine cycles. Five transient tests were averaged together for each parameter change.

6.3 Propane-Fueled Step Throttle Transients

Two transient effects were investigated for propane-fueled transients. The effects investigated were both a high-low load transients and low-high load transients. The high-

low transient consisted of starting at 100% load and step changing to 55% load. The low-high transient consisted of starting at 55% load and step changing to 100% load.

6.5 Propane-Fueled High/Low Throttle Transient Results

Results of the five run ensemble averaged propane-fueled high-low step throttle transients may be seen in Figure 6.1.

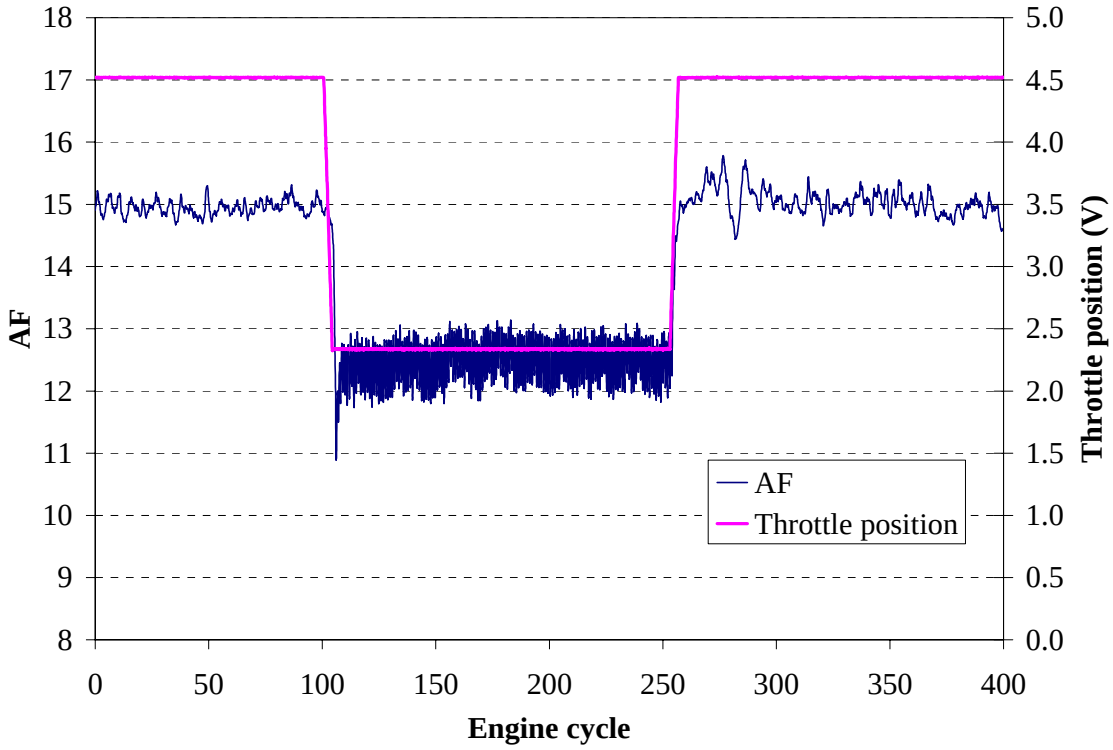

Figure 6.1 Propane fueled high/low throttle transient results, 5 tests averaged.

In Figure 6.1 it may be seen that a rich excursion occurs following the initial closing of the throttle. This rich excursion lasts for approximately 2 cycles before attaining the steady state 55% load A/F ratio. Since the gaseous fuel cannot form a fuel film in the intake port, this effect is a result of either air flow dynamics, or sensor effects. During the throttle opening it may be seen that there is no visible excursion present. This

behavior would be expected since the gaseous fuel does not allow for fuel films that effect transient response.

6.5 Propane-Fueled Low/High Throttle Transient Results

Results to the five run ensemble averaged propane-fueled low-high step throttle transients may be seen in Figure 6.2.

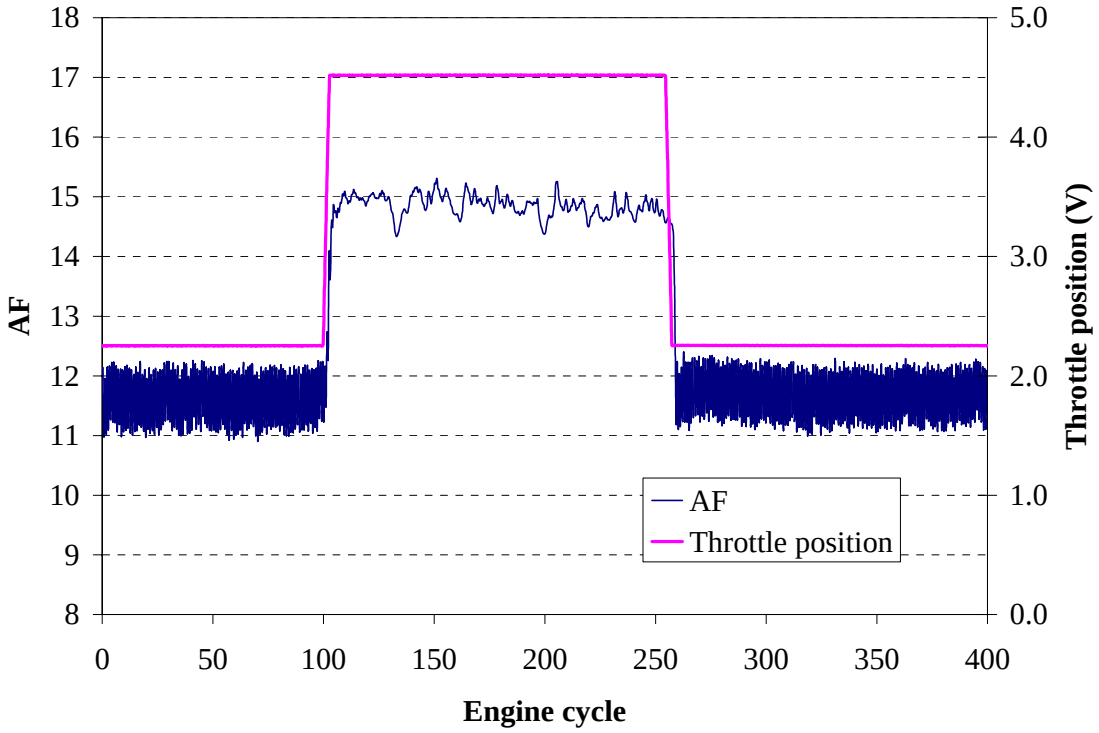

Figure 6.2 Propane fueled low/high throttle transient results, 5 tests averaged.

From Figure 6.2 it may be seen that no rich or lean excursion occurs for either the opening or closing of the throttle plate during the transient, as was seen during the 100th engine cycle in Figure 6.1. Since both transient tests differed only in the change in direction of the load transient, results suggest that the overshoot in Figure 6.1 is a sensor issue rather than mixing effect.

6.4 Indolene-Fueled Step Throttle Transients

High and low pressure siphon-tube fuel injection tests were conducted under similar high-low and low-high throttle transients as the propane data presented in section 6.3. Since the siphon-tube fuel injection system uses a fuel injector to meter fuel, low pressure long duration fuel metering during the intake stroke was investigated to better mimic carburetor fuel metering conditions. This was done to investigate the potential effects that fuel metering has on step throttle transients. Throttle transients under reversed load directions were conducted to determine if the direction of the transient would have various effects on fuel films.

6.5 High Injection Pressure Throttle Transient Results

Results of the five run ensemble-averaged indolene-fueled high-pressure siphon-tube injection high/low step throttle transient may be seen in Figures 6.3. From Figure 6.3 it may be seen that a rich A/F excursion occurs at the onset of the closing of the throttle from 100 to 55% load. This overly rich excursion lasts for approximately 20 engine cycles before reaching a steady value. The duration of the excursion is much greater than that seen in Figure 6.1. This indicates that the excursion is not caused by sensor effects. A lean excursion occurs during the opening of the throttle from 55 to 100% load, and lasts for approximately 50 engine cycles before reaching a steady A/F ratio. No lean excursion was present for the propane transients displayed in Figures 6.1 and 6.2.

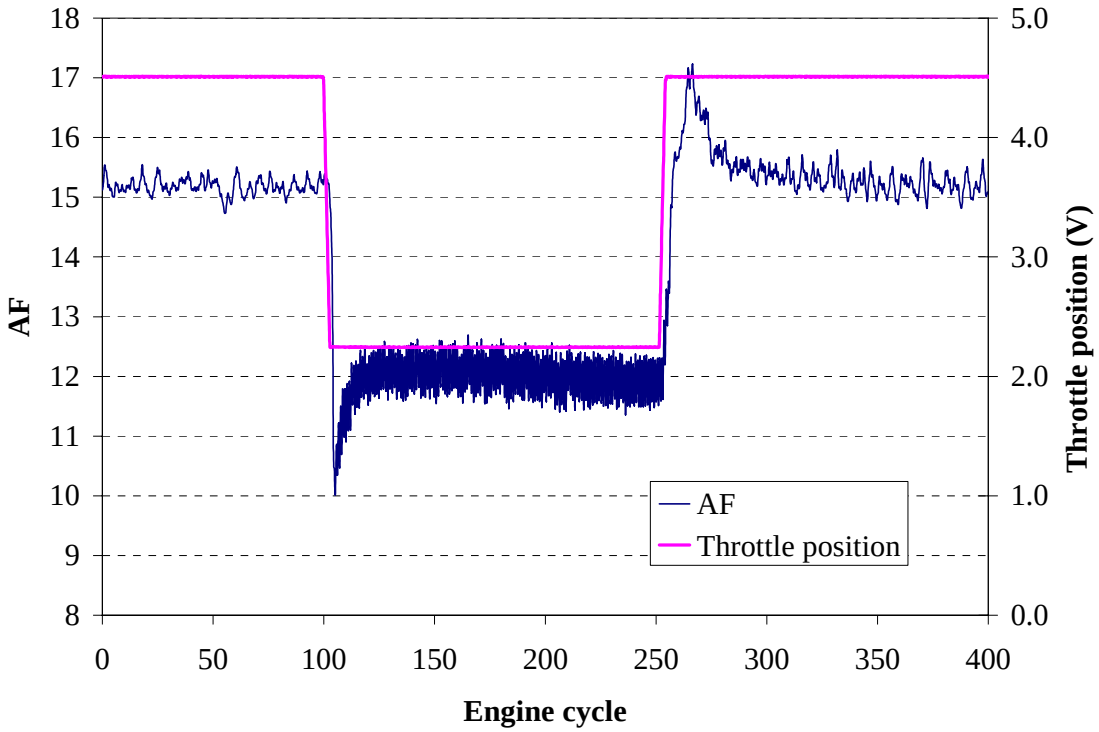

Figure 6.3 Indolene fueled high/low-high pressure throttle transient results, 5 tests averaged.

The presence of rich and lean A/F excursions is indicative of the presence of fuel films in the intake manifold. The intake port fuel film mass decreases as the engine goes from high to low load. This is deduced from the initially overly rich condition during throttle closure. As the throttle opens, the overly lean conditions denote an insufficient fuel film mass, later settling to a steady state value. This is indicative of an increase in overall film mass [22].

Figure 6.4 displays the reverse load transient presented in Figure 6.3. It may be seen in Figure 6.4 that an overly lean condition exists during the throttle opening. This overly lean condition lasts approximately 50 engine cycles, as was the case with the high-low transient. It may also be seen in Figure 6.4 that an overly rich excursion occurs

during throttle closure. This overly rich excursion lasts approximately 15 engine cycles before reaching the steady state A/F value.

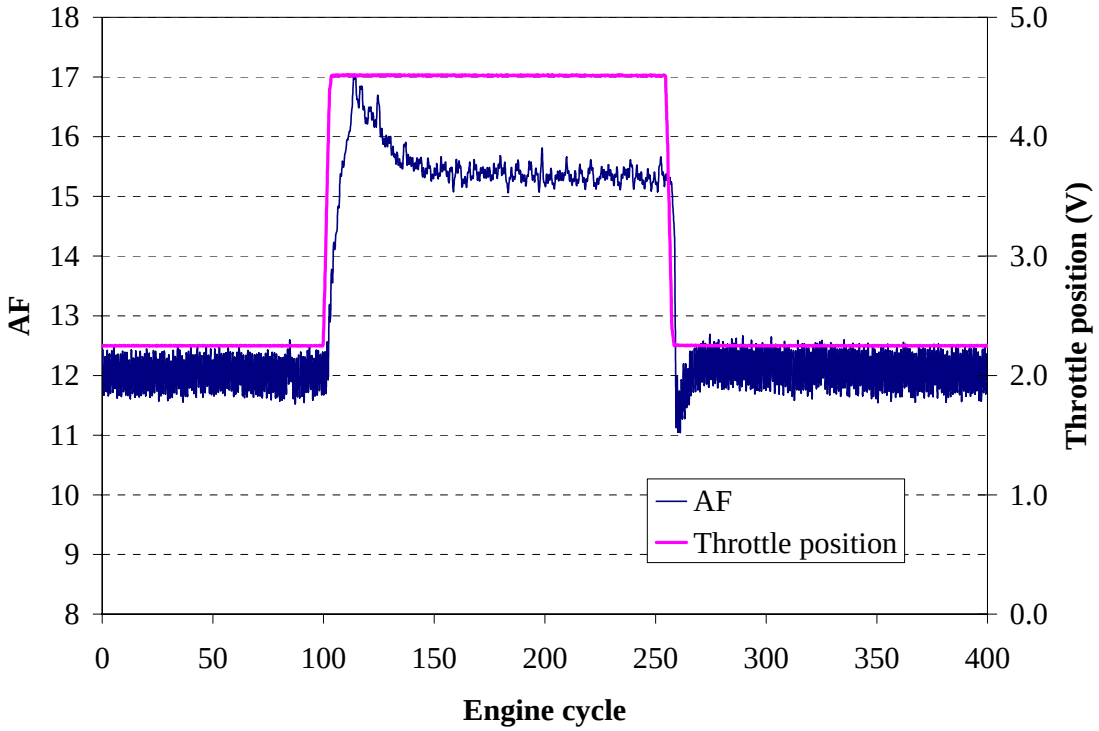

Figure 6.4 Indolene fueled low/high-high pressure throttle transient results, 5 tests averaged.

In comparing Figures 6.3 and 6.4, it may be seen that lean excursions occur when the throttle opens from low to high load conditions, and that rich excursions occur when the throttle closes from full to partial load. This behavior is indicative of a delay in the response of the fuel delivered to the engine during the transient due to the fuel film. As the throttle opens, the air responds faster to the transient and more air is induced into the cylinder. Two effects of the increased air flow are imparted on the fuel film: increased mass transfer potential and increased shear stress on the fuel. Increased mass transfer potential would assist in vaporizing the fuel, and one might find a rich excursion following throttle opening. However, directly following throttle opening, one finds a

lean excursion. Modeling of fuel films has found that the increased shear stress imparted on the fuel film takes time before the film is drawn into the cylinder [13]. Two dynamics waves travel through the film; a transverse wave orthogonal to the port and a longitudinal wave along the port imparting shear stress. The longitudinal wave has been noted to take more than a second to travel the length of a manifold. This delay causes a lean excursion that decays as the overall fuel film mass reduces due to the increased intake charge shear stress. As the throttle closes, less air is introduced causing the rich excursion. The reduction in air flow allows the film mass to increase resulting in steady operation After a certain number of engine cycles. This behavior has been noted in various other transient studies [12, 17], and time constants for the fuel film have been found to be on the order of one minute [11]. In this study, it was found that the time constants are significantly smaller relative to a minute (approximately 2 seconds). This is most likely due to the increased intake port temperature of the air-cooled engine. Although the film depletion time constant is much smaller than that found in the above noted studies, it might be expected that the fuel film would be eliminated within few cycles, especially in this test case in which port wall temperatures are relatively high [7].

6.5 LOW INJECTION PRESSURE THROTTLE TRANSIENTS

Results to the five run ensemble averaged low-pressure indolene-fueled siphon-tube injection for both high/low and low/high step throttle transients may be seen in Figures 6.5 and 6.6. By comparing Figures 6.3/6.4 and 6.5/6.6 it may be seen that the relative A/F signal is less stable during the low pressure injection transient tests. The steady state A/F ratio has considerably more variability in the low pressure case. The relative A/F

stability is an indication of cycle-to-cycle stability. Therefore, this behavior is indicative of better A/F mixture preparation for the high-pressure fuel injection case. Although the siphon-tube injector is directly connected to the inlet of venturi tube, the high pressure short duration injection introduces the fuel with significantly more energy than the low pressure case. The increased pressure injection may assist in atomizing a portion of the fuel at the exit of the venturi. Also, the high pressure, short duration injection event introduces the fuel approximately 13 ms earlier than the low-pressure case, allowing the fuel to reside in the intake port longer allowing for better mixing prior to entering the combustion chamber. This would result in increased combustion stability.

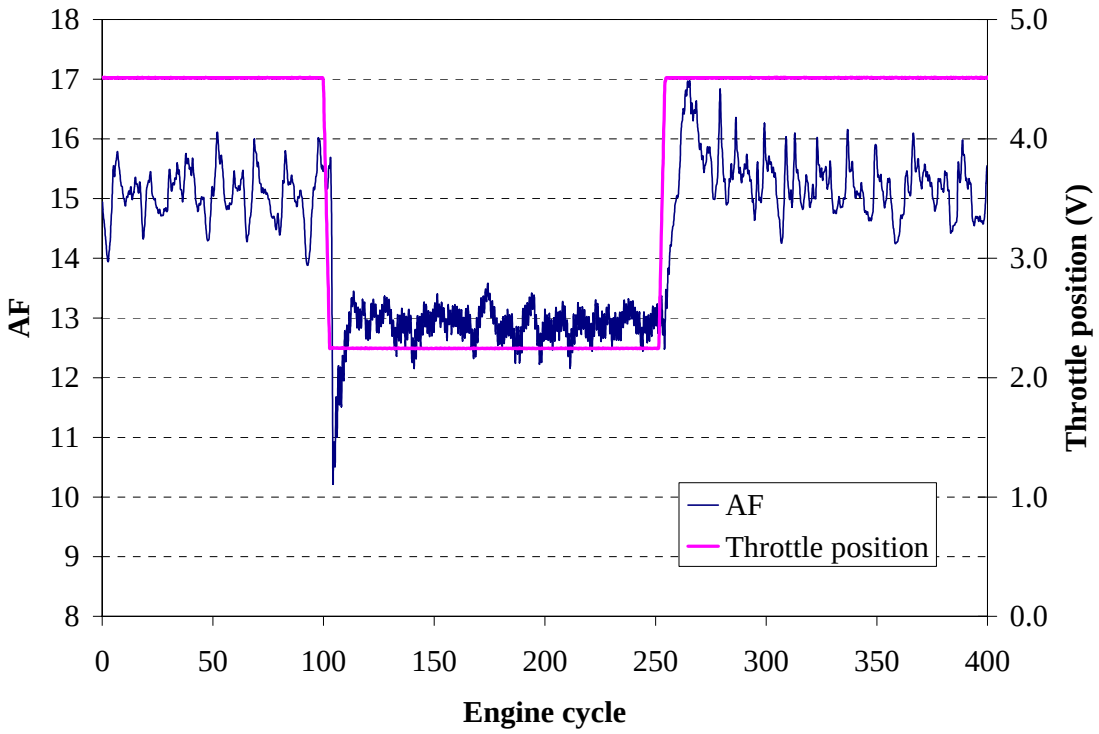

Figure 6.5 Indolene fueled high/low-low pressure throttle transient results, 5 tests averaged.

In Figure 6.5 it may be seen that both an overly rich and overly lean excursion occur during throttle opening and closure. During throttle closure, the rich excursion

lasts approximately 10 engine cycles before settling into a steady state A/F value. During throttle opening, the overly lean excursion lasts approximately 25 engine cycles. The relative duration of the excursions is less than those observed during the high pressure injection transient tests.

In Figure 6.6 an overly lean condition may be seen during throttle opening. This overly lean condition lasts approximately 15 engine cycles.

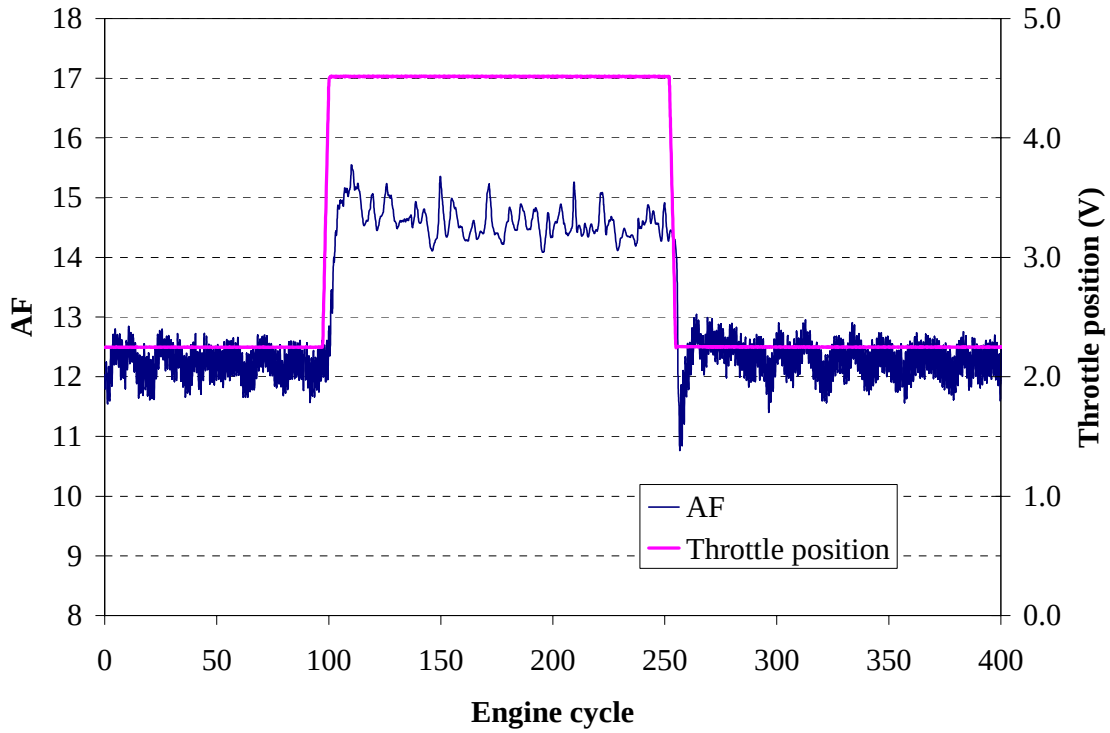

Figure 6.6 Indolene fueled low/high-low pressure throttle transient results, 5 tests averaged.

Further inspection of Figure 6.6, however, does not indicate a drastic rich excursion during throttle closure as was seen in prior results. Under these low-pressure injection conditions, fuel is metered at 13.8 kPa (gage). For the high-pressure cases, fuel is metered at 345 kPa (gage). It is likely that the high-pressure injection case causes a significant portion of the fuel to impinge the relatively cool carburetor body directly

across from the siphon-tube. This would increase the fuel film under high-pressure cases resulting in more predominant excursions during throttle transients.

6.5 Summary

It has been found that low-to-high load change transients result in a lean excursion caused by the increased reaction rate of the intake air. High-to-low load transients result in rich excursions also caused by the increased reaction rate of the intake air. These excursions are substantially greater in magnitude and longer in duration than that found for propane indicating the presence of fuel films. Also, the relative magnitude of excursions is greater than that found for fixed throttle, transient fueling tests conducted in Chapter 5. This indicates that intake air motion plays a significant role in affecting intake port fuel films. The relative instability of the low pressure throttle transient tests is thought to be caused by a lack of time for the fuel to fully mix with the intake air resulting in better homogeneity.

7

CAPACITANCE SENSOR FUEL FILM MEASUREMENTS

7.1 Introduction To Capacitance Film Measurements

The basic premise for capacitance film measurements involves forming a capacitance between a sensor and grounded object separated by a dielectric medium. Typical sensor design involves driving a center electrode by an AC potential, then shielding the electrode from stray capacitance with an insulating shield driven at the same potential as the electrode. By driving the outer sleeve at the same potential, the electric field of the electrode and the sleeve are equivalent, eliminating the capacitance between them. A diagram of a capacitance sensor used for measuring fuel films may be seen in Figure 7.1.

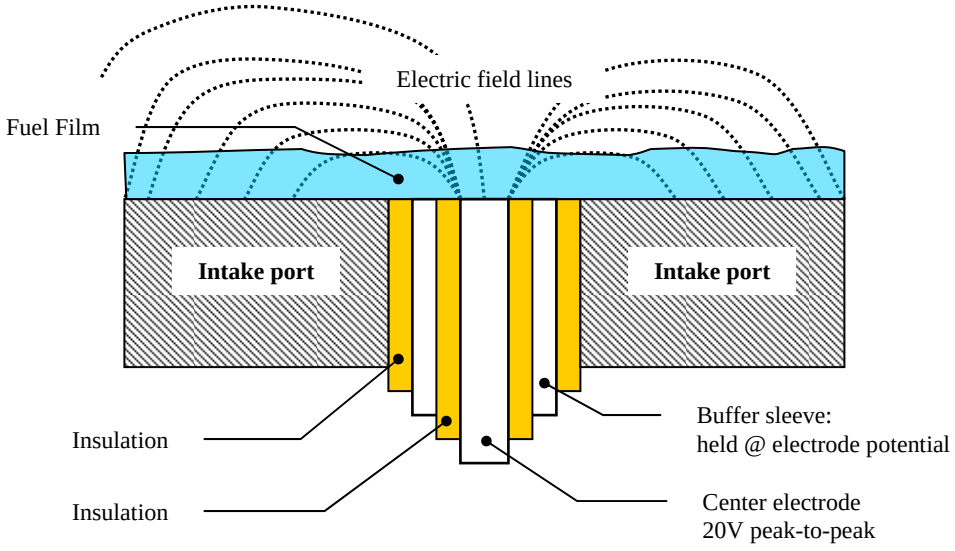

Figure 7.1 Capacitance sensor design diagram.

Although it is more common to align the ground directly opposing the capacitance electrode, stray electric field lines may be used to measure changes in capacitance as well, as is seen in Figure 7.1. By aligning the ground directly across from the electrode and taking advantage of certain geometries the capacitance becomes linear with dielectric and is easier to calibrate. This is done for convenience when applicable. Aligning the ground directly across from the electrode was not possible for this application.

7.2 Capacitance Sensor Design

The design criteria for the capacitance sensors of this study required that they be small, thermally durable, hydrocarbon fuel resistant, and relatively simple to make. Material availability constraints also had to be taken into account (i.e. tube size availability).

For the final sensor design, stainless steel was chosen as the electrode material. Hypodermic stainless steel tubing was chosen as the buffer sleeve in order to minimize the distance between the center electrode and the grounded surface. Polyimide tubing was chosen as the insulation material due to its high temperature resistance, thin walled construction, and electrical resistance properties. High temperature epoxy was chosen to assemble the various components. Table 7.1 lists the final sensor component dimensions.

Sensor Component	Material	Dimension
Center electrode	Stainless steel rod	0.107” dia.
Inner insulation	Polyimide tubing	0.001” thick (ID = 0.107”)
Buffer sleeve	Hypodermic tubing	0.003” thick (ID = 0.112”)
Outer insulation	Polyimide tubing	0.002” thick (ID = 0.116”)

Table 7.1 Capacitance sensor component specifications.

In order to get the outer polyimide shield to fit over the stainless steel buffer sleeve, the sleeve's outer diameter needed to be slightly reduced. This was accomplished by turning the sleeve in a drill press and using 600 grit sandpaper. After making this slight modificaiton, the final sensor diameter was determined to be 0.121". The final capacitance sensor design may be seen in Figure 7.2.

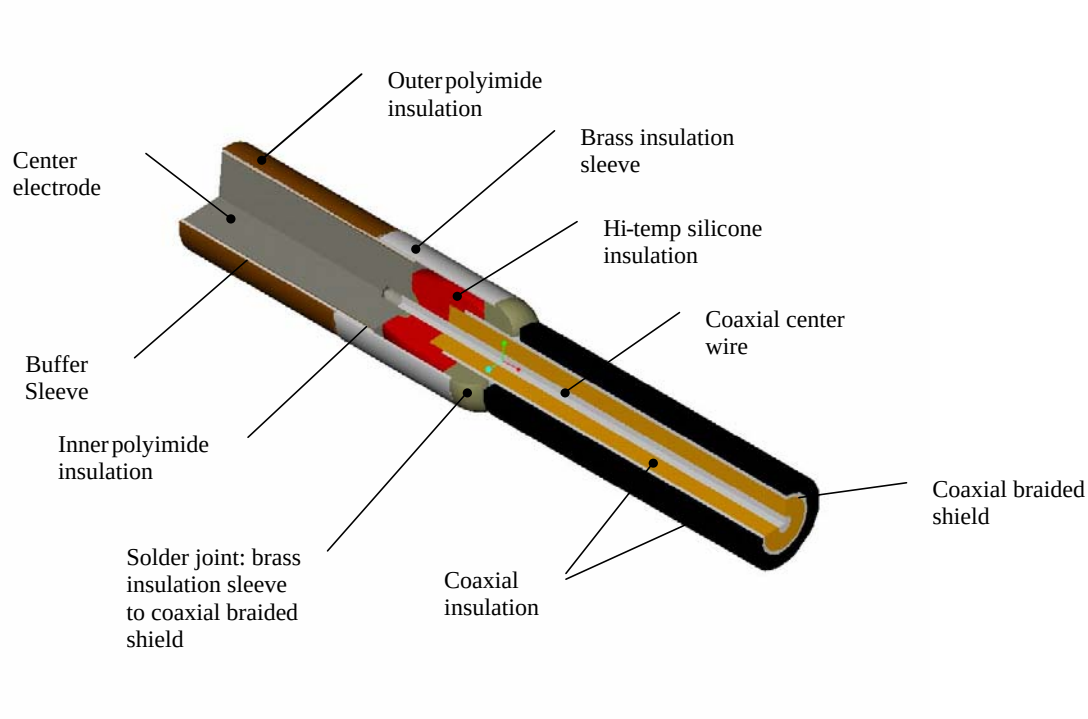

Figure 7.2 Capacitance fuel film sensor design.

7.3 Capacitance Probe Calibration

Two methods of calibrating the capacitance sensors were conducted: gravimetric and directly using a film of known thickness. Although two techniques were used, both were similar in principle; a film of known dielectric was placed over the sensor and the voltage from the capacitance circuit recorded. By knowing the film thickness and voltage, calibration curves were completed using both a liquid and solid film. For the gravimetric

calibration technique, indolene fuel was used for the film. For the thin film calibration technique, thin clear tape was used.

7.3.1 Gravimetric Calibration Technique

The gravimetric technique consisted of manufacturing a precisely machined lightweight aluminum cup (total cup weight was 15.5 grams). The sensor was located at the base of the cup and the dimensions of the cup were precisely known. The cup and the sensor were then placed on a scale capable of measuring weight to within 1 μg. Indolene fuel was placed in the cup and the mass of the fuel measured. Various masses were recorded over time by letting the fuel evaporate. By having knowledge of the density of the fuel, cup dimensions, and weight of the sample measured, the film thickness could be determined. Figure 7.3 displays the cup used to gravimetrically calibrate the sensors.

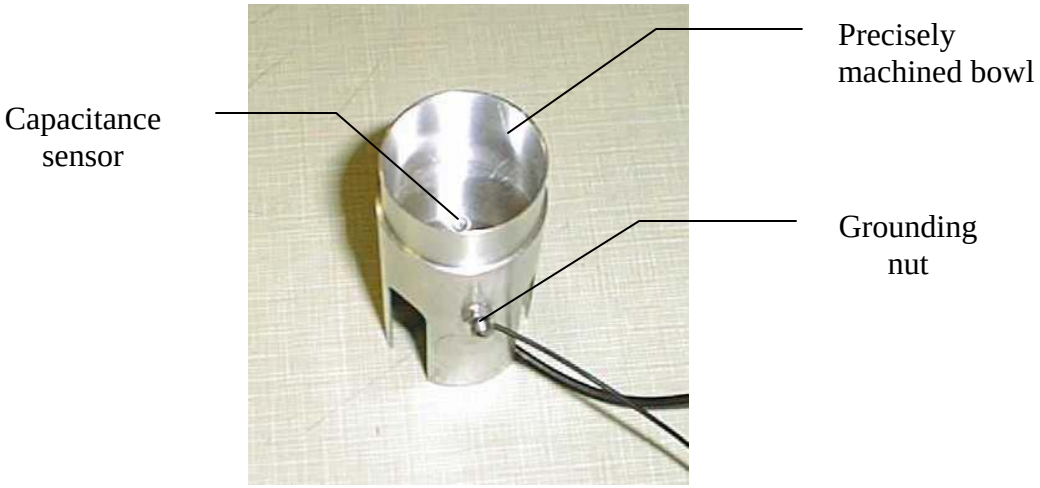

Figure 7.3 Capacitance sensor gravimetric calibration cup.

An example of the calibration curve using this technique may be seen in Figure 7.4.

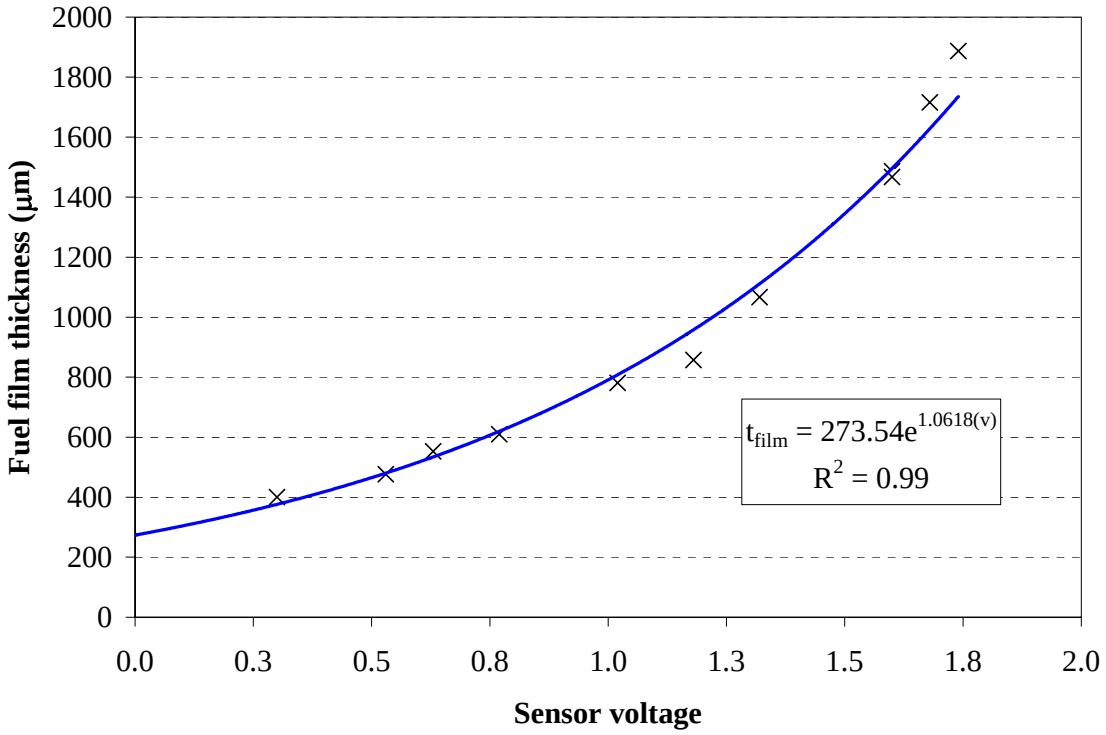

Figure 7.4 Capacitance sensor gravimetric calibration curve.

From Figure 7.4 it may be seen that the calibration curve follows an exponential trend. The calibration curve does not, however, settle to a zero datum as would be expected. This was caused by surface tension effects of the fuel above the sensor in the calibration cup. As the fuel evaporated, a small bead of fuel settled over the sensor and did not form a uniform thin film. Although care was taken in making sure that the sensor rested flush against the base of the cup, the slight cavity around the sensor tip was sufficient in forming a bead. Also, due to capillary action of the fuel film, ideal thin films were not observed over the sensor. This led to variations in readings. It was determined that this technique did not allow for thin film calibration within the range desired. Although this

technique works well for relatively thick films in which surface tension and capillary effects are negligible, a second technique was required.

7.3.2 Thin Film Calibration Technique

The second technique consisted of placing thin strips of tape over the sensor while the sensor was located in the engine intake port. With direct knowledge of the dielectric constant of the tape and its measured thickness, the sensors output voltage could be calibrated (details to the determination of the tape dielectric may be seen in Appendix B-3). This calibration was achieved by using Scotch® brand clear adhesive tape and layering pieces of tape yielding various thickness. Each of the varied tape thickness was located over the sensor and the voltage recorded. The capacitance circuit DC offset was adjusted such that no tape corresponded to 0 V. The results of the tape calibration may be seen in Figure 7.5.

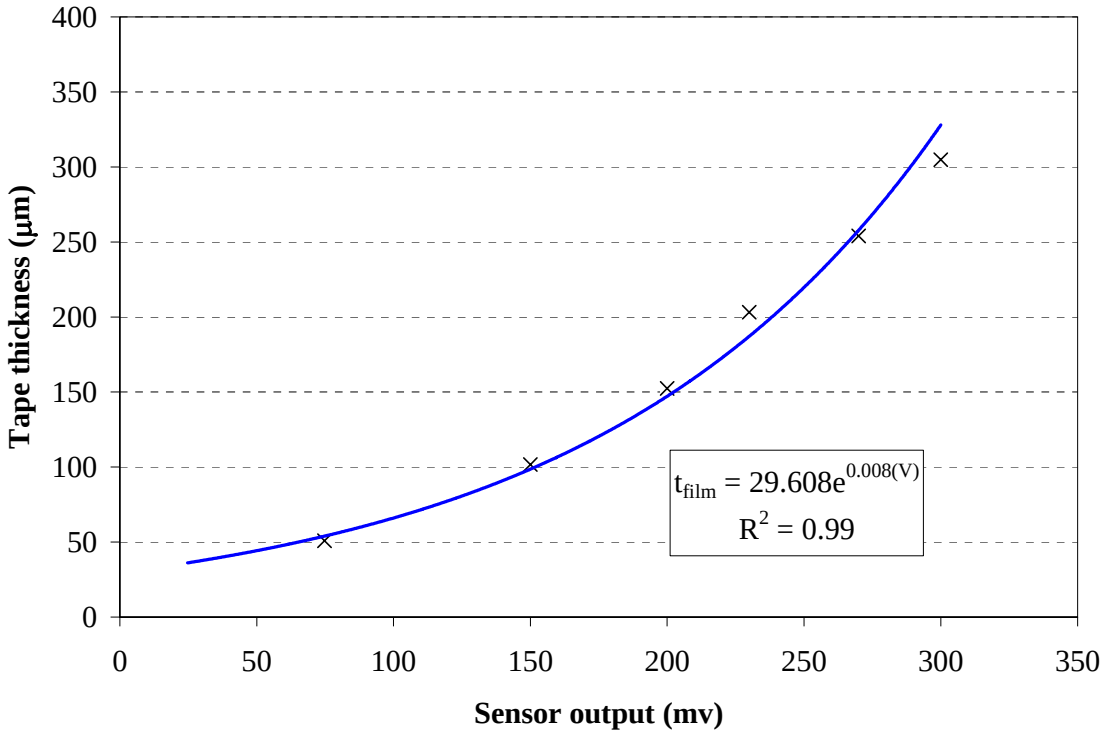

Figure 7.5 Capacitance sensor solid film calibration curve.

Utilizing the tape technique it was also found that an exponential function fit the calibration data relatively well. This technique was shown to measure thinner film thickness to a greater degree of accuracy. In order to directly correlate this technique to the fuel film, the dielectric constant of the tape would have to be equivalent to the fuels. For these tests the dielectric constants were not equivalent (approximately 2 for indolene, and approximately 7 for tape). To overcome this, there are films that have dielectrics equivalent, though slightly elevated from indolene. Thin films of poly-ethyl-ethyl-ketone (PEEK) with a dielectric of 3.3 could be used in lieu of tape. In order to match the dielectric of the fuel and PEEK, 3-pentanone could be added to the indolene to raise its dielectric constant. Since 3-pentanone contains similar evaporative characteristics as indolene, yet contains a much higher dielectric constant (approximately 17), vaporization

properties would not be significantly affected while matching the dielectric properties. This would allow for direct calibration of indolene and film thickness in an identical manner presented above.

7.4 Motored Engine Fuel Film Measurement Results

After developing calibration techniques for the sensors, a capacitance fuel film sensor was placed in the intake port. This first sensor was located at the top of the intake port directly across from the combustion head surface. This spot was chosen due to geometrical constraints. A second sensor was located in the intake port after conducting tests for the first sensor. This sensor was located at the base of the intake port, orthogonal to the combustion head surface. The location of the two sensors may be seen in Figure 7.6.

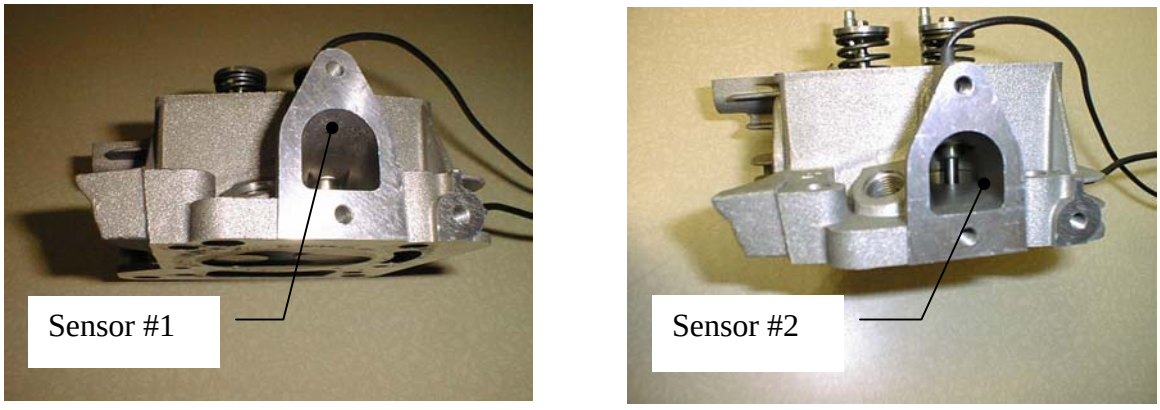

Figure 7.6 Locations of capacitance sensors.

Tests consisted of firing the engine at 3060 RPM under various fuel injection rates and various throttle positions. Under relatively rich running conditions (~11:1), no change in the output of sensor #1 was observed. Varying the throttle position also

showed no effect on the sensor output. This indicated that no fuel film was generated, or that the sensor was located where no fuel film was present. Since transient fueling and throttle tests indicated the presence of fuel film, it was deduced that no film existed in the region investigated.

To further investigate the presence of films, a second sensor was placed in the intake port. The throttle plate direction was reversed such that fuel would be directed off the throttle plate in the general direction of sensor #2. It was again found that no discernible film was present under identical testing conditions for sensor #1.

To test the validity of the sensors a motored test sequence was conducted. The engine was brought to operating temperature by running the engine approximately half an hour under steady state WOT conditions. The siphon-tube fuel injection system was then removed from the engine. The engine was motored at 2000 RPM and indolene fuel from a syringe was directed towards the sensors. This test was conducted to determine if the sensors would detect the presence of fuel films for a hot spinning engine. The results to the sensor response for sensor #2 may be seen in Figure 7.7, along with the UEGO signal which was used to identify times that fuel was inducted into the engine.

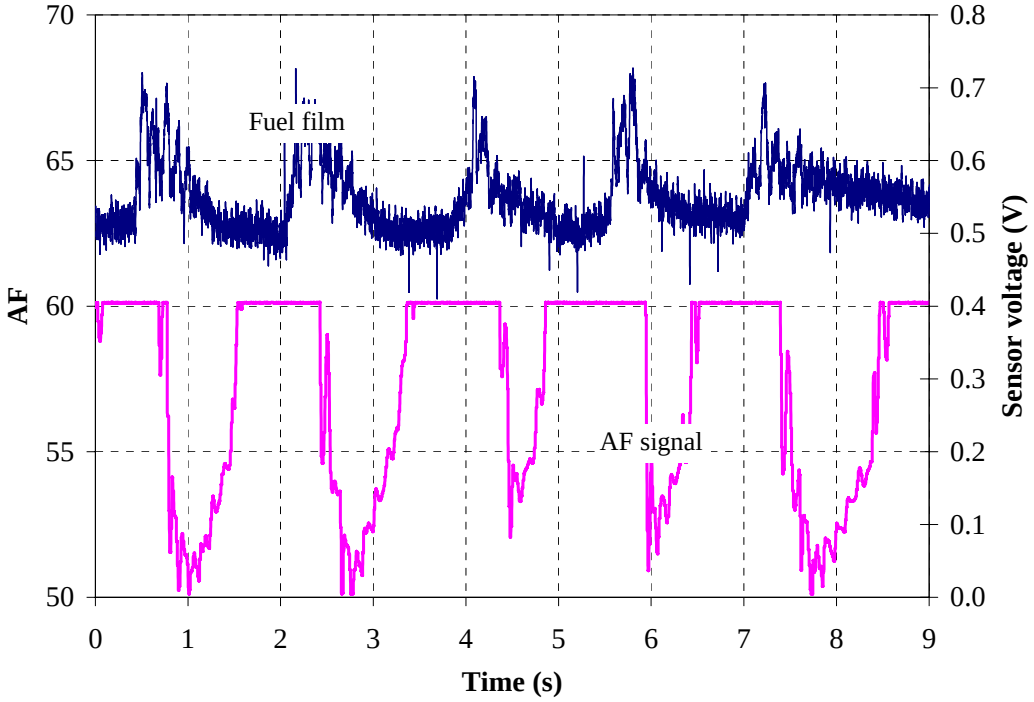

Figure 7.7 Capacitance sensor #2 fuel film response, 2000 RPM motored engine tests.

It was determined that both sensors responded presence of fuel. This is indicated by the increase in sensor voltage. Directly following the increase in the capacitor sensor voltage is a decrease in AF ratio detected by the UEGO sensor as the induced fuel passes out the exhaust port. The spark plug was activated during the tests and partial combustion was noted.

Conclusions from the calibrations and motored tests determined that the sensors had the capability of measuring fuel films in the intake port. However, no film was detected where the sensors were located. Since the tape calibration was conducted with a dielectric approximately 3 times greater than that of the fuel, it is expected that a film thickness of 150 μm could be detected. Thus, it is believed that fuel films that were present were less than 150 μm in thickness at this location. The geometrical constraints

of the intake port did not allow for large numbers of sensors to be mounted, nor did it allow for sensors to be located in the venturi just downstream of the main fuel jet.

7.5 Summary

A technique of capable of measuring low dielectric fuel films to within 50 μm has been developed. A reliable technique of using solid films of various thickness (Scotch® brand clear adhesive tape) was implemented to calibrate the sensors. Due to adhesion of the film, the gravimetric technique of calibrating the sensors was found to be insufficient in the range of fuel films desired. Two sensors were located within the intake port of the research engine, but were unsuccessful in measuring films. Since transient tests concluded the presence of fuel films, it was concluded that the sensors were located in regions in which no fuel film exists. Motored engine tests in which fuel was applied over the sensors via a syringe confirmed that the sensors worked. Spatial limitations of the engine limited sensor location and number.

8

FFID SKIP-INJECTION/STOP-INJECTION HYDROCARBON SAMPLING

8.1 Introduction

In chapter six, behavior indicative of fuel films was observed by conducting fixed fuel flow, transient throttle position tests. To further quantify these films, the skip and stop-injection method of quantifying the total steady state mass of the fuel film was utilized. The skip-injection method consisted of measuring the exhaust hydrocarbon concentration utilizing a FFID during both combustion and skip-injection engine cycles. The skip-injection event consisted of not injecting fuel for one or three engine cycles. The engine was run at steady state and fuel injection skips occurred every 30 engine cycles. The stop-injection tests consisted of impulsively ceasing fuel flow altogether while the engine was running under steady state conditions. Exhaust stream hydrocarbon concentration was measured prior to and after the skip- and stop-injection fueling events. The time-resolved measured exhaust stream hydrocarbon concentration was converted to an equivalent fuel mass to the determine fuel inducted into the engine during the skip- and stop-injection cycles. Parameters investigated were propane-fueled injection, high and low pressure indolene-fueled injection, and engine load. Details of the skip-injection sampling system may be found in sections 3.7 and 3.8.

Although a small portion of the measure HC concentration may come from either residual crevice volume effects or oil desorption, the significant contribution is thought to

be from the intake port film mass. By using propane, the relative crevice volume effect was investigated. Insight into the oil absorption/desorption was gained using iso-octane.

8.2 Propane Skip-Injection Tests

In order to separate partial combustion and crevice effects from fuel film effects, a series of propane-fueled skip-injection tests were conducted. Five tests were conducted for each parameter change to ensure statistical viability. These tests consisted of running the engine at steady state and skipping fuel injection every 30 engine cycles. Fuel pressure was set to 620 kPa (gage) for all tests. Injection duration was set to 3.1 ms. This injection duration resulted in a steady state air/fuel ratio approximately 14.7:1. Fuel injection timing was the parameter investigated, with timings set at both 180 BTDC and TDC of the intake stroke.

The engine was run approximately one half hour prior to any transient tests to ensure steady state operation. After that time, engine oil temperature reached a steady value of 113 ^{o}C. Engine speed was set at 3060 RPM, with fluctuations caused by the engine inertial change due to the non-combustion events. Exhaust pressure was set at a constant 1.87 mm Hg vacuum. In Figure 8.1, the hydrocarbon concentration and cylinder pressure results to a single skip-injection test may be seen. The pressure trace allowed for determination of whether or not partial burning occurred during the skip-injection event (this is later shown for indolene-fueled skip-injection tests).

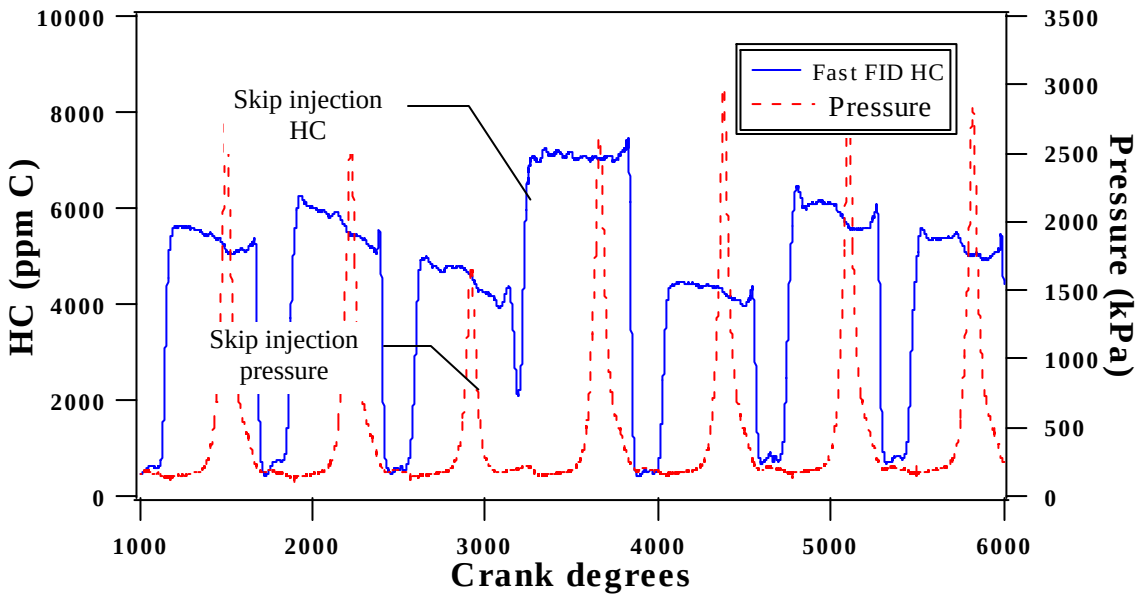

Figure 8.1 Propane-fueled TDC injection 1 cycle skip-injection HC concentration, test #4.

It may be seen in Figure 8.1 that a rise in the hydrocarbon concentration occurs directly following the skip-injection event. Since propane cannot form fuel films, this rise in concentration is most likely due to crevice volume contributions. The measured in-cylinder peak pressure reduces significantly during the skip-injection event indicating no combustion. Further, analysis of the trace shows no late cycle burning normally indicated by an increase in the pressure on the expansion stroke.

In Figure 8.2, the results of a three-cycle skip-injection test may be seen. The numbers shown correspond to the cycle number for the three cycles in which propane was not introduced.

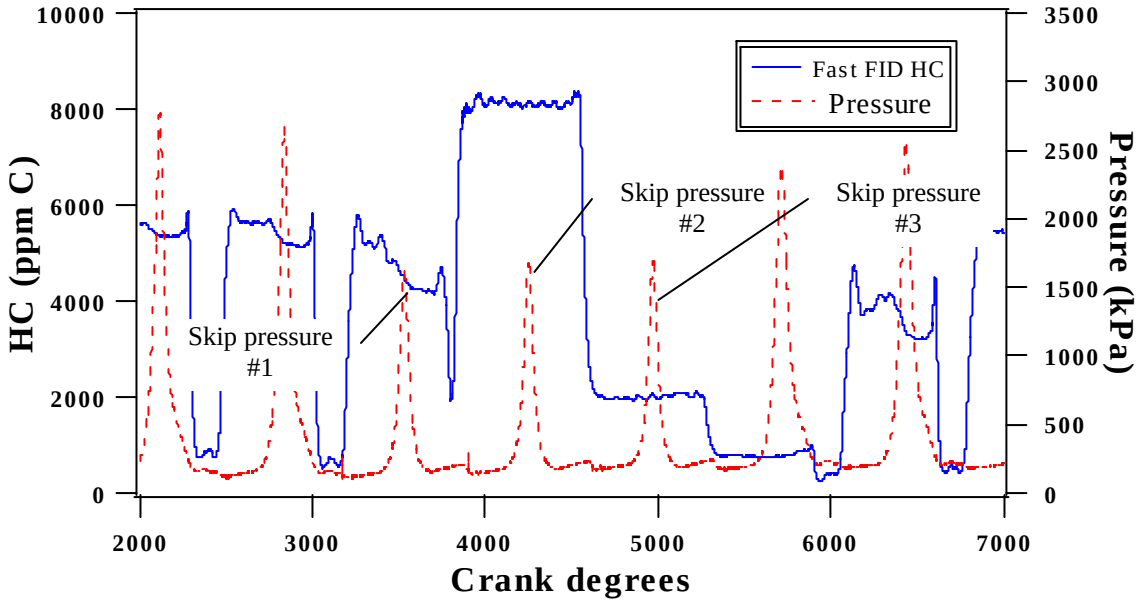

Figure 8.2 Propane TDC injection 3 cycle skip-injection HC concentration, test #2.

From Figure 8.2, a similar rise in hydrocarbon concentration following the first skip-injection event may be seen. This first cycle increase is similar in magnitude to that found in Figure 8.1. Directly following the first skip-injection is a decrease in the hydrocarbon concentration. By the third cycle, the concentration is significantly lower than the concentration present during the combustion events. This is expected since the majority of crevice volume hydrocarbons should be vacated.

After collecting the hydrocarbon concentration data, the results were converted to a mass basis. This required converting the hydrocarbon mole fraction to a mass fraction. The equation used to convert the mole fraction to mass fraction is as follows

$$m_{fuel} = \frac{y_f}{1-y_f} m_{air} = \frac{x_{c1} \cdot MW_{c1}}{(1-x_{c1})MW_{air}} m_{air} \qquad (8.2)$$

where m_{fuel} is the equivalent mass of fuel that passed through the engine unburned per cycle, y_f is the mass fraction of the fuel, m_{air} is the mass of air per cycle, x_{c1} is the carbon mass fraction (single carbon basis), MW_{c1} is the molecular weight of indolene or propane on a single carbon basis, and MW_{air} is the molecular weight of air. The air flow was calibrated as a function of engine load, and the mole fraction of c_1 is measured by the FFID. This determined the mass of HC present. This method of converting the hydrocarbon concentration to a mass basis was applied to propane- and indolene-fueled cases, the only difference being slight differences between the mass fraction equations of indolene and propane (see Appendix A-5 for details). The results of the amount of fuel required per cycle under various loads for propane and indolene may be seen in Figure 8.3. This may be used as reference throughout the chapter.

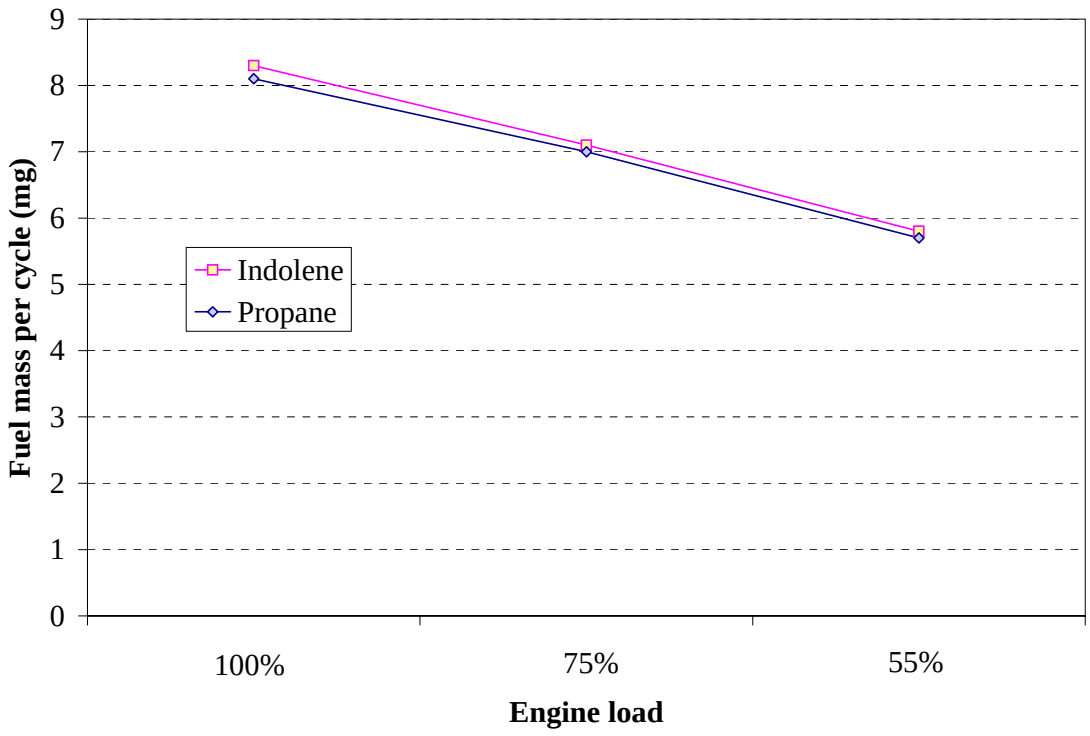

Figure 8.3 Fuel required per engine cycle, full load, A/F = 14.7:1, η_v = 75%.
For indolene: 100% load = 8.3 mg, 75% load = 7.1 mg, 55% load = 5.8 mg.
For propane: 100% load =8.1 mg, 75% load = 7.0 mg, 55% load = 5.7 mg.

8.3 Fuel Injection Timing Effect On Propane-Fueled 3 Cycle Skip Tests

An example of the mass results for a three-cycle skip-injection propane-fueled test with fuel injection timing set to TDC may be seen in Figure 8.4. For the sake of brevity, only this case is presented. For reference, under full load conditions, A/F equal to 14.7:1, 75% volumetric efficiency, the mass of propane delivered per cycle was 8.1 mg.

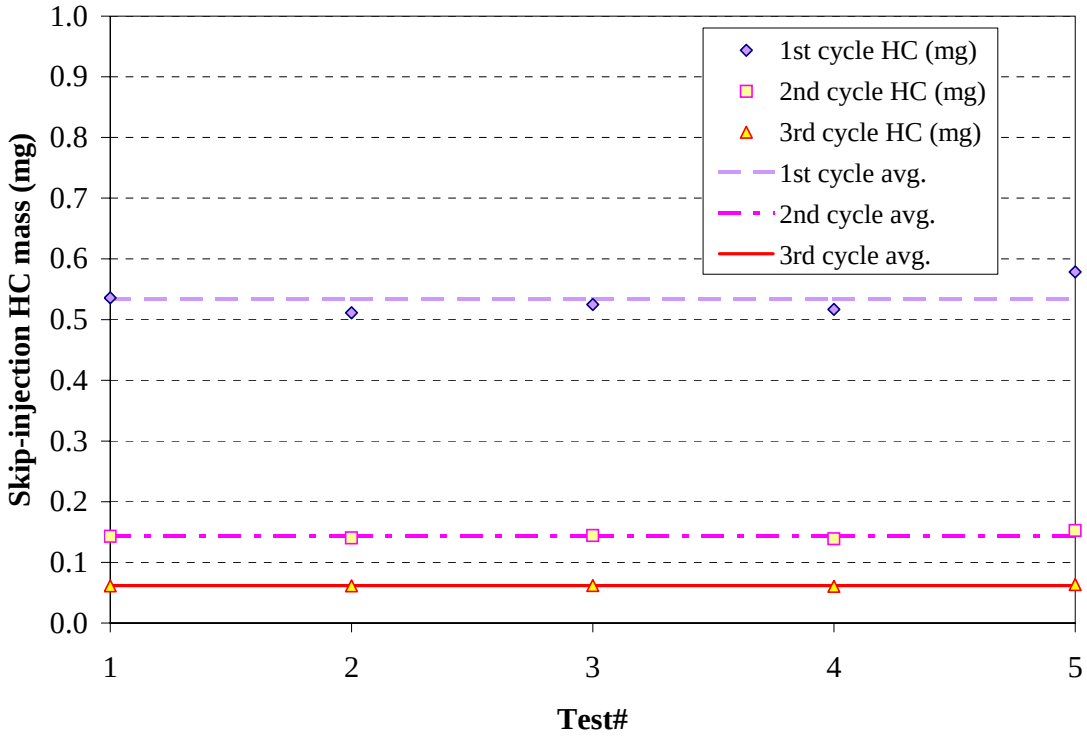

Figure 8.4 Propane TDC injection 3 cycle skip-injection HC mass, 5 test averages.

From Figure 8.4 it may be seen that the overall HC mass decreases continually from the first to final stop-injection event. The masses presented correspond to 6.6%, 1.8% and 0.8% of an engine cycle worth of propane for the first, second, and third skip, respectively. Since gaseous propane does not form a fuel film in the intake port, the presence of HC after the skip-injection event are predominately a result of crevice volume hydrocarbons. As the inducted A/F mixture is compressed, a portion of the

intake charge is forced into the ringpack and other crevices within the combustion chamber. As combustion occurs the flame is quenched prior to entering the crevices and the hydrocarbons escape oxidation. During the latter stages of exhaust blowdown the pressure in the ringpack exceeds the cylinder pressure, and the hydrocarbons are returned to the combustion chamber. Also, hydrocarbons that escaped combustion in other crevice locations are released following peak pressure (i.e. spark plug threads, oil absorption, piston top ring-land). It may also be seen in Figure 8.4 that by the third skip-injection event the mass of crevice hydrocarbons is virtually depleted.

After conducting similar stop-injection tests while varying injection timing, the five runs were averaged together and compiled into a single figure. The effect of injection timing on propane-fueled skip-injection testing may be seen in Figure 8.5.

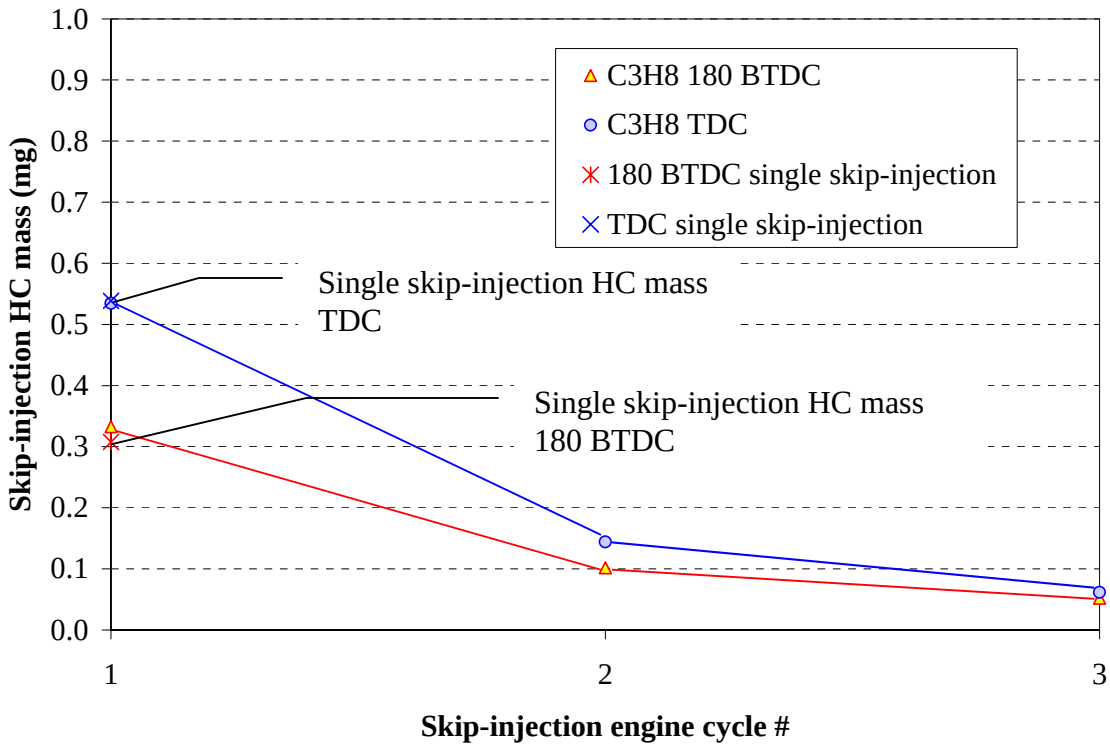

Figure 8.5 Fuel injection timing effect on propane-fueled 3 cycle skip-injection HC mass (Full load, A/F = 14.7:1, η_v = 75%, 1 engine cycle of propane = 8.1 mg).

From Figure 8.5 it may be seen that the relative hydrocarbon mass is negligible by the third skip-injection event for both 180^{o} BTDC and TDC injection timing. The first skip-injection mass for TDC and 180^{o} BTDC timings contain 6.1% and 4.1% of a standard engine cycle mass of propane, respectively. This value decreases to 0.7% by the third skip engine cycle. Included in Figure 8.5 are the results to the single skip-injection hydrocarbon masses. It may be seen that the first cycle hydrocarbon mass for the three skip-injection tests correlates well with the single skip-injection masses. Both fuel injection timings display similar trends as the number of skip-injection cycles increases, with the TDC injection timing case containing slightly elevated hydrocarbons over 180^{o} BTDC injection timing. This would be expected since earlier injection of propane allows for better mixing prior to combustion, with the increase in homogeneity resulting in more complete combustion.

8.4 Indolene-Fueled Skip-Injection Tests

After determining the relative effects of propane fuel on skip-injection tests, similar tests were conducted using indolene fuel. For the indolene tests, two siphon-tube fuel injection pressures were investigated: 345 kPa and 14 kPa (gage). In Chapter 6 differences were found in engine stability using high and low injection pressure. Due to the stability of the A/F ratio with high-pressure injection, it is thought that better fuel mixture preparation was obtained with the siphon-tube injection system using high pressure injection, and that low pressure injection better mimics carburetor behavior.

Five tests were conducted for each condition to ensure statistical viability. Similar to propane, the tests consisted of running the engine steady state and skipping one

or three cycles of fuel injection every 30 engine cycles. Running the engine approximately one half hour prior to any transient tests ensured steady state operation. After that time, engine oil temperature reached a steady value of 113 °C. Engine speed was set at 3060 RPM, with fluctuations caused by the engine inertial change due to the three non-combustion events. Exhaust pressure was set at a constant 1.87 mm Hg vacuum. The same technique of converting the hydrocarbon concentration to a mass basis was used as outlined in section 8.2.

8.4.1 Engine Load Effect On High Pressure Siphon-Tube Fuel Injection, Skip Tests

The first set of indolene-fueled skip-injection tests investigated the effects of engine load on fuel film mass. Injection duration was set to 3.8 ms at TDC, and fuel injection pressure was set to 345 kPa. The results of a single skip-injection test may be seen in Figure 8.6.

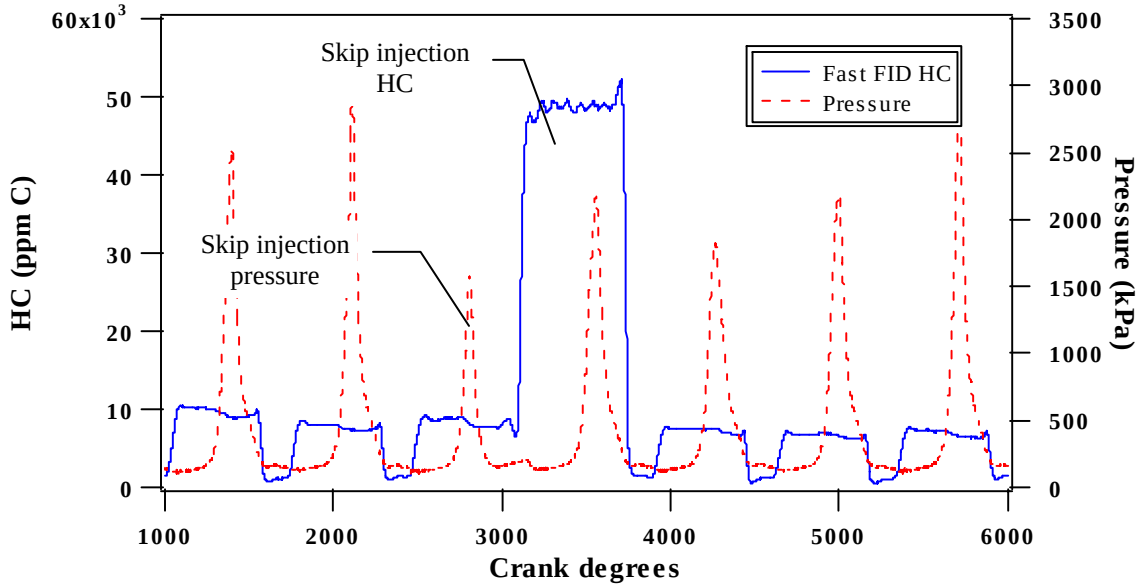

Figure 8.6 Indolene-fueled TDC injection 100% load 1 cycle skip-injection HC concentration, test #2 (Full load, A/F = 14.7:1, η_v = 75%, 1 engine cycle of indolene = 8.3 mg).

As was seen in Figure 8.2, the exhaust stroke following the skip-injection cycle shows a significant increase in hydrocarbon concentration. This concentration is equivalent to 3.0 mg of fuel. Under these testing conditions, this rise in hydrocarbon concentration equates to approximately 36% of the fuel mass for a standard engine cycle. These masses are much higher than the results found for propane in section 8.2. This verifies the presence of a fuel film, which continues to contribute fuel mass to the engine in the absence of fuel injection.

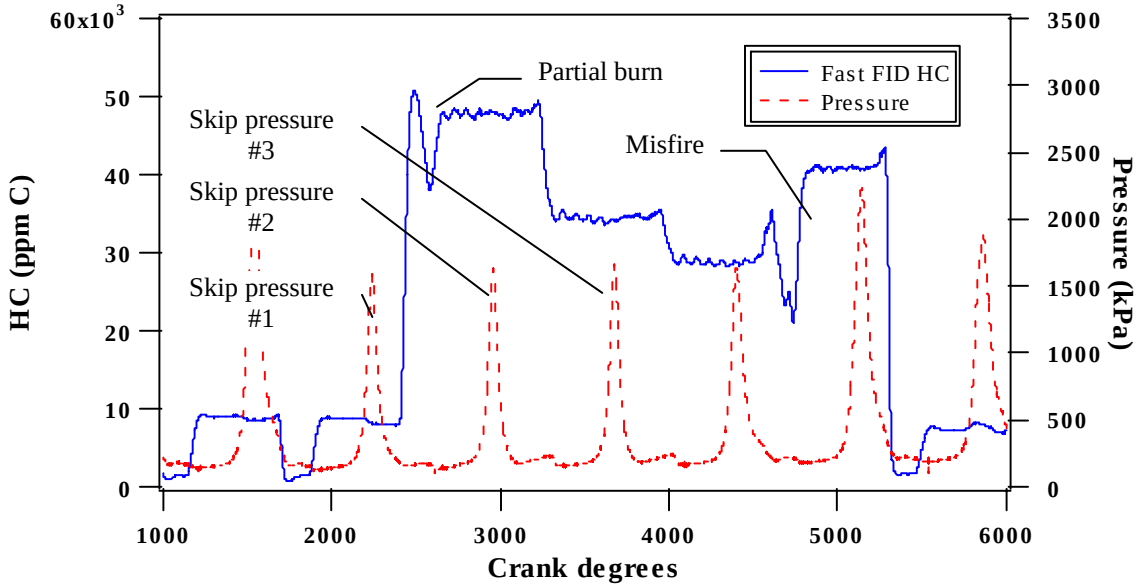

Figure 8.7 Indolene-fueled TDC injection 100% load 3 cycle skip-injection HC concentration, test #3.

Figure 8.7 shows the results to an indolene-fueled three skip-injection tests with fuel injection timing set to TDC. A decrease in hydrocarbon concentration may be seen for the skip-injection cycles following the first skip-injection event. The first cycle hydrocarbon concentration is slightly less (47,000 ppm compared to 50,000 ppm) than that found for the single skip-injection test presented in Figure 8.5. This reduction in the first cycle of the skip-injection event is caused by a partial combustion in the first skip-

injection cycle. Since the spark plug was not disabled during the skip-injection tests, certain testing conditions led to partial combustion during the first skip-injection cycle. This partial combustion reduces the first cycle hydrocarbon concentration during the three cycle skip-injection event. This partial burn was not seen for single skip-injection tests.

After conducting similar skip-injection tests for varied engine load, the five runs were averaged together and compiled into a single figure. The effect of engine load on indolene-fueled skip-injection testing may be seen in Figure 8.8.

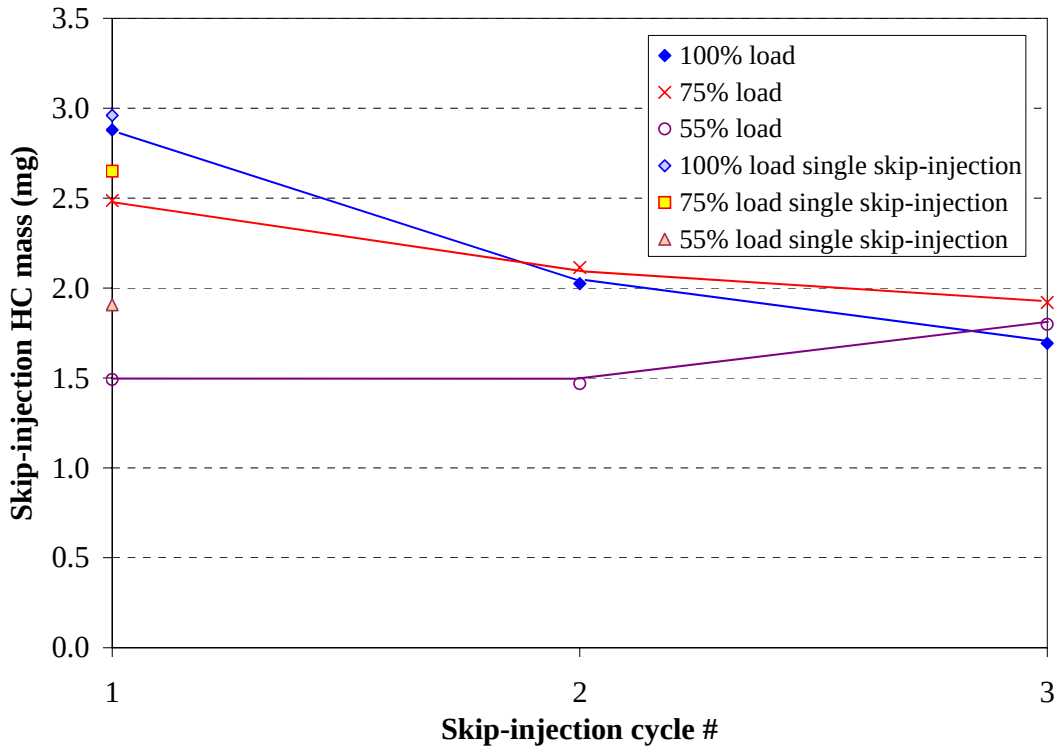

Figure 8.8 Engine load effect on high pressure indolene-fueled 3 cycle skip-injection HC mass.

From Figure 8.8 it may be seen that the initial intake port fuel film mass for the 100% load case is on the order of 2.9 mg during the first skip-injection cycle, and 2.5 mg

for the 75% load case. The single skip-injection values indicated on the chart are slightly higher than the first cycle value measured for the three skip-injection tests as a result of the partial burning. Also, for the 55% load case, the trend of decreasing fuel film mass for the skip-injection events is not observed. Insight into this behavior may be gained from Figures 8.9 and 8.10. Figure 8.9 displays the results for a single cycle skip-injection test at 55% load, and Figure 8.10 displays the results for a three cycle skip-injection test.

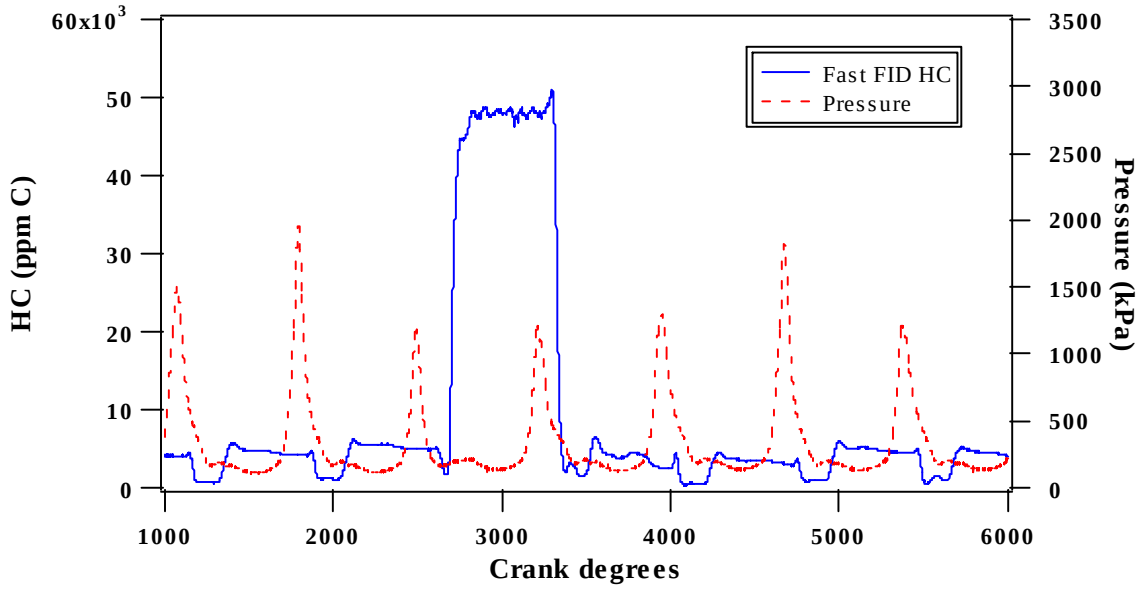

Figure 8.9 55% load high pressure load indolene-fueled 1 cycle skip-injection HC concentration, test #5.

From Figure 8.9, it may be seen that for 55% load single skip-injection exhaust hydrocarbon concentration is approximately 49,000 ppm. This is equivalent to approximately 2.0 mg of fuel under the given test conditions. However, the five cycle average for the first skip-injection during three skip-injection case presented in Figure 8.10 is significantly less (~ 1.5 mg). By inspecting the three cycle skip-injection results, insight into this behavior is gained.

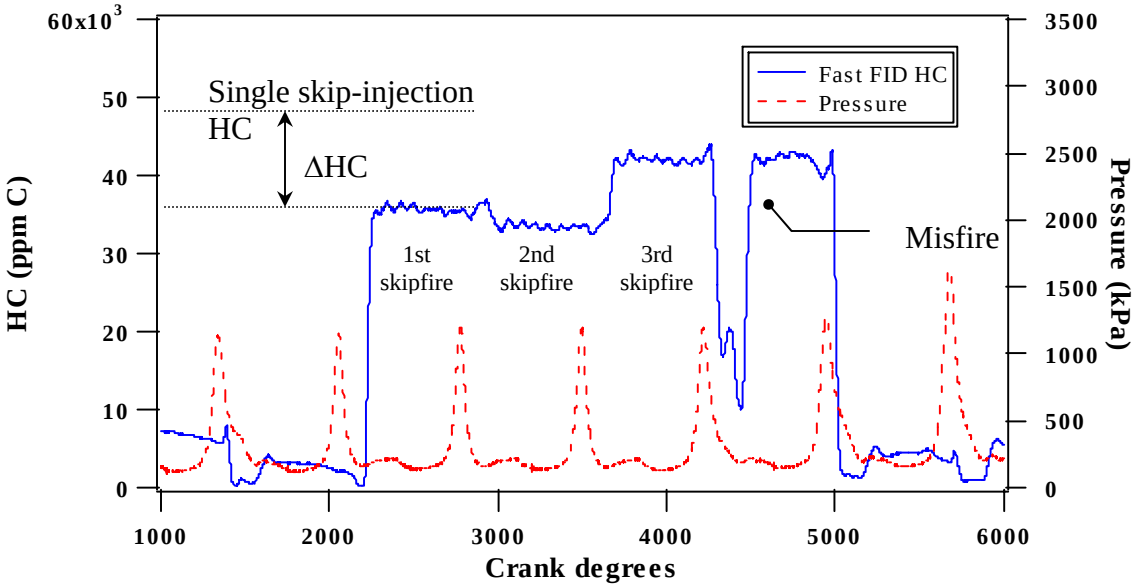

Figure 8.10 55% load high pressure indolene-fueled 3 cycle skip-injection HC concentration, test #5.

It may be seen in Figure 8.10 that the third cycle hydrocarbon concentration is higher than the first two skip-injection cycles, and that the rate of depletion between the first and second cycle is slight. This is not physically consistent with what is expected.

It is believed that the observed fuel film dynamics are being dominated by engine instability caused by the three skip-injection cycles. During the three cycle skip-injection tests the engine speed varied significantly due to the lack of combustion stability. Also, it may be seen that there is an engine misfire after the third skip-injection. This misfire was seen consistently for the 55% load case. Since a portion of the injected fuel goes to form a film during the first cycle that fuel is introduced, there is insufficient fuel during the first non skip-injection engine cycle for a complete combustion event. This occurs for only one cycle after skip-injection has ceased, at which point the engine resumes normal operation. However, since three cycles are misfires due to skipping fuel injection, and the fourth cycle misfires, a total of four cycles out of every thirty engine cycles are

misfires. Under low load these four cycles drastically affect smooth engine operation. Similar behavior was observed for other indolene-fueled tests as well. It was found that by skipping fuel injection for three engine cycles the engine instability became too great and erroneous results, not indicative of actual fuel film behavior, were obtained.

8.4.2 Fuel Injection Timing Effect On High Pressure Siphon-Tube Fuel Injection Skip Tests

The next parameter investigated for high pressure siphon-tube injection was fuel injection timing. Two timings were investigated: 180^{o} BTDC and TDC injection. Injection pressure was set to 345 kPa (gage) and injection duration set to 3.8 ms. This equated to a steady state air fuel ratio of approximately 14.7:1. Five tests were averaged together for each timing change, the results of which may be seen in Figure 8.11.

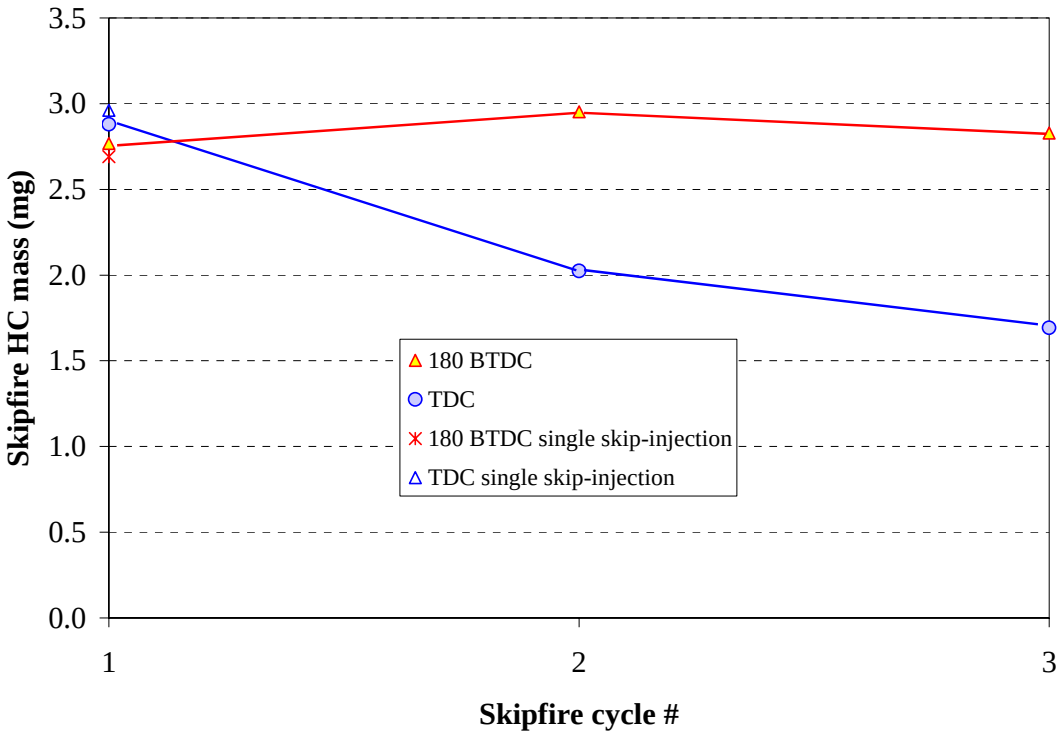

Figure 8.11 Fuel injection timing effect on high pressure indolene-fueled 3 cycle skip-injection HC mass.

From Figure 8.11 it may be there is no strong correlation between fuel injection timing and initial fuel film mass for the first cycle of skip-injection as may be seen by the first cycle results. The magnitude of the first cycle hydrocarbon mass for the three cycle skip-injection correlates well with the single skip-injection results. This indicates that the engine instability issue is not as significant for the single skip-injection tests, and that the results are fairly reliable. However, fuel film dynamics again appear to be dominated by engine instability for the three cycle skip-injection tests, which was discussed in section 8.3.1.

8.4.3 Engine Load Effect On Low Pressure Siphon-Tube Fuel Injection Skip Tests

The second set of indolene-fueled skip-injection tests involved investigating low pressure, long duration siphon-tube fuel injection. By introducing the fuel during the intake stroke under low pressure conditions, carburetor behavior is thought to be better mimicked. Fuel pressure was set to 13.8 kPa (gage) and fuel injection duration ranged from 10 to 16 ms depending upon engine load. These settings equated to a steady state air-fuel ratio of approximately 14.7:1. For each load change, five runs were completed and averaged together to ensure testing repeatability. The results of engine load on low pressure siphon-tube injection may be seen in Figure 8.12.

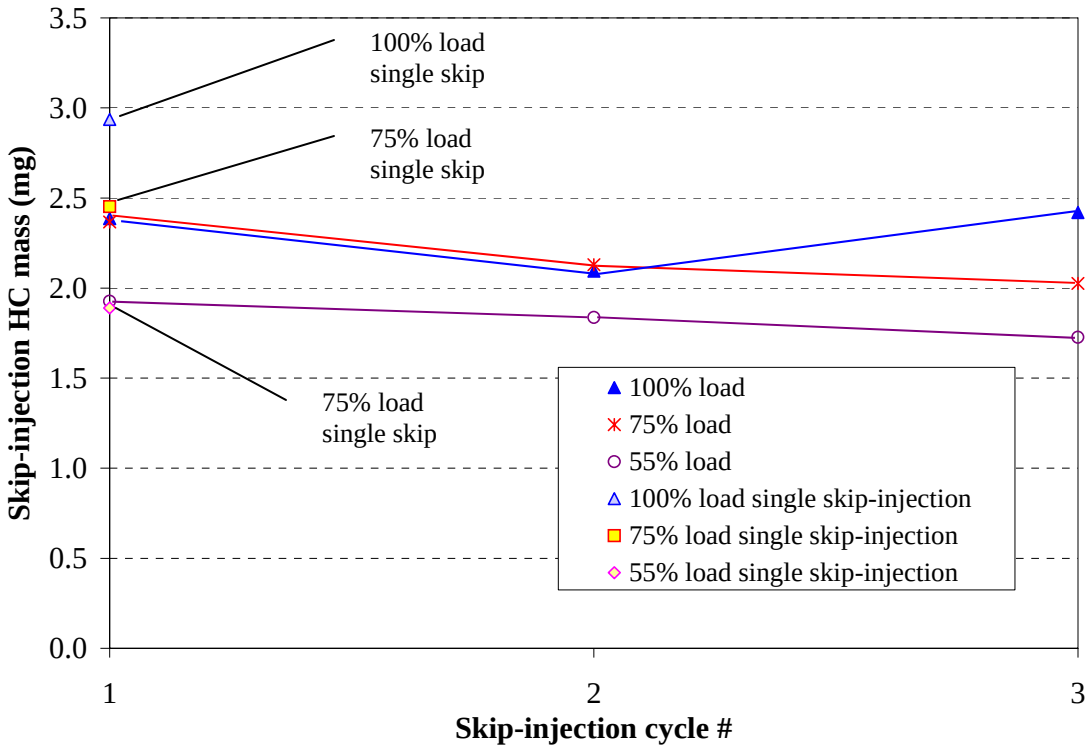

Figure 8.12 Engine load effect on low pressure indolene-fueled 3 cycle skip-injection HC mass.

It may be seen in Figure 8.12 that the hydrocarbon mass for the first cycle of the three skip-injection tests do not correlate well with the single skip-injection tests. These results are again attributed to the rough engine operating conditions encountered during three skip-injection events. However, the results to the single skip-injection tests presented on Figure 8.12 are similar to the results found for the high pressure skip-injection tests presented in section 8.4.1. Results indicate that approximately 33% of the fuel contributed to the cylinder by the fuel film per engine cycle, regardless of fuel injection pressure or engine load.

8.5 Stop-Injection Tests

These tests consisted of running the engine on propane and liquid fuel under steady state conditions, and impulsively stopping fuel injection altogether. The exhaust stream hydrocarbon concentration was measured before and after fuel injection ceased using the FFID. The measured exhaust stream hydrocarbon concentration was then converted to a mass. This technique allowed for cumulative intake port fuel film mass determination. The effects of high and low pressure siphon-tube indolene fuel injection, propane fuel injection, and engine load were investigate. Both 40 and 450 engine cycles worth of data were investigated for the propane- and indolene-fueled tests.

8.5.1 40 Cycle Propane-Fueled Stop-Injection Tests

Propane tests served as a datum for the indolene-fueled stop-injection tests. For these tests, the engine was run under full load conditions. Fuel pressure for these tests was set to 620 kPa (gage). Fuel injection duration was set to 3.0 ms. This injection duration

resulted in a steady state air/fuel ratio approximately 14.7:1. Fuel injection timing was set to TDC.

Running the engine approximately one half hour prior to any transient tests ensured steady state operation. After that time, engine oil temperature reached a steady value of 113 °C. Engine speed was set at 3060 RPM. Exhaust pressure was set at a constant 1.87 mm Hg vacuum. Results of a series of five 40 cycle propane-fueled stop-injection tests may be seen in Figure 8.13.

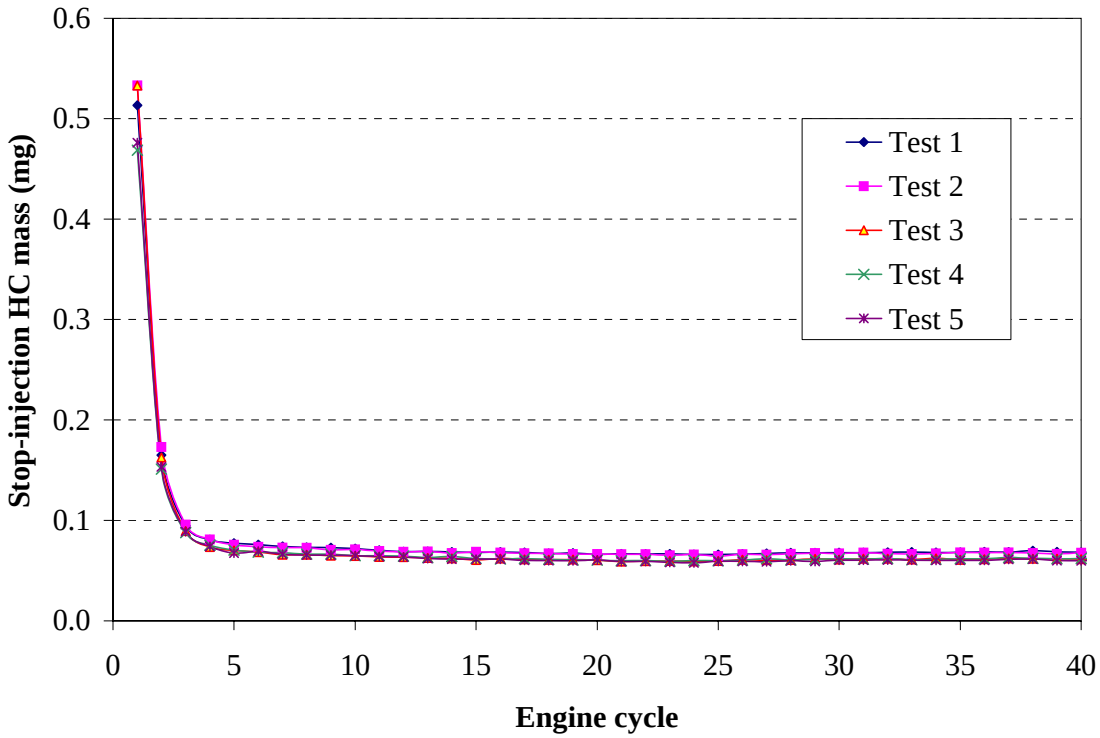

Figure 8.13 Propane-fueled 40 cycle stop-injection tests.

From Figure 8.13 it may be seen that by the third engine cycle the measured hydrocarbon mass has reached a negligible steady state mass of approximately 0.06 grams. This value is equivalent to 0.75% of an engine cycle worth of propane. The hydrocarbons present this late after the cessation of fuel injection are thought to be due to

the release of fuel from oil diffusion (unlikely with propane), or perhaps direct oil consumption.

8.5.2 450 Cycle Propane-Fueled Stop-Injection Tests

After conducting the 40 cycle stop-injection tests, a series of 450 cycle stop-injection tests were conducted. These longer durations were investigated to determine whether or the hydrocarbon concentration would go to zero since this did not occur after 40 engine cycles. The results to the 450 cycle propane-fueled stop-injection tests may be seen in Figure 8.14.

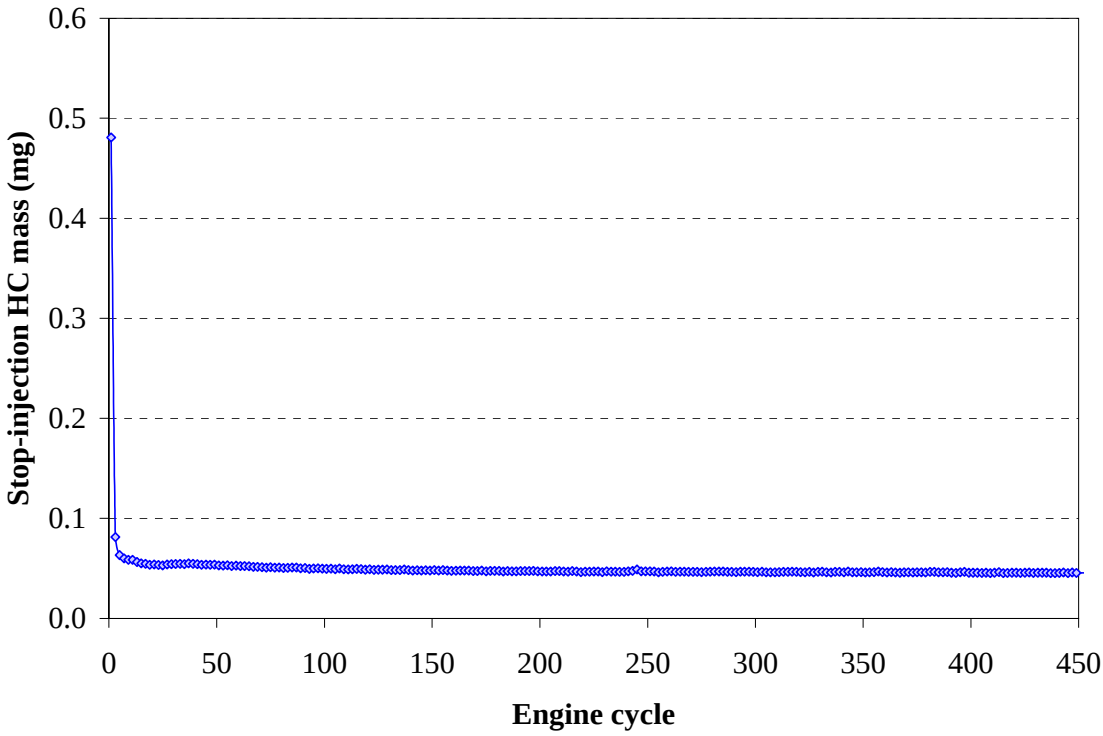

Figure 8.14 Propane-fueled 450 engine cycle stop-injection tests.

From Figure 8.14 it may be seen that by the third stop-injection cycle the stop-injection hydrocarbon concentration is significantly less than an engine cycle worth of

fuel. However, as was the case during the 40 cycle stop-injection tests, there still existed some measurable hydrocarbon concentration at the conclusion of 450 engine cycles. Close inspection of the data finds the mass was 0.045 grams at the conclusion of 450 engine cycles, as opposed to the 0.068 grams recorded at the conclusion of the 45 cycle tests. Although the hydrocarbons did not reach a zero datum, the quantity was slowly reducing.

To see whether this was an issue with the FFID, the purge gas was sent to the FFID collection head following the tests. This resulted in negligible hydrocarbon readings. Sampling directly following purging again resulted in a small amount of measurable hydrocarbons. Five tests lasting 60 engine cycles were collected at approximately 15 second intervals. The results to these tests may be seen in Figure 8.15.

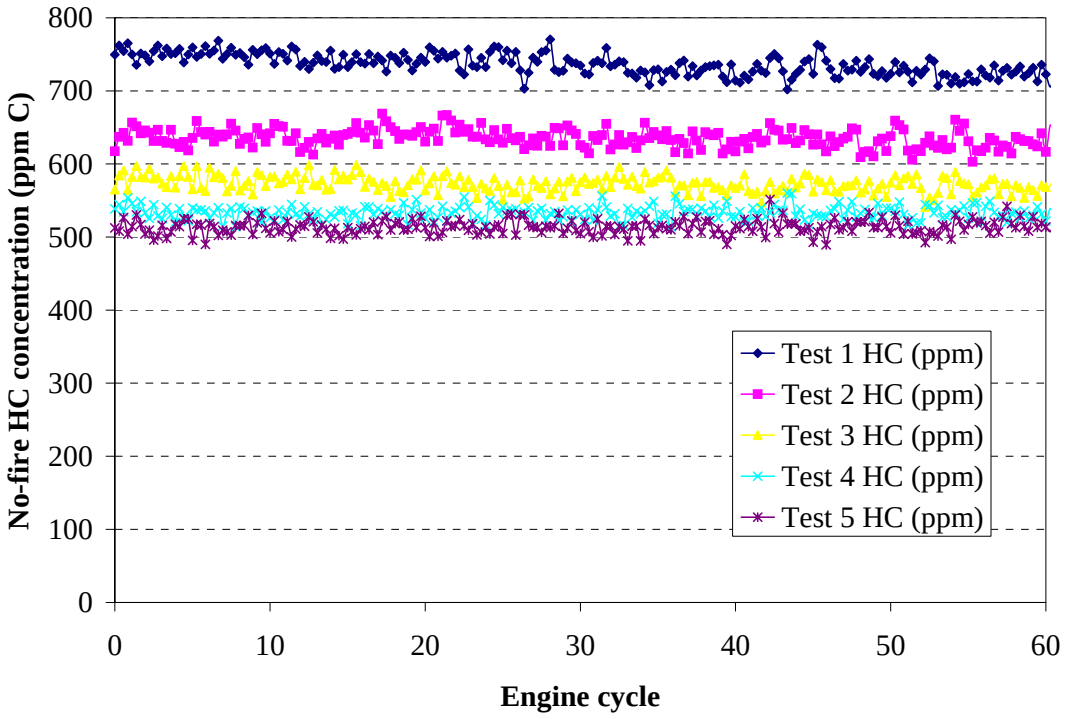

Figure 8.15 Residual hydrocarbon mass following fuel injection cessation and FFID purging.

From Figure 8.15 it may be seen that the hydrocarbon mass decreases as time continues following the ending of fuel injection. Since propane does not form a fuel film, and there are no other long term storage mechanisms (i.e. crevice volumes) for the fuel, this suggests that the source of hydrocarbons is the engine oil film.

8.4.3 40 Cycle Indolene-Fueled Stop-Injection Tests

Indolene was used to investigate the extent of fuel film effects, and was compared to the results for propane stop-injection tests. Both engine load and siphon-tube fuel injection pressure were investigated.

High pressure for these tests was set to 345 kPa, and low pressure set to 13.8 kPa. Fuel injection duration was set to 2.9 and 10 ms for the high and low pressure cases, respectively. This equated to a steady AF ratio of 14.7:1 for both cases. Running the engine approximately one half hour prior to any transient tests ensured steady state operation. After that time, engine oil temperature reached a steady value of 113 ^{o}C. Engine speed was set at 3060 RPM. Exhaust pressure was set at a constant 1.87 mm Hg vacuum. Results of a series of five 40 cycle indolene-fueled stop-injection tests may be seen in Figure 8.16.

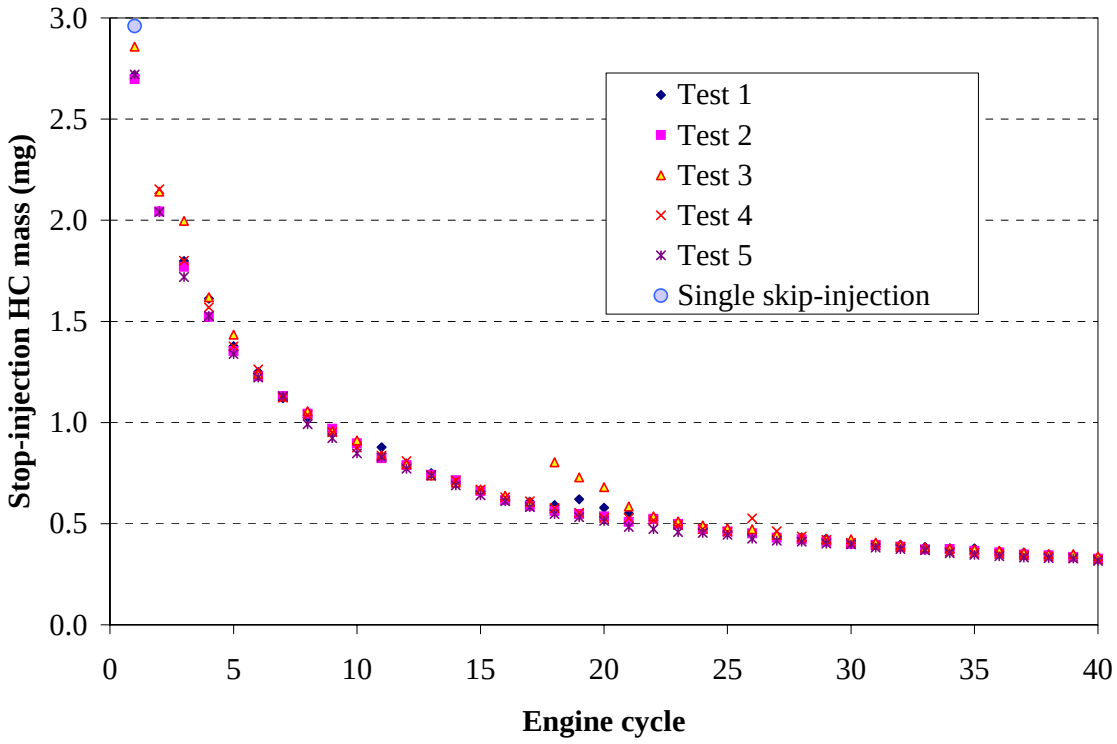

Figure 8.16 40 Cycle stop-injection high pressure indolene-fueled hydrocarbon sampling tests.

From Figure 8.16 it may be seen that the initial intake port fuel film mass starts at approximately 2.8 mg and steadily decays to approximately 0.35 grams near the 40th engine cycle. The overall magnitude of the hydrocarbon mass and rate of depletion is significantly higher than that found for propane, indicating a strong fuel film effect. The slight hydrocarbon increase for test #3 data at the 17th engine cycle is most likely due to oil being inducted through the valve guides or past the piston rings. However, this increase was not seen for other tests and is not considered consistent behavior. The first cycle hydrocarbon mass corresponds closely to the results found using the single skip-injection technique.

To determine if siphon-tube fuel injection pressure affected the overall port mass, low pressure tests were also conducted. Fuel injection timing for the low pressure tests

was set to TDC and the duration of injection set to mimic intake stroke carburetor fueling behavior. The results of the five tests may be seen in Figure 8.17.

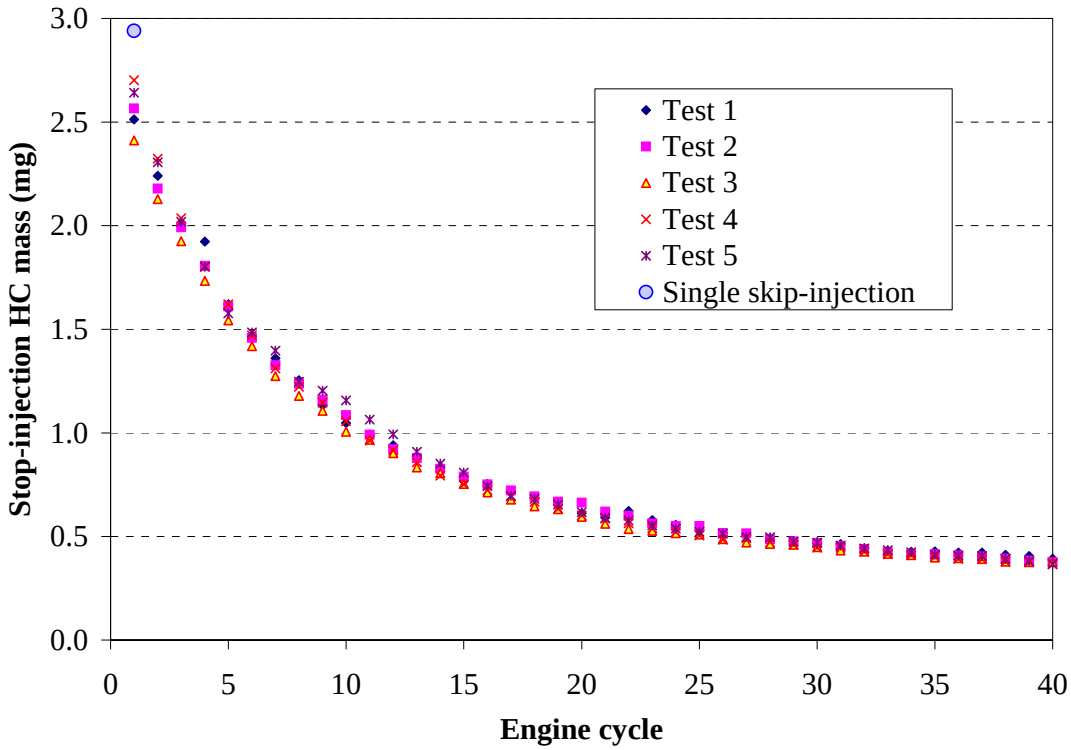

Figure 8.17 40 Cycle stop-injection low pressure indolene-fueled hydrocarbon sampling tests.

It may be seen from Figure 8.17 that the relative magnitude and rate of decay for the five low pressure tests is similar to the results found for the high pressure presented above. The averages of the five tests were taken and the results placed on a single figure for comparison. These results may be seen in Figure 8.18.

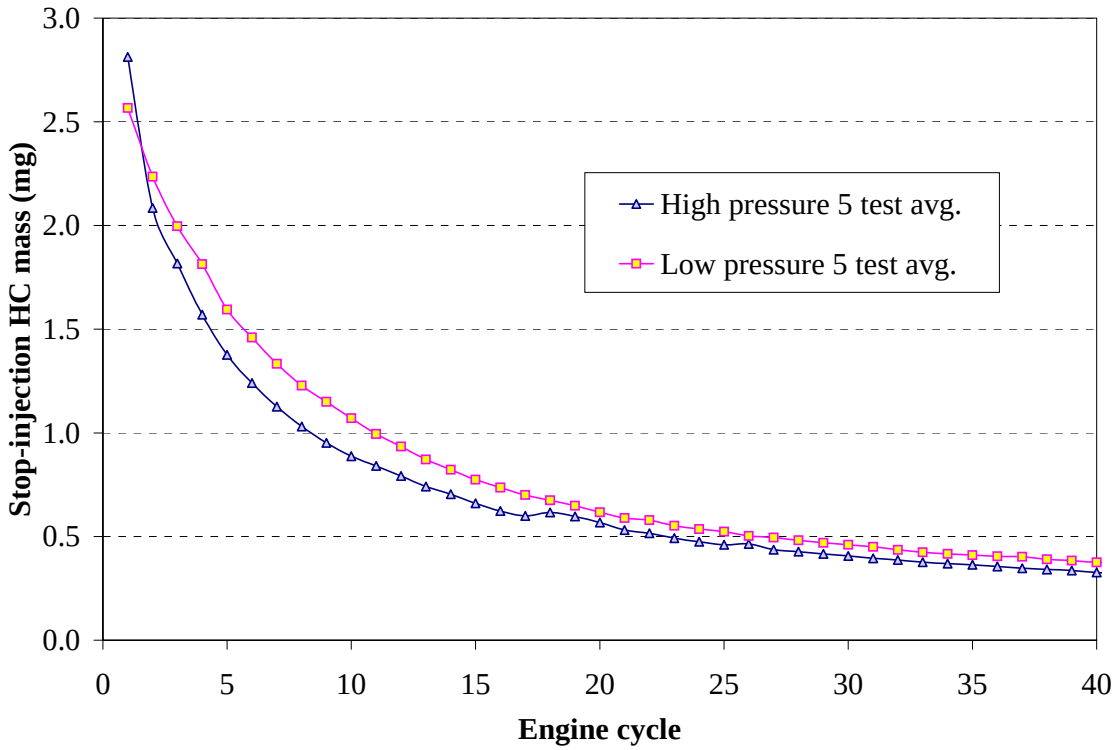

Figure 8.18 High/low siphon-tube fuel injection pressure 40 cycle stop-injection 5 run average.

From Figure 8.18 it may be seen that the effect injection pressure is minimal. The first cycle of intake port fuel film for the high pressure case is slightly higher than the low pressure case. However, the rate of film depletion and final depletion value are similar. Also, the hydrocarbon mass for the first stop-injection engine cycle is consistent with the values obtained for the single skip-injection case under similar testing conditions. To determine the cumulative mass difference between the high and low pressure stop-injection cases, both the high and low pressure tests were integrated over the 40 engine cycles. The results to the integration may be seen in Figure 8.19.

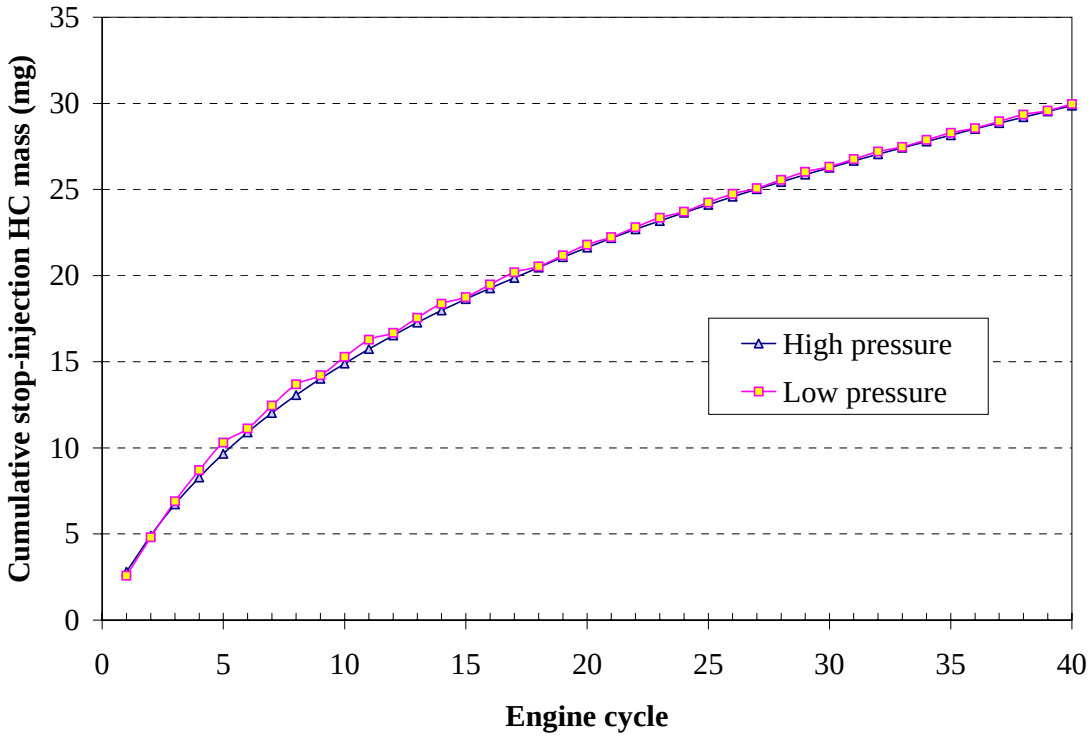

Figure 8.19 High/low siphon-tube fuel injection pressure 40 cycle cumulative stop-injection HC mass.

From Figure 8.19 it may be seen that the overall cumulative stop-injection mass over 40 engine cycles is nearly identical for high and low injection pressure. This indicates that the relative fuel film mass deposited is nearly identical for both cases. However, the cumulative mass does not level to a steady value as might be expected. To investigate this behavior, a series of 450 engine cycle indolene-fueled stop-injection tests were conducted for the low pressure fuel injection case. This was done to see if the cumulative mass would reach a finite value as might be expected.

8.4.4 450 Cycle Indolene-Fueled Stop Injection Tests

A series of load tests were conducted using low pressure injection. The three loads investigated were 100%, 75% and 55% load. Five runs were completed for each parameter change, and the results averaged together. The results of these tests along with the 450 cycle propane-fueled stop-injection tests may be seen in Figure 8.20. Included are the results of the single skip-injection tests, located on the right vertical axis for convenience.

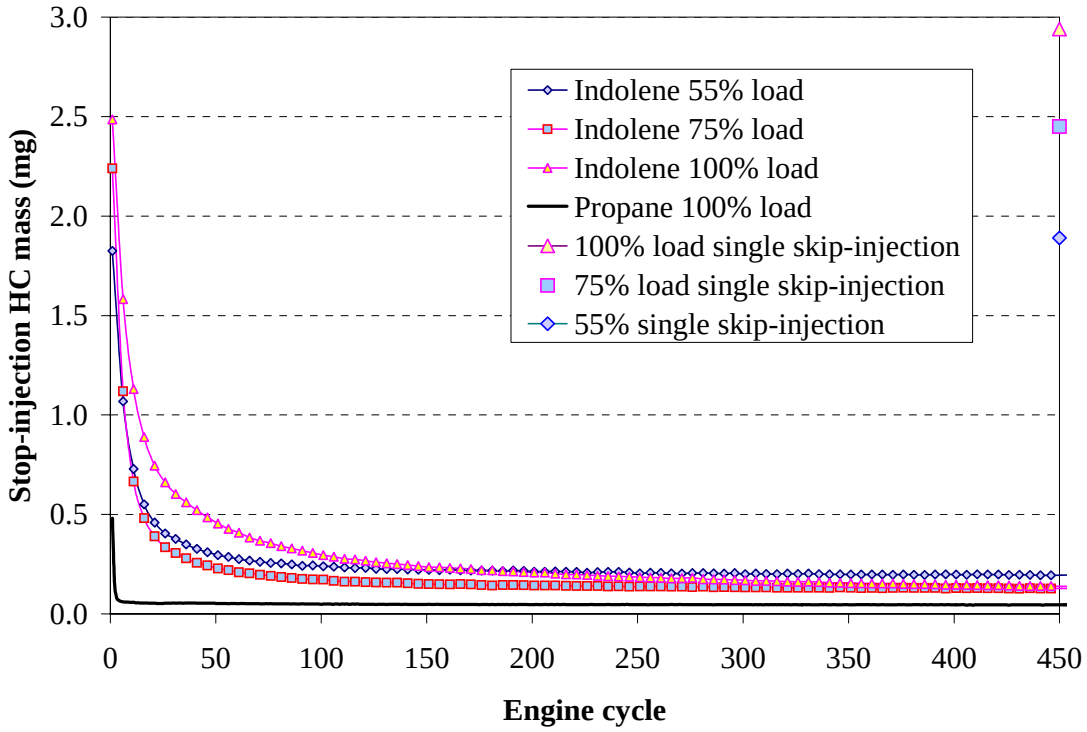

Figure 8.20 450 cycle stop-injection load effect, low pressure siphon-tube injection.

In comparing the results of the indolene-fueled tests in Figure 8.15 to the propane results, one finds significantly greater hydrocarbons present for indolene for all engine loads. This is caused by the presence of fuel films. The results to the single skip-injection tests are slightly elevated from the first stop-injection cycle. Although the

single skip-injection results were consistent with one another, smooth engine operation was also affected for the single skip tests, though not to the extent of the three skip tests. Since the stop-injection tests do not result in erratic engine operation that could affect the fuel film dynamics, the results here are considered more reliable and indicative of the actual film mass. It was earlier noted that rough engine operation for the three cycle skip-injection tests resulted in altering the fuel film mass under certain conditions.

From Figure 8.20 it may also be seen that the greatest first cycle mass of fuel present occurs for the 100% load case, followed by the 75% load case. These initial quantities of mass are 35.4%, 34.5%, and 32.6% of an engine cycle worth of fuel for the 100%, 75%, and 55% load cases, respectively. Thus it is seen that although the mass that the fuel film contributes to the cylinder is proportional to engine load, the relative percent of the mass is nearly equal, regardless of engine load. Past approximately 20 engine cycles, the 55% load case contains a greater mass of film than the 75% load case. There are two competing effects with the formation of fuel film: increased intake port temperature and throttle impingement. As the load increases, so does the intake port surface temperature and its ability to vaporize fuel. Also, as load decreases the air stream is throttled downstream of the point of induction for the fuel. The throttle plate acts as an impingement surface for the incoming fuel, which may affect fuel film formation. A combination of the low port temperature and the impingement surface for the 55% load case may result in it exceeding the 75% load case past approximately 20 engine cycle presented in Figure 8.20. Another explanation is variability in hydrocarbon measurements for the stop-injection tests. The following validation tests indicated this variability.

In order to validate the data, 100% load stop-injection tests were conducted a week following the original data collection period. All the parameters to the 100% load case were matched and 5 tests conducted. The results were then averaged together and compared to the original data run. The results may be seen in Figure 8.21.

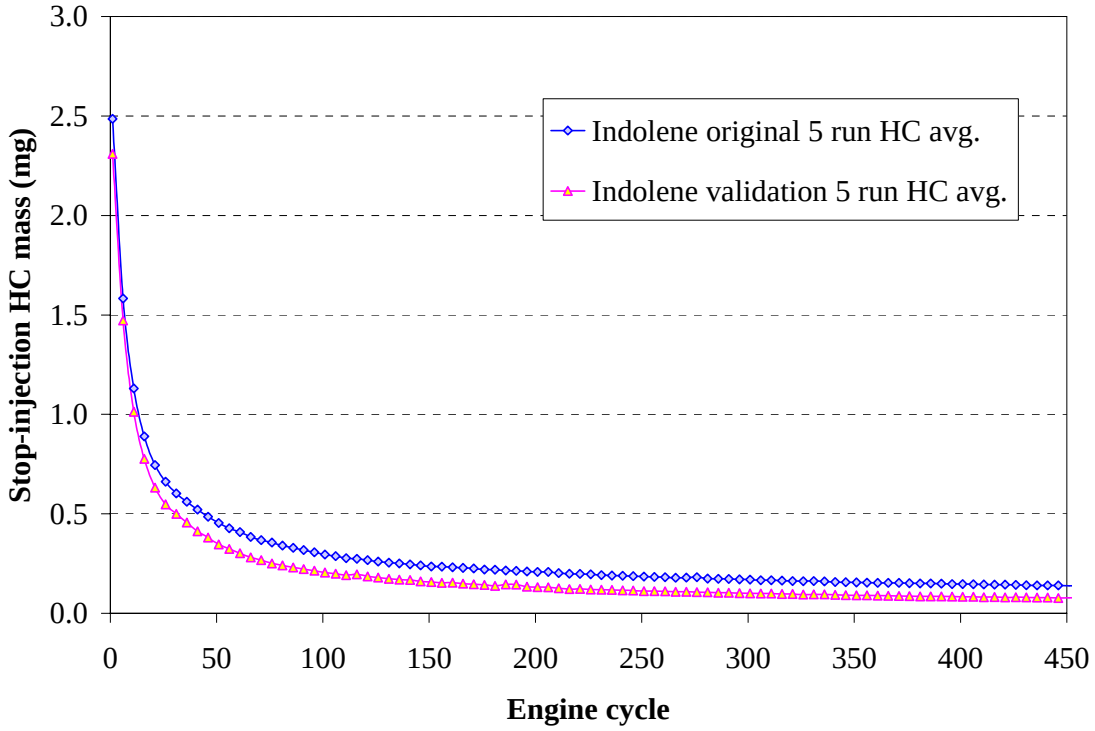

Figure 8.21 450 Cycle 100% load testing validation run.

From Figure 8.21 it may be seen that there is a slight variation in the validation run from the original test run. Although the relative trend between the two cases is nearly identical, the validation tests are slightly less in magnitude than the original tests. This variation is well within the range of hydrocarbon measurements seen in Figure 8.20 for the low load cases. This is most likely due to the slight variation in the steady A/F ratio prior to ceasing fuel injection. Pressure to the fuel injector is controlled via a hand dial, and slight variations in fuel pressure result in altered A/F ratios. Although the testing

conditions were matched as best as possible, matching the desired 14.7:1 A/F ratio exactly was not possible because of noise in the A/F signal, which was significant due to the low pressure injection (refer to section 6.4.2 for explanation).

The integrated masses for the results presented in Figure 8.20 were also determined. The results of the cumulative film mass to the various load cases may be seen in Figure 8.22.

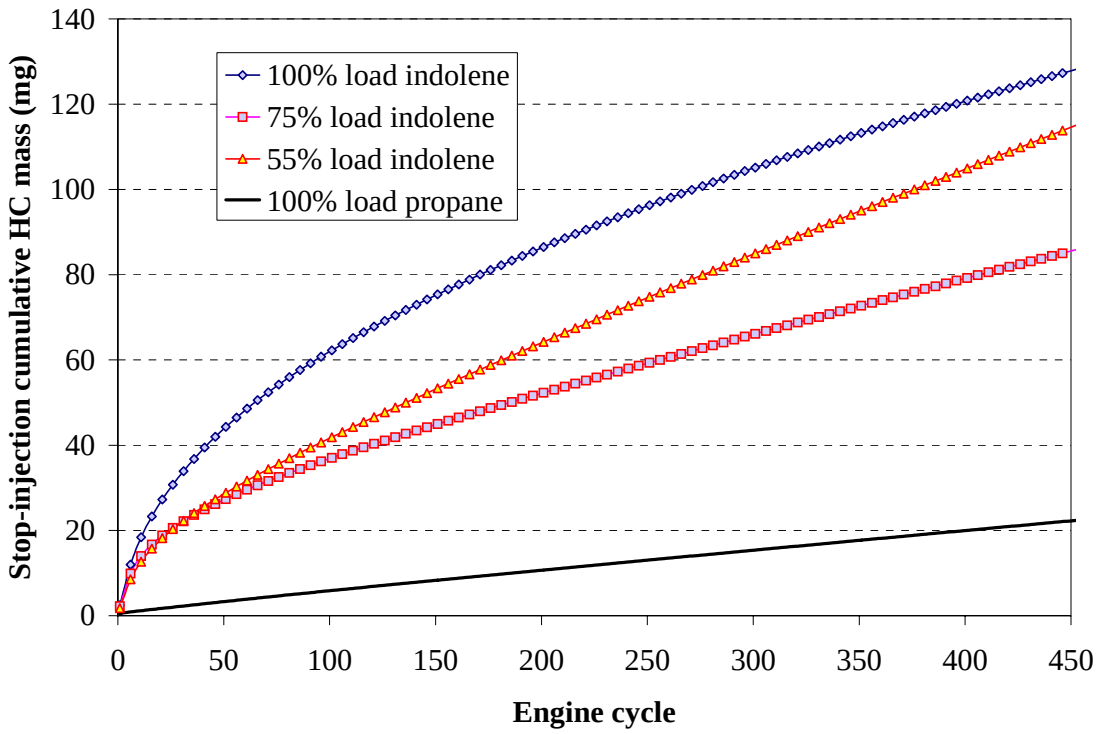

Figure 8.22 Low siphon-tube fuel injection pressure 450 cycle cumulative stop-injection HC mass.

From Figure 8.22 it may be seen that the cumulative hydrocarbon mass has still not reached a finite value after 450 engine cycles even for propane. The total mass at cycle 450 was 15.8, 12.5, and 20.6 engine cycles worth of fuel for the 100%, 75%, and

55% load cases, respectively. For the 100% case, this equates to a single spherical droplet of indolene fuel 6.93 mm in diameter.

Since it was not expected that the fuel film would persist after this duration (~20 seconds) due to high port temperature, tests were conducted to determine whether the measured hydrocarbons were due to the fuel was desorbing from the oil. This was accomplished by conducting a series of iso-octane-fueled tests.

8.4.5 450 Cycle Iso-Octane-Fueled Stop-Injection Tests

In order to investigate the effects of fuel diffusion into engine oil, a series of iso-octane-fueled stop-injection tests were conducted. Since iso-octane has similar diffusion characteristics into oil as indolene, yet has a much lower boiling point (160^{o}C for the 90% distillation of indolene versus 100^{o}C for iso-octane), stop-injection tests provide information on the relative contribution of oil absorption/desorption on stop-injection hydrocarbon concentrations.

Varied load tests were conducted similar to the load tests presented in section 8.4.4. Fuel injection pulsewidths were set to 10, 9.5, and 8.7 ms for the 100% load, 75% load, and 55% load cases respectively. Five tests were run at each condition and the results averaged together. The results of the tests, along with the indolene presented in section 8.4.4 may be seen in Figure 8.23.

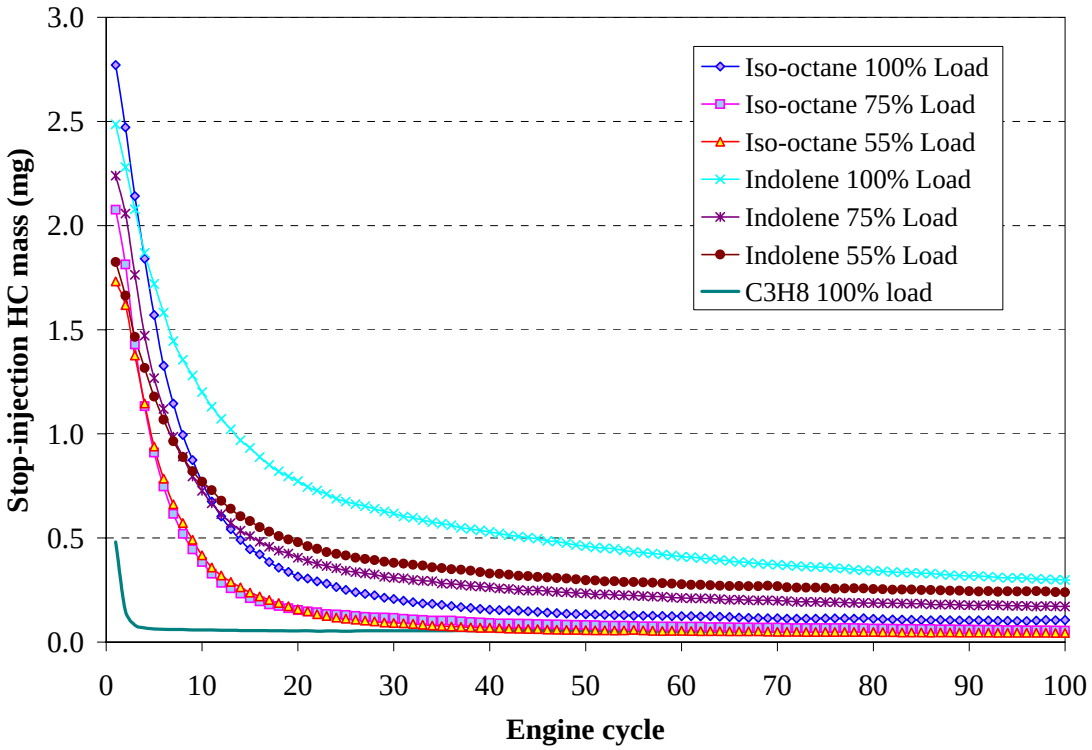

Figure 8.23 Low siphon-tube fuel injection pressure 450 cycle cumulative stop-injection HC mass.

From Figure 8.23 it may be seen that iso-octane, under all load conditions results in a smaller fuel film contribution than indolene. Even though the first cycle mass for the 100% load case is greater for iso-octane than indolene, the hydrocarbon mass decays more rapidly. Around the 100th engine cycle, iso-octane approaches the propane hydrocarbon contribution. Since the boiling point of iso-octane is significantly less than that of indolene, yet has similar diffusion properties into oil, this is suggestive that diffusion into oil does not play a significant role releasing hydrocarbons long after fuel injection has ceased.

To gain more insight into the film behavior, the cycl-resolved propane hydrocarbon mass was subtracted from the indolene and iso-octane results. Since propane does not form a fuel film yet can have crevice volume hydrocarbon emissions,

subtracting its contribution removes the crevice volume hydrocarbon contribution. Also, issues associated with oil consumption or other engine physics may be removed. The results after removing the propane contribution and integrating the hydrocarbon masses, may be viewed in Figure 8.24.

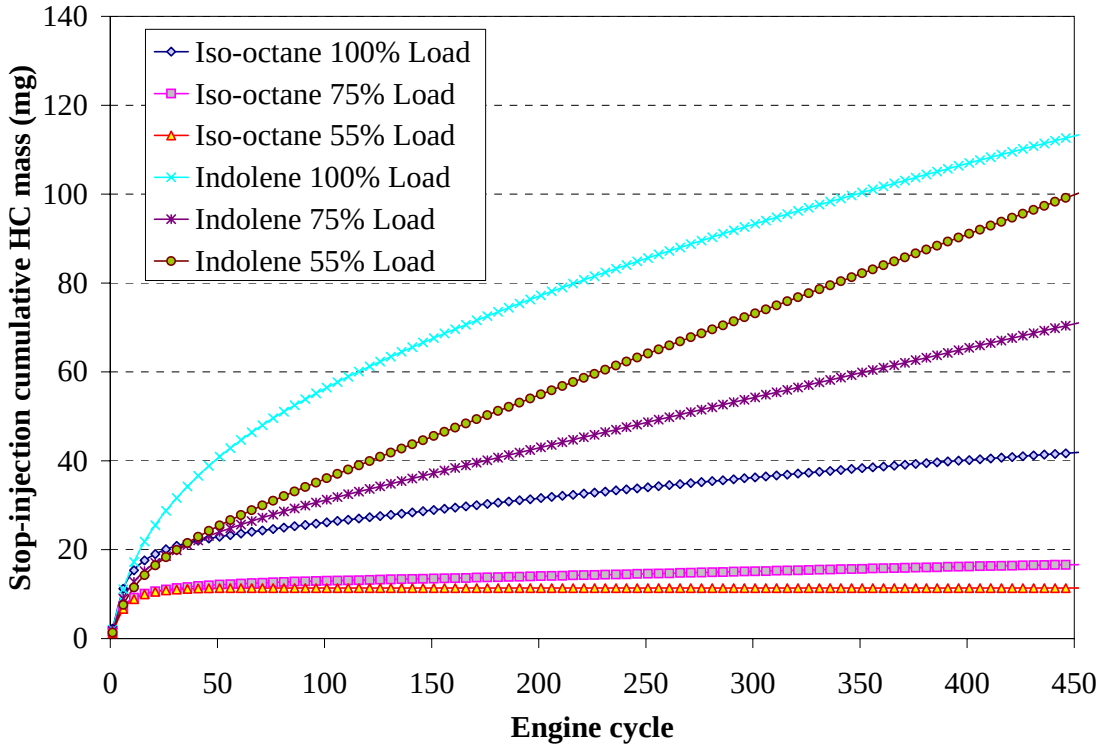

Figure 8.24 Low siphon-tube fuel injection pressure 450 cycle cumulative stop-injection HC mass: propane contribution removed.

From Figure 8.24 one finds that the iso-octane fuel film depletes more rapidly than does indolene. For both the 55% and 75% load iso-octane case, the film has nearly evaporated indicated by the near constant cumulative mass. The integrated fuel film mass for the iso-octane is much less than that of the indolene for all load cases. This overall reduction in mass indicates that the higher boiling point of indolene has a strong effect on the rate of fuel film depletion. Since both fuels exhibit roughly the same oil

diffusive properties, results also suggest that oil absorption does not contribute significantly to the overall hydrocarbon mass detected.

A final assessment of the relative differences between high and low pressure siphon-tube fuel injection was conducted with iso-octane. These iso-octane-fueled stop-injection tests consisted of matching operating conditions and varying the fuel injection pressure. Engine load was set to 100%, and theA/F ratio set to 14.7:1. Fuel injection timing set to TDC. The engine was run at 3060 RPM, and after reaching steady state conditions, five data sets were collected for both high and low pressure. The results were then averaged together. Figure 8.25 displays the results.

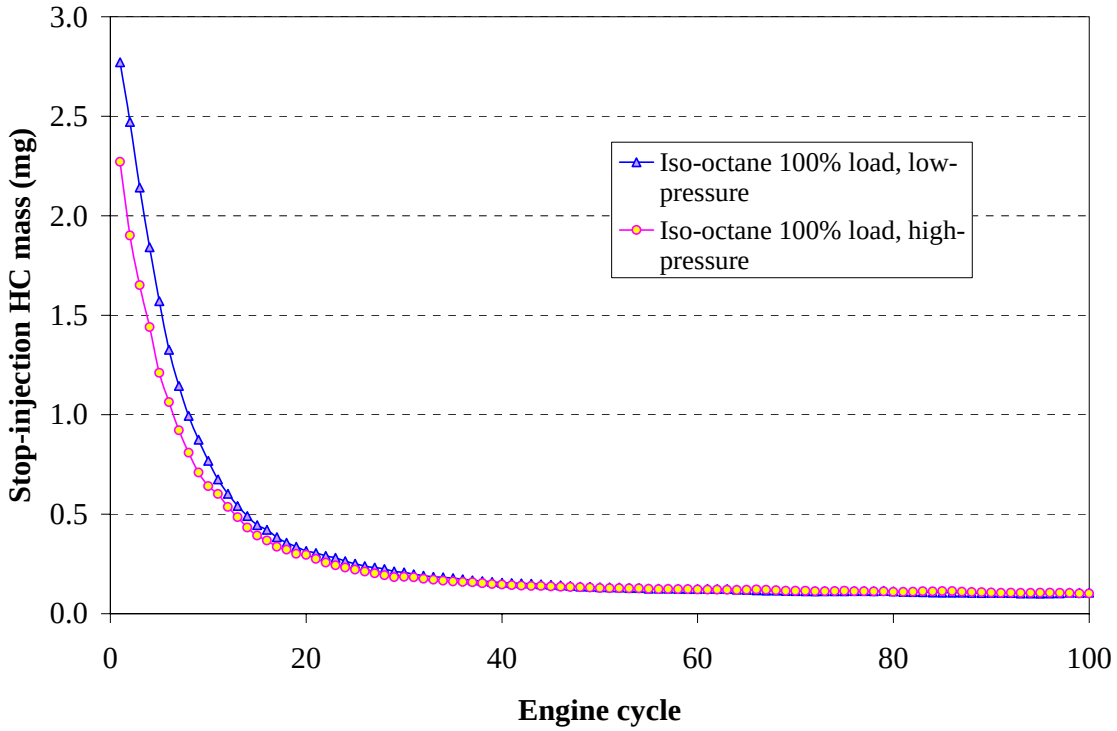

Figure 8.25 Low siphon-tube fuel injection pressure 450 cycle cumulative stop-injection HC mass.

From Figure 8.25, it may be seen that the initial fuel film mass under high pressure conditions is less than that of low pressure. Results indicate that 33% of the fuel inducted per cycle comes from the fuel film for the low pressure case, and 27% of the fuel for the high pressure case. In viewing hydrocarbon depletion, one finds the rate of depletion and final datum is nearly identical for both runs. The reduction in mass for the high-pressure case may be due to the increased contact time the fuel has with the warm port wall assisting in vaporization. The boiling point of iso-octane is much less than indolene affecting the rate of film depletion, and this appears to be the dominant factor in film depletion.

Summary

Results to the three- cycle skip-injection tests indicate that dynamics other than fuel film dynamics lead to erroneous results. The results are thought to be caused by engine dynamic excursions brought on by the engine misfires. Results to the single skip-injection tests correlate well with the first cycle hydrocarbon masses found for the stop-injection tests. Stop-injection tests were found to be a reliable and accurate testing method for measuring fuel film masses.

A summary of the skip- and stop-injection tests may be seen in Table 8.1. It was found that contribution to the fuel inducted into the engine per cycle is approximately 33%, regardless of engine load or siphon-tube fuel injection pressure. This was found for both iso-octane and indolene. Generally, mass decreases with load, with the exception of the 55% load case using indolene. The cumulative fuel film masses were found to be significantly large for all indolene cases, with hydrocarbons still present after 450 engine cycles of stop-injection. Iso-octane contributed less to overall fuel film masses, and was due to the lower boiling point of the fuel. Results indicate that vaporization characteristics of the fuel dominate all other effects (i.e. load, injection pressure).

Fuel	Load (%)	Injection pressure	Single Skip-Injection: % mass contributed by fuel film	Stop-Injection: % mass contributed by fuel film	Cumulative mass # cycle 450: corrected by C_3H_8 (mg)	Steady mass?
Indolene	100	high	36	-	-	-
	75	high	37	-	-	-
	55	high	33	-	-	-
	100	low	35	30	116.1	N
	75	low	35	32	73.6	N
	55	low	33	31	104.3	N
Iso-octane	100	low	-	33	42.6	N
	75	low	-	29	16.8	Y
	55	low	-	30	11.4	Y

Table 8.1 Skip- & Stop-Injection testing results.

9

SUMMARY AND RECOMMENDATIONS

9.1 Summary

Five methods of quantifying and characterizing fuel films during transient engine operation were utilized. These methods were fixed throttle, transient fueling tests, fixed fuel mass flow, transient throttle tests, capacitive fuel film measuring tests, skip-injection FFID exhaust sampling tests, and stop-injection FFID exhaust sampling tests.

Propane-fueled step fueling transients allowed for determination of UEGO sensor response. These results were compared to indolene-fueled step transient test. Results to the indolene-fueled tests did not indicate a large perturbation of the fuel film, yet indicated the presence of fuel films by compromised sensor response time. Results to the step throttle transient tests indicated the presence of a fuel film due to A/F excursions following the transient. These excursions were not present for propane-fueled tests. It was found that lean excursions occur during throttle opening, and that rich excursions occur for throttle closing.

Skip-injection test results were not indicative of fuel film behavior due to dynamic engine excursions caused by the misfires. Stop-injection tests were found to be the most accurate method of determining a global fuel film mass, and the mass of fuel inducted into the cylinder per cycle from the fuel film. The localized capacitance technique of calibrating and measuring thin fuel films was developed, however location of two sensors in the intake port did not indicate the presence of fuel films. This was attributed to the locations of the sensors, which were compromised by spatial constraints.

9.1.1 Summary Of Step-Fueling Transient Tests

Propane-fueled step fueling transient tests determined the minimum UEGO sensor response time to be one-half of an engine cycle under full load conditions. No apparent transient excursions were found. Sensor response time was determined as the sum of two time constants: τ_1, the amount of time it takes the sensors to see the exhaust gas after EVO, and τ_2, the amount of time it takes the sensor to respond as modeled by a first order equation. Similar indolene-fueled transient tests determined that transient excursions were minimal. Results indicated the sensor response to be approximately twice that found for propane tests. This suggests that impulsive fuel transients do not disturb the fuel film to a great extent. The longest sensor response time for indolene-fueled tests was found at 90^o ATDC injection timing.

9.1.2 Summary Of Step-Throttle Transient Tests

Results to the propane-fueled tests indicated a very slight excursion during throttle closing during the high-to-low load transient tests. Since propane does not form a fuel film, results indicated either a slight mixing or sensor response effect. These results were not seen for the tests conducted under identical conditions, in the reverse transient direction (low-to-high transient tests). This indicated that sensor response was most likely the cause of the anomaly.

High and low pressure indolene-fueled tests indicated a lean excursion during throttle opening, while a rich excursion occurring during throttle closing. This was caused by the increased reaction rate of the air to the transient. Low pressure throttle

transient tests indicate that the A/F mixture preparation is not as homogeneous as the high pressure case, though the excursions were still present.

The overall excursion magnitude for throttle transient tests is significantly greater than for step-fueling transients. This indicates that intake air charge motion plays a more significant role in the formation of fuel films than fuel delivery.

9.1.3 Summary Of Capacitance Sensor Fuel Film Measurements

A capacitive technique capable of measuring fuel films to within 50 μm was developed. Small minimally intrusive sensors were designed and fabricated that were temperature and solvent resilient. Two techniques were used to calibrate the sensors: a wet film gravimetric technique, and a dry film technique. Due to adhesion of the film, the gravimetric technique of calibrating the sensors was found to be insufficient in the range of fuel films desired. Using tape as a dry film, the sensors were reliably calibrated to within 50μm.

After calibration, two sensors were located within the engine intake port. The engine was run under a variety of loads and A/F ratios at steady state, yet the sensors did not detect any fuel film. To test the sensors, the engine was motored and fuel was directed over the sensors via a syringe. These tests confirmed that the sensors worked. It was concluded that no fuel film was present in the vicinity of the sensors.

9.1.4 Summary Of Skip-Injection Tests

Results to the single and three cycle tests indicated high hydrocarbon concentrations during the engine cycles in which fuel injection was disabled. This indicated the

presence of significant fuel film formation. Tests were conducted using propane and indolene fuel, with the single cycle hydrocarbon indolene-fueled concentration approximately seven times greater than that of propane. Three cycle skip-injection tests resulted in behavior not indicative of the depletion of a fuel film as would be anticipated. Data for the three cycle skip-injection tests showed that four out of every thirty engine cycles were usually misfires (three due to the skip-injection, the fourth often caused by a portion of the fuel reforming the depleted fuel film after three skips). The frequency of the misfires led to engine dynamics that altered fuel film behavior, i.e. an increase in fuel film after fuel injection cessation.

The single skip-injection tests were consistent with the stop-injection results, the only deviation being a slight elevation in the single skip-injection mass to the first cycle of the stop-injection tests. This was thought to be caused by the slight engine dynamics due to the misfire. It was determined that the single skip-injection method was an accurate method of determining the contribution of fuel film the mass of fuel inducted per cycle. Test results indicated that approximately 35% of the fuel inducted per cycle comes from the fuel film, regardless of engine load or siphon-tube fuel injection pressure.

9.1.5 Summary Of Stop-Injection Tests

Both 45 and 450 cycle stop-injection tests were conducted using propane and indolene fuel. This technique allowed for global determination of fuel film masses and behavior. After 45 cycles, it was found that a small but definitive hydrocarbon mass was being measured for both indolene and propane. This led to conducting a series of 450 cycle stop-injection tests (taking approximately 20 seconds to complete after the cessation fuel

injection). Results to propane, indolene, and iso-octane all indicated that a measurable hydrocarbon concentration still existed. This concentration was on the order of 600 ppm for propane and the low load tests for iso-octane, and on the order of 2400 ppm for indolene. This indicated that a fuel film was still present for all of the indolene fueled tests and the 100% load case for iso-octane.

By subtracting out the propane contribution, it was found that indolene formed a cumulative fuel film equivalent to well over 10 cycles worth of engine fuel, and that the time constant for the depletion of the film relatively slow. Although the mass of fuel inducted per cycle from the fuel film for iso-octane was comparable to indolene, the rate of depletion was much faster for iso-octane, reaching a final value comparable to that of propane. This indicated that oil absorption/desorption was not a significant contributor to the hydrocarbon concentration.

For both indolene and iso-octane, the mass of fuel contributed to the cylinder from the fuel film to the engine cylinder per cycle was also found to be approximately 32%, regardless of load or siphon-tube fuel injection pressure. These results correlate well with those found for the single skip-injection tests. The cumulative mass of iso-octane is significantly less than that of indolene, and generally, the fuel film mass decreases with load, with the exception of the 55% load case using indolene.

9.2 Recommendations

Win the lottery, don’t go to grad school. The amount of sleep you get will be exponential.

By fixing fuel injection while varying throttle position, and conversely by fixing throttle and varying fuel injection, real world transient operation is not truly encountered. Although these techniques allow for insight into fuel film behavior, transient tests should be conducted using an actual carburetor setup. Results to such tests could then be compared to the decoupled tests conducted in this work to further determine the difference between impulsive air or fuel transients, and their respective effect.

The capacitance thin fuel film measuring technique presented in this work shows promise. The main problem with using this technique for this work was spatial constraints. However, it was shown that very thin films could be measured, and the rate at which the sensor operates would allow for cycle resolved film measurements. There currently exist techniques of applying conductive and flexible ceramic inks to thin films (such as polyimide). Such techniques could be applied to develop very thin and flexible sensors that could be shielded from stray capacitance as was done in this work. An array of these thin sensors could be located in the intake port, on the throttle plate, and within the throttle body of the carburetor and would allow for spatial cycle resolved fuel film measurements.

The issue of hydrocarbons still present after 450 engine cycles following the cessation of fuel injection was not fully addressed. This behavior was present not only for indolene and iso-octane, but propane as well. It is difficult to imagine that such a significant fuel film could exist in an air-cooled engine with a relatively small and hot intake port. It is my belief that oil absorption does play a role after the majority of the fuel film has been inducted. Perhaps a method of sending a fraction of the crank-case oil

through a gas-chromatograph and analyzing speciating the oil could shed light into the relative percent of fuel that exists in the oil under various operating conditions.

Since results to the work indicate that the lower boiling point fuel, iso-octane, forms a fuel film that depletes much faster than indolene, tests need to be conducted to determine the relative transient excursions that occur when it is used. Since it appears that the fuels vaporization characteristics have the largest effect in fuel film behavior, these tests may confirm a reduction in excursions. This could lead to experiments involving the heating of the manifold, throttle body, throttle plate, or pre-heating the fuel itself. These tests would could gain insight into the relative effects that certain engine components have on fuel vaporization, and the extent to which they reduce A/F excursions. Insight into this behavior could be used to design fuel-metering devices that may release the fuel in such a manner as to contact hotter surfaces assisting in excursion reductions, or perhaps designs that would involve pre-heating of the fuel.

REFERENCES

1) Heywood, J.B., *Internal Combustion Engine Fundamentals*, McGraw-Hill Publishing Company: New York, N.Y., 1988.

2) Bonneau, B.J., "Development of a Homogeneous Mixture System and Comparison with Carbureted Utility Engine Emissions and Performance", M.S. Thesis, Mechanical Engineering Department, University of Wisconsin-Madison, 1994

3) Westrate, B., "The Development of Diagnostics and Testing Methods for the Characterization of Carburetor Exit Flow Conditions", M.S. Thesis, Mechanical Engineering Department, University of Wisconsin-Madison, 1994

4) Cunningham, M.J., "Effects of Mixture Preparation Parameters on Utility Engine Performance and Emissions", M.S. Thesis, Mechanical Engineering Department, University of Wisconsin-Madison, 1996

5) Itano, E., "Characterization of Carburetor Exit Flow", M.S. Thesis, Mechanical Engineering Department, University of Wisconsin-Madison, 1996

6) Boyce, B.P., "Effect of Air Fuel Ratio and Ignition Timing on Thermal Loading and Engine Performance of a Spark Ignited, Homogenous Charged, Four Stroke, Air-Cooled Engine", M.S. Thesis, Mechanical Engineering Department, University of Wisconsin-Madison, 1998.

7) Strauss, S., "Investigation of Fueling Strategies for the Transient Operation of a Small Four Stroke Engine", M.S. Thesis, Mechanical Engineering Department, University of Wisconsin-Madison, 1999.

8) Strucel, J.E., "Experiments and Computational Predictions of Thermal Energy Flows Occurring Within a Spark Ignited, Homogeneous Charge, Four Stroke, Air Cooled Engine", M.S. Thesis, Mechanical Engineering Department, University of Wisconsin-Madison, 2000

9) Kay, I.W., "Manifold Fuel Film Effects in an SI Engine", SAE Paper 780944, 1978.

10) Aquino, C.F., "Transient A/F Control Characteristics of the 5 Liter Central Fuel Injection Engine", SAE Paper 810494, 1981.

11) Hires, S.D., Overington, M.T., "Transient Mixture Strength Excursions- An Investigation of Their Causes and the Development of a Constant Mixture Strength Fueling Strategy", SAE Paper 810495, 1981.

12) Aquino, C.F., Fozo, R.S., "Steady State and Transient A/F Control Requirements for Cold Operation of a 1.6 Liter Engine with Single-Point Fuel Injection", SAE Paper 850509, 1985.

13) Bardon, M.F., Rao, V.K., Gardiner, D.P., "Intake Manifold Fuel Film Transient Dynamics", SAE Paper 870569, 1987.

14) Yamada, T., Hayakawa, N., Kami, Y., Kawai, T., "Universal Air-Fuel Ratio Heated Exhaust Gas Oxygen Sensor and Further Applications", SAE Paper 920234, 1992.

15) Shayler, P.J., Scarisbrick, A., "Determining Fuel Transfer Characteristics for Mixture Control During Transient Operation", IMechE paper, C469/008, 1993.

16) Chen, G., Vincent, M.T., Gutermuth, T.R., "The Behavior of Multiphase Fuel-Flow in the Intake Port", SAE Paper 940445, 1994.

17) Bourke, M. C., Evers, L.W., "Fuel Film Dynamics in the Intake Port of a Fuel Injected Engine", SAE Paper 940446, 1994.

18) Almkvist, G., Eriksson, S., "A Study of Air to Fuel Transient Response and Compensation with Different Fuels", SAE Paper 941931, 1994.

19) Mooney, J.J., Hwang, H.S., Daby, K.O., Winberg, J.R., "Exhaust Emission Control of Small 4-Stroke Air Cooled Utility Engines An Initial R&D Report", SAE Paper 941807, 1994.

20) Shayler, P.J., Teo, Y.C., Scarisbrick, A., "Fuel Transport Characteristics of Spark Ignition Engines for Transient Fuel Compensation", SAE Paper 950067, 1995.

21) Johnen, T., Haug, M., "Spray Formation Observation and Fuel Film Development Measurements in the Intake of a Spark Ignition Engine", SAE Paper 950511, 1995.

22) Almkvist, G., Denbratt, I., Josefsson, G., Magnusson, I., "Measurements of Fuel Film Thickness in the Inlet Port of an S.I. Engine by Laser Induced Flourescence", SAE Paper 952483, 1995.

23) Ladommatos., N., Rose, D.W., "On the Causes of In-Cylinder Air-Fuel Ratio Excursions During Load and Fuelling Transients in Port-Injected Spark-Ignition Engines", SAE Paper 960466, 1996.

24) Curtis, E.W., Aquino, C.F., Trumpy, D.K., Davis, G.C., "A New Port and Cylinder Wall Wetting Model to Predict Transient Air/Fuel Excursions in a Port Fuel Injected Engine", SAE Paper 961186, 1996.

25) Chen, G., Asmus, T.W., Weber, G.T., "Fuel Mixture Temperature Variations in the Intake Port", SAE Paper 961194, 1996.

26) Skippon, S.M., Nattrass, S.R., Kitching, J.S., Hardiman, L., Miller, H., “Effects of Fuel Composition on In-Cylinder Air/Fuel Ratio During Fueling Transients in an SI Engine, Measured Using Differential Infa-Red Absorption”, SAE Paper 961204, 1996.

27) Itano, E., Shakal, A.J., Martin, J.K., Shears, D., Engman, T.J., “Carburetor Exit Flow Characteristics”, SAE Paper 961730, 1996.

28) Imatake, N., Saito, K., Morishima, S., Kudo, S., Ohhata A., “Quantitative Analysis of Fuel Behavior in Port-Injection Gasoline Engines”, SAE Paper 971639, 1997.

29) Hentschel, W., Grote, A., Langer, O., “Measurement of Wall Film Thickness in the Intake Manifold of a Standard Production SI Engine by Spectroscopic Technique”, SAE Paper 972832, 1997.

30) Stiyer, M.J., Ghandhi, J.B., “Direct Calibration of LIF Measurements of the Oil Film Thickness Using the Capacitance Technique”, SAE Paper 972859, 1997.

31) Bauer, W., Balun, P., Heywood, J.B., “Heat Transfer and Mixture Vaporization in Intake Port of a Spark Ignited Engine”, SAE Paper 972983, 1997.

32) Phase 2 Emission Standards for New Nonroad Spark-Ignition Engines At or Below 19 Kilowatts, Federal Register: January 27, 1998 (Volume 63, Number- 17), Proposed Rules, From the Federal Register Online via GPO Access [wais.access.gpo.gov], Environmental Protection Agency.

33) Graham, J., Kryzeminski, M., Popovic., Z., “Capacitance based scanner for thickness mapping of thin dielectric films”, Review of Scientific Instruments, Vol. 71, Number 5., 1996.

34) Simon, Dr. Ing. N., Bosch, R., “Kraftstoffwandefilmuntersuchungen Im Saugrohr des Ottomotors mit Zentraleinspritzung”, Reihe 12, Verkehrstechnik/Fahrzeugtechnik, Nr. 141., 1990.

35) Horiba Mexa 110 Lambda Instruction Manual, February 1992.

Appendix A

Calibrations

Appendix A-1
Calibration Of The Throttle Position Sensor With Respects To Engine Load

For the following throttle position calibration, the engine was run at 3060 RPM for approximately a half hour to reach steady state. Propane was selected as the fuel, and injection pressure set to 90 psi. A/F ratio was set to approximately 14.7:1. This calibration was used to set engine loads during tests.

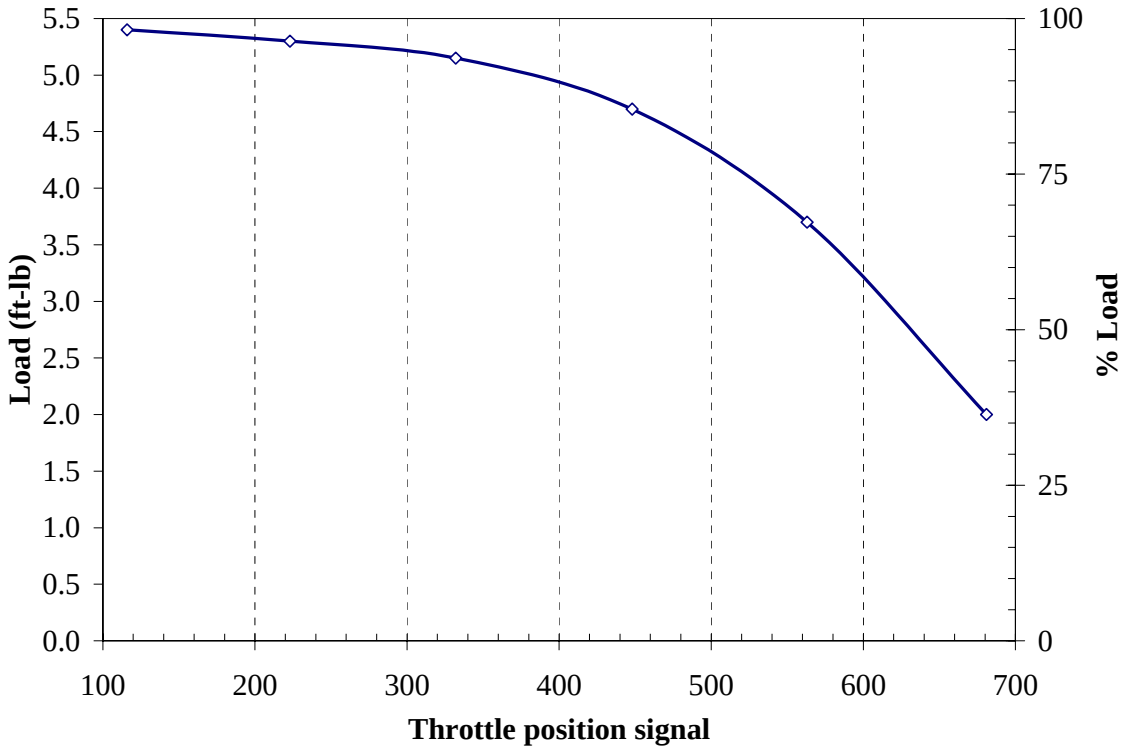

Appendix A-2
Calibration Of The Throttle Position Sensor Voltage With Respects To Engine Load

The following throttle position calibration, the sensor output voltage was correlated to the digital readout from the calibration in Appendix A-1. This was required for some of the concentration to mass conversions during the FFID tests.

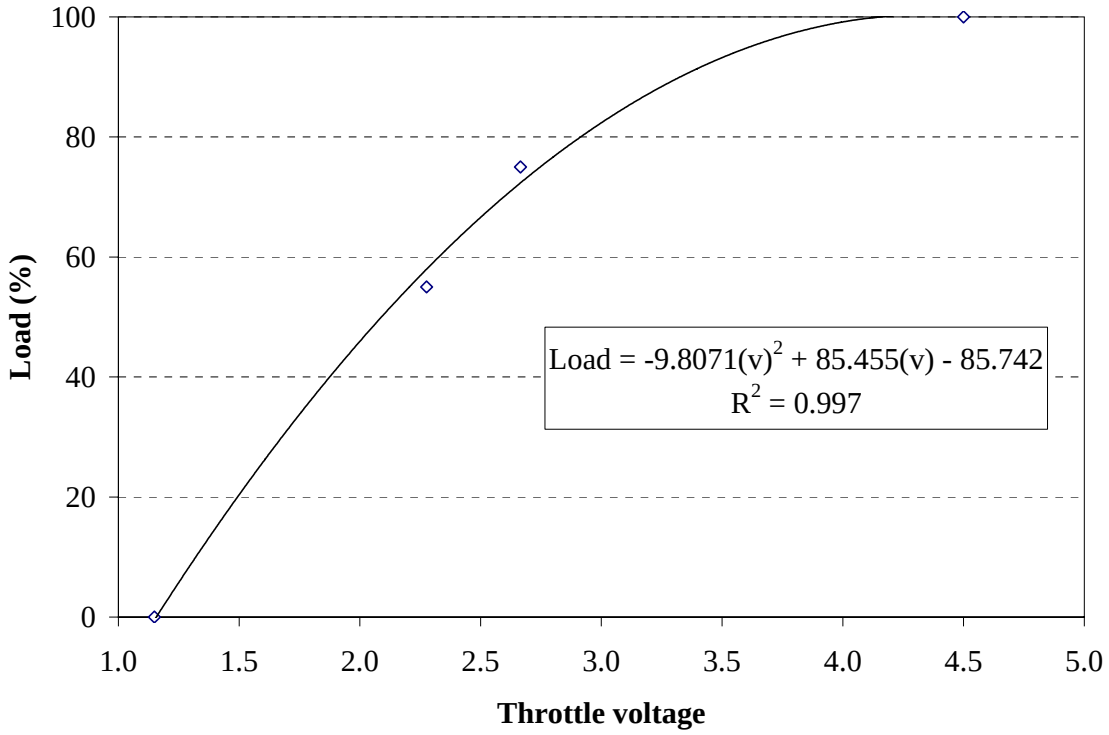

Appendix A-3
Calibration Of Pressure Transducer

The following calibration was conducted on a Kistler model 6061B, serial number 1013178 pressure transducer on 12/25/99. Charge amplifier settings were set to 200 divisions per volt, and the long time constant setting was used.

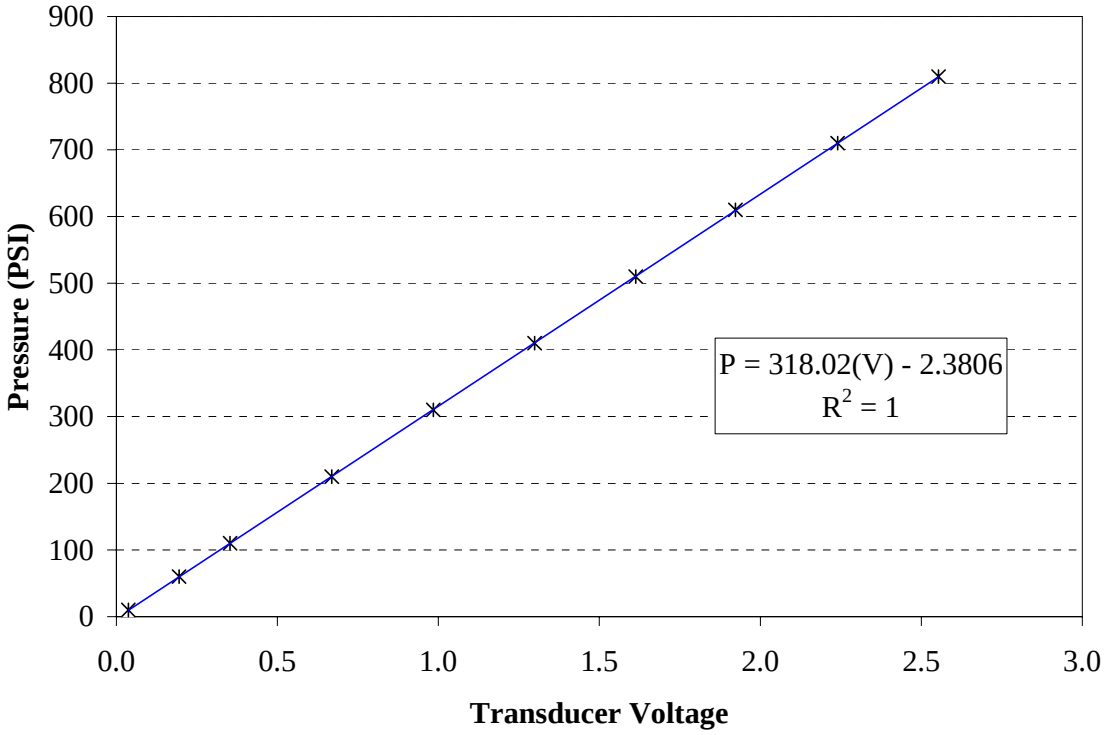

Pressure PSI	V_0	V(P)	V_{end}	ΔV
10	0.006	0.036	0.004	0.037
60	0.005	0.194	0.003	0.195
110	0.006	0.352	0.004	0.353
210	0.006	0.668	0.004	0.669
310	0.005	0.984	0.004	0.985
410	0.005	1.298	0.003	1.299
510	0.005	1.613	0.005	1.613
610	0.005	1.921	0.002	1.923
710	0.004	2.239	0.002	2.240
810	0.005	2.552	0.002	2.554

Appendix A-4
Calibration Of Engine Mass Airflow

For the following mass air flow calibration, the engine was run at 3060 RPM for approximately a half hour to reach steady state. Mass air flow was determined for both propane and indolene. Fuel injection pressure for propane was set to 620 kPa. Fuel injection pressure for indolene was set to 345 kPa. Fuel injection timing was set to TDC of the intake stroke for both cases. A/F ratio was held at approximately 14.7:1 for both calibrations. Humidity was recorded 20%, and barometric pressure at 743 mm Hg. Temperature was recorded at 21.7 ^{o}C.

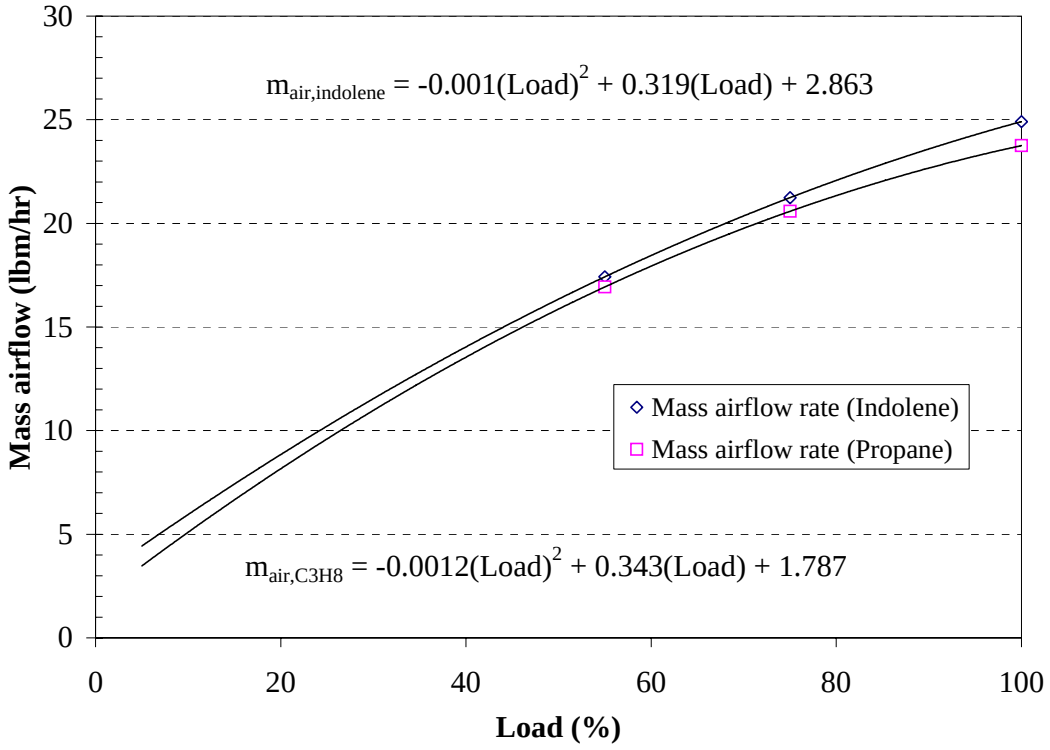

```
"Program to calculate the Air/Fuel Ratio indicated by the HMS and the Yardman in B121"
"8/20/00 used forrest jehlik    adapted from Mike Cunningham 6/12/95"

"Required Inputs form the Yardman bench:
        Mass air flow rate is a function of pressure drop across the laminar element (Delta_P_15).
        There are slight corrections for temp, humidity, inlet pressure, etc."
    humd        =20         "Relative Humidity Ratio"
    baro        =74.4 - 0.53    "Barometric Pressure in cm of Hg: recorded in B119"
    temp        =70         "Air temperaure before LFE, Thermocouple 1 on first dial"
    DELTA_P_15  =1.14       "Differential Pressure in inches of H2O:  Digital manometer"
    inps        =13.4       "Inlet Pressure to LFE:   U-tube monometer mounted next to
Yardman"

"Calculate the mass flow rate of fuel:
    ex. if the fuel flow is know comment out air fuel ratio specification to calculate it in the solution
        likewise if mass flow of fuel is desired comment it out"
    A\F = 14
    m_dot_fuel  = air_dot / A\F

"Constants"
    b           = 5.2634
    c           = 0-.14191
    visc_std    = 181.87
    temp_std    = 529.67
    pres_std    = 14.696
    dens_std    = 0.074884

"Calculations"
    corinps     = inps * (62.366 / 62.426) * (51.75 / 27.71)
    baro_conv   = baro * (1000 / 100)
    P_f_1       = corinps + baro_conv
    P_f         = P_f_1 * (1 / 51.75)
    T_f         = 459.67 + temp
    DELTA_P     = DELTA_P_15 * (62.366 / 62.426)

"Viscosity of the wet air calculated from lookup table"
    rho     = Interpolate('rho','humidity',humidity=humd)
    rho_1   = Interpolate('rho_1','humidity',humidity=humd)
    rho_2   = Interpolate('rho_2','humidity',humidity=humd)
    frhv    = rho + rho_1 * temp + rho_2 * temp^2
    vwetair = ((14.58 * (((459.67 + temp) / 1.8)^1.5))/(((459.67 + temp ) / 1.8)+110.4))*frhv

"Density of Air from lookup table"
    denscf  = Interpolate('density ratio','temperature',temperature=temp)
    pdrywet = 1 + (denscf * humd / 20 * 0.01)
    pwetdry = 1 / pdrywet
    svfl    = (b * DELTA_P+c * delta_P^2) * (visc_std / vwetair) * (temp_std / T_f) * (P_f /
pres_std) * pwetdry
    air_dot = svfl * dens_std * 60
```

Appendix A-5
Propane & Indolene C_1 Mass Fraction Factor-
Used For PPM-To-Mass Conversions For FFID Analysis

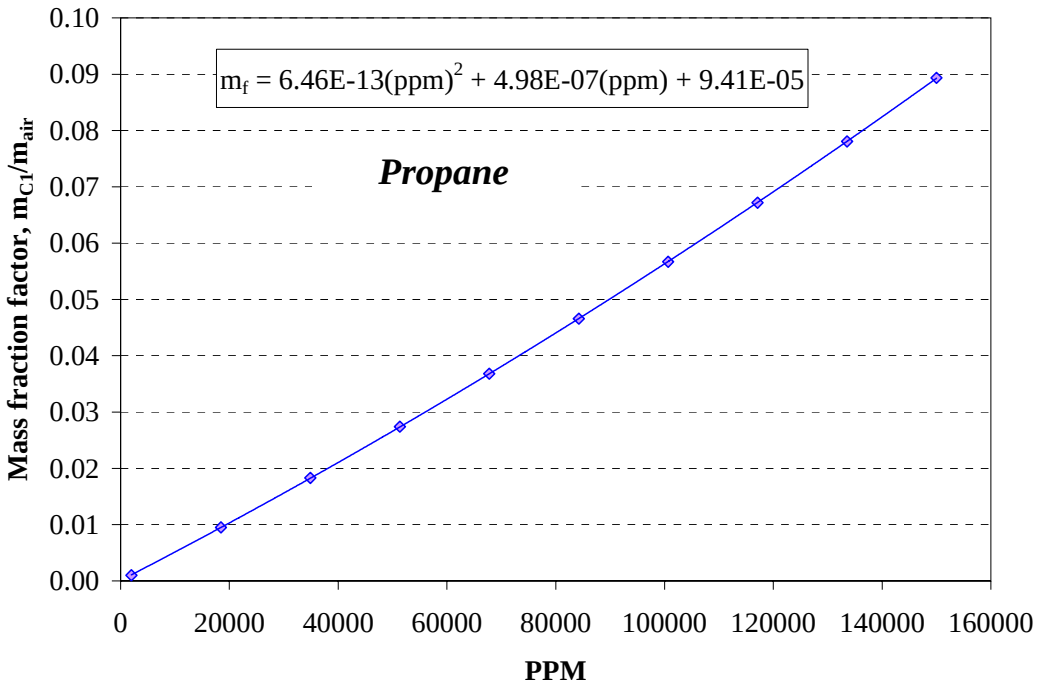

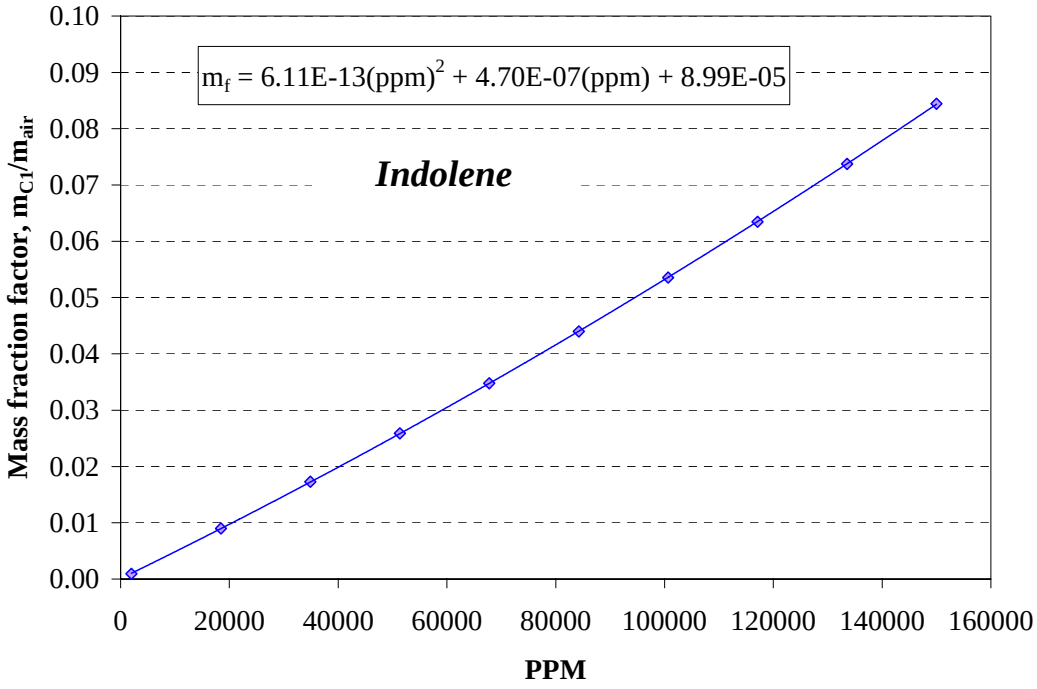

Appendix B

EES Programs

Appendix B-1 UEGO sensor response τ_1 and τ_2 determination
Appendix B-2 Propane fuel injection delivery tube propane storage potential
Appendix B-3 Tape dielectric constant determination

Appendix B-1
UEGO Sensor First Order Response Determination

This program calculates τ_1 and τ_2 by doing minimizing the least squared difference between the sensor response and the collected A/F data. The A/F data is presented in a lookup table.

```
function response(time, tau1,tau2,AF1,AF2)
if (time<tau1) then
    response:=AF1
else
    response:=AF2+(AF1-AF2)*exp(-(time-tau1) / tau2)
endif
end

AF1=15.57; AF2=11.72;
    duplicate i=1,136
        time[i]=lookup(i,'time')
        af[i]=lookup(i,'af')
        r[i]=response(time[i], tau1,tau2,AF1,AF2)
    end

SSQ=sum((af[i]-r[i])^2,i=1,136)
```

Appendix B-2
Cycles Of Propane Stored In The Propane Fuel Injection System Delivery Tube

This EES program calculates number of engine cycles of propane that may be stored in the propane fuel injection system delivery tube.

```
"the following calculates the mass of fuel used per cycle for the Briggs engine running WOT with
75% percent volumetric efficiency"
"also included is a calculation of the volume of fuel that a single injection event displaces"

"lists constants"
      AF_ratio=          14.7
      displacement=      146                  "cm3"
      eta_V=             0.75                 "engine is 75% volumetric efficient"
      P=                 101.235              "ambient pressure, kPa"
      T=                 300                  "port temperature, Kelvin"
      R=                 8.3145               "universal gas constant, kJ/kmol-K"
      MW_air=            MOLARMASS(air)       "kg/kmol"
      MW_c3h8=           MOLARMASS(C3H8)      "kg/kmol"

"calculates air and fuel densities"
      rho_air=           P * MW_air / ( R * T )          "kg/m3"
      rho_c3h8=          P * MW_c3h8 / ( R * T )         "kg/m3"

"calculates mass of fuel/cycle"
      m_air_cycle=       eta_v * displacement * CONVERT(cm3, m3) * rho_air
          "kg"
      m_fuel_cycle=      1 / AF_ratio * m_air_cycle * CONVERT(kg, mg)
      "mg"
      v_fuel_cycle=      m_fuel_cycle / rho_c3h8 * CONVERT(mg, kg) * CONVERT(m3,cm3)
      "cm3"

"calculates volume of 1/8 in tubing from injector to intake port"
      diameter=          0.125 - 2 * 0.014    "diameter of tube minus wall thickness, inches"
      length=            2                    "variable tube length"
      v_tubing=          PI * ( diameter^2 / 4 )* length * CONVERT(in3, cm3)

"calculates engine cycles of fuel stored in tubing"
      num_cycles=        v_tubing / v_fuel_cycle
```

Solution:

AF_{ratio} = 14.7	diameter = 0.097 [in]	displacement = 146 [cm3]	η_V = 0.75	length = 2 [in]	MW_{air} = 28.97 [kg/kmol]
MW_{c3h8} = 44.1 [kg/kmol]	$m_{air,cycle}$ = 0.0001287 [kg]	**$m_{fuel,cycle}$ = 8.757 [mg]**	**num_{cycles} = 0.0495**	P = 101.2 [kpa]	R = 8.315 [kj/kmol-k]
ρ_{air} = 1.176 [kg/m3]	ρ_{c3h8} = 1.79 [kg/m3]	T = 300 [k]	$v_{fuel,cycle}$ = 4.893 [cm3]	v_{tubing} = 0.2422 [cm3]	

Appendix B-3
Tape Dielectric Determination

This program calculates the dielectric constant of the Scotch® brand tape used for calibrating the capacitance sensor using the tape method. From the solution , the dielectric constant of tape was found to be approximately 7.

$$d_m = dist \cdot 0.000001$$

$$cap_{air} = \frac{0.000049}{d_m}$$

$$v_{tape} = 2.319 + 0.81666 \cdot \ln(cap_{tape})$$

$$ratio = \frac{cap_{tape}}{cap_{air}}$$

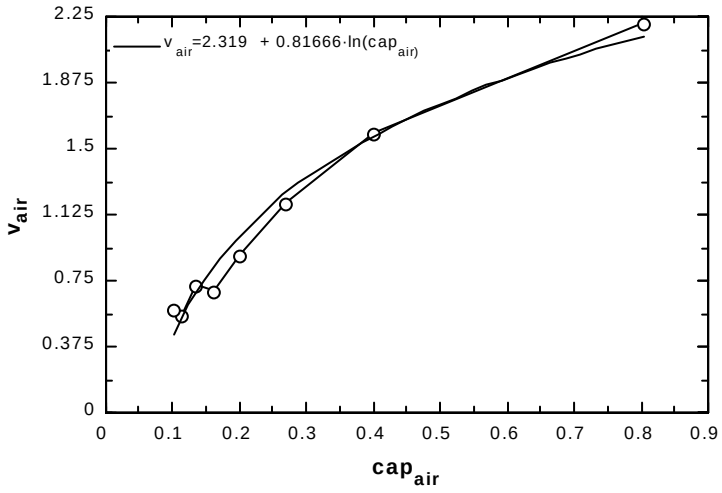

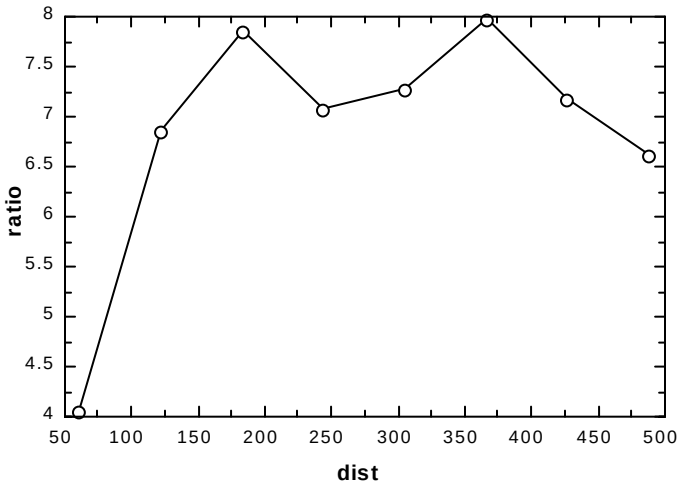

Appendix C

Visual Basic Data Analysis Programs

Appendix C-1 Transient fuel injection data analysis
Appendix C-2 Transient throttle data analysis

Appendix C-1
Transient Fuel Film Data Analysis Program:
Written By Adam Salvo

The following program analyzed the raw data runs from the Hi-Techniques data acquisition system for the step fueling transient tests. The program aligned five runs by finding a digital high signal that occurred at the onset of the transient. The five files were averaged together and reduced in size to a single file.

```
Option Explicit
Private trace1 As New dat      'Pressure
Private trace2 As New dat      'A/F
Private trace3 As New dat      'Injector Signal
Private trace4 As New dat      'Trigger
Private files1(20) As String
Private files2(20) As String
Private files3(20) As String
Private files4(20) As String
Public outputFile As String
Public numberOfFiles1
Public numberOfFiles2
Public numberOfFiles3
Public numberOfFiles4
Public filesLoaded As Boolean

Public Sub StartInjectorVariable()
'-------------------------------------------------------------------------------------
Dim index As Double
Dim j As Integer
Dim condensed(5000)
Dim xValue
Dim fileCount          'what file on
Dim total(725000)
Dim dumpPoint          'What data point to cut off unecessary data(count back 125 cycles)
Dim files As New FilePath
Dim channel
Dim temp
Dim triggerPoint       'where does trigger go high?
Dim count
'-------------------------------------------------------------------------------------
'LOAD FILES AND SUCH
'-------------------------------------------------------------------------------------
files.Show vbModal
If files.filesLoaded = False Then
   MsgBox "No files loaded - Exiting Sub", vbOKOnly, "No files loaded"
   Exit Sub
End If

numberOfFiles1 = files.numberOfFiles1
numberOfFiles2 = files.numberOfFiles2
numberOfFiles3 = files.numberOfFiles3
numberOfFiles4 = files.numberOfFiles4
```

```
If numberOfFiles2 <> numberOfFiles3 Or numberOfFiles3 <> numberOfFiles4 Then
   MsgBox "Channel 2, Channel 3, and Channal 4 have a different number of input files!", vbOKOnly,
"Channel 2/3 Input Files"
   Exit Sub
End If

MainForm.CDlg.ShowSave
outputFile = MainForm.CDlg.fileName

MainForm.MousePointer = vbHourglass

'Init File Path Arrays.  Need to save memory
channel = 1
Open App.Path & "\files.txt" For Input As #1

Do
   Input #1, temp
   If temp = "**********" Then
      channel = channel + 1
      index = 0
   Else
      If channel = 2 Then
         files2(index) = temp
         index = index + 1
      End If
      If channel = 3 Then
         files3(index) = temp
         index = index + 1
      End If
      If channel = 4 Then
         files4(index) = temp
         index = index + 1
      End If
   End If
Loop Until channel = 5

Close #1

'---------------------------------------------------------------------------------
'Initalize Arrays
'---------------------------------------------------------------------------------

trace2.Initialize (750000)
trace3.Initialize (750000)
trace4.Initialize (750000)

'---------------------------------------------------------------------------------
'Main Procedure Loop
'---------------------------------------------------------------------------------

For fileCount = 0 To numberOfFiles3 - 1

'#################################################################################
'Load Data channel 4
   MainForm.ProgramStatus.Caption = "Loading Channel #4 for file #" & fileCount + 1
```

```
    MainForm.ProgressBar1.Visible = True
    MainForm.Refresh

    If trace4.Load_File(files4(fileCount)) Then
        MainForm.MousePointer = vbDefault
        MsgBox "Error Loading File, Exiting CalcInjecter Sub", vbOKOnly, "File I/O Error"
        Exit Sub
    End If

'#########################################################################################
'Find where trigger goes high.
    MainForm.ProgramStatus.Caption = "Locating where trigger(Channel 4) goes high for file #" fileCount
+
    MainForm.Refresh

    For index = 0 To trace4.numberOfPoints
        If trace4.GetDataPoint(index) > 4 Then
            triggerPoint = index
            Exit For
        End If
    Next index

'#########################################################################################
'Load data channel 3
    MainForm.ProgramStatus.Caption = "Loading Channel #3 for file #" & fileCount + 1
    MainForm.ProgressBar1.Visible = True
    MainForm.Refresh

    If trace3.Load_File(files3(fileCount)) Then
        MainForm.MousePointer = vbDefault
        MsgBox "Error Loading File, Exiting CalcInjecter Sub", vbOKOnly, "File I/O Error"
        Exit Sub
    End If

'#########################################################################################
'Find next the point where the next injector pulse goes high.  This should be the first
'fat injector pulse width!
    MainForm.ProgramStatus.Caption = "Locating first(fat) injector pulse after trigger for file #" &
fileCount + 1
    MainForm.Refresh

    For index = triggerPoint To trace3.numberOfPoints
        If trace3.GetDataPoint(index) > 3.5 Then
            dumpPoint = index - 144000              'count back 100 cycles
            Exit For
        End If
    Next index

'#########################################################################################
'Read Channel 2
    MainForm.ProgramStatus.Caption = "Reading channel 2 for file #" & fileCount + 1
    MainForm.Refresh

    If trace2.Load_File(files2(fileCount)) Then
        MainForm.MousePointer = vbDefault
        MsgBox "Error Loading File, Exiting CalcInjecter Sub", vbOKOnly, "File I/O Error"
```

```
      Exit Sub
   End If
'#############################################################################################
'Align channel 2 data
   MainForm.ProgramStatus.Caption = "Aligning Channel #2 for file #" & fileCount + 1
   MainForm.Refresh

   trace2.numberOfPoints = trace2.numberOfPoints - dumpPoint

   For index = 0 To trace2.numberOfPoints
      Call trace2.SetDataPoint(index, trace2.GetDataPoint(index + dumpPoint))
      total(index) = total(index) + trace2.GetDataPoint(index)
   Next index

Next fileCount

'#############################################################################################
'Output average fuel/air mixture
MainForm.ProgramStatus.Caption = "Outputting average Air/Fuel Mixture."
MainForm.Refresh
Open outputFile For Output As #1
xValue = 0
If MainForm.Condense.value = 0 Then
   For index = 0 To trace2.numberOfPoints
      total(index) = total(index) / fileCount
      Print #1, total(index)
   Next index
Else
   For index = 0 To trace2.numberOfPoints
      If j = 160 Then
         j = 0
         condensed(count) = condensed(count) / (160 * fileCount)
         Print #1, xValue & "," & condensed(count)
         xValue = xValue + 0.111111111111
         count = count + 1
      Else
         condensed(count) = condensed(count) + total(index)
         j = j + 1
      End If
  Next index
End If
```

Close

```
'#############################################################################################
MainForm.MousePointer = vbDefault
MainForm.ProgramStatus.Caption = "Injector Calculations Finished"
MainForm.Refresh

End Sub
```

Appendix C-2
Transient Throttle Data Analysis Program:
Written By Adam Salvo

The following program analyzed the raw data runs from the Hi-Techniques data acquisition system for the throttle transient tests. The program aligned five runs by finding a digital high signal that occurred at the onset of the transient. The five files were averaged together and reduced in size to a single file.

```
Option Explicit
Private trace1 As New dat      'Pressure
Private trace2 As New dat      'A/F
Private trace3 As New dat      'Injector Signal
Private trace4 As New dat      'Trigger
Private files1(20) As String
Private files2(20) As String
Private files3(20) As String
Private files4(20) As String
Private outputFile As String
Private outputFile2 As String
Public numberOfFiles1
Public numberOfFiles2
Public numberOfFiles3
Public numberOfFiles4
Public filesLoaded As Boolean

Public Sub StartInjectorSlope()
'-------------------------------------------------------------------------------
Dim index As Double
Dim j As Integer
Dim condensed(5000)
Dim iCondensed(5000)
Dim xValue
Dim fileCount          'what file on
Dim total(725000)
Dim total2(725000)
Dim dumpPoint          'What data point to cut off unnecessary data(count back 125 point)
Dim files As New FilePath
Dim channel
Dim temp
Dim triggerPoint       'where does trigger go high?
Dim count

'-------------------------------------------------------------------------------
'LOAD FILES AND SUCH
'-------------------------------------------------------------------------------
files.Show vbModal
If files.filesLoaded = False Then
   MsgBox "No files loaded - Exiting Sub", vbOKOnly, "No files loaded"
   Exit Sub
End If

numberOfFiles1 = files.numberOfFiles1
```

```
numberOfFiles2 = files.numberOfFiles2
numberOfFiles3 = files.numberOfFiles3
numberOfFiles4 = files.numberOfFiles4

If numberOfFiles2 <> numberOfFiles3 Or numberOfFiles3 <> numberOfFiles4 Then
   MsgBox "Channel 2, Channel 3, and Channal 4 have a different number of input files!", vbOKOnly,
"Channel 2/3 Input Files"
   Exit Sub
End If

MainForm.CDlg.ShowSave
outputFile = MainForm.CDlg.fileName

'MainForm.CDlg.ShowSave
'outputFile2 = MainForm.CDlg.fileName

MainForm.MousePointer = vbHourglass

'Init File Path Arrays.  Need to save memory
channel = 1
Open App.Path & "\files.txt" For Input As #1

Do
   Input #1, temp
   If temp = "**********" Then
      channel = channel + 1
      index = 0
   Else
      If channel = 2 Then
         files2(index) = temp
         index = index + 1
      End If
      If channel = 3 Then
         files3(index) = temp
         index = index + 1
      End If
      If channel = 4 Then
         files4(index) = temp
         index = index + 1
      End If
   End If
Loop Until channel = 5

Close #1

'--------------------------------------------------------------------------------
'Initalize Arrays
'--------------------------------------------------------------------------------

trace2.Initialize (750000)
trace3.Initialize (750000)
trace4.Initialize (750000)

For fileCount = 0 To numberOfFiles3 - 1
'--------------------------------------------------------------------------------
'Main Procedure Loop
```

```
'-------------------------------------------------------------------------------
'#############################################################################################
####
'Load data channel 3
   MainForm.ProgramStatus.Caption = "Loading Channel #3 for file #" & fileCount + 1
   MainForm.ProgressBar1.Visible = True
   MainForm.Refresh

   If trace3.Load_File(files3(fileCount)) Then
      MainForm.MousePointer = vbDefault
      MsgBox "Error Loading File, Exiting CalcInjecter Sub", vbOKOnly, "File I/O Error"
      Exit Sub
   End If

'#############################################################################################
'Load Data channel 4
   MainForm.ProgramStatus.Caption = "Loading Channel #4 for file #" & fileCount + 1
   MainForm.ProgressBar1.Visible = True
   MainForm.Refresh

   If trace4.Load_File(files4(fileCount)) Then
      MainForm.MousePointer = vbDefault
      MsgBox "Error Loading File, Exiting CalcInjecter Sub", vbOKOnly, "File I/O Error"
      Exit Sub
   End If

'#############################################################################################
'Find where trigger goes high.
   MainForm.ProgramStatus.Caption = "Locating where trigger(Channel 4) goes high for file #" &
fileCount + 1
   MainForm.Refresh

   For index = 0 To trace4.numberOfPoints
      If trace4.GetDataPoint(index) > 4 Then
         triggerPoint = index
         Exit For
      End If
   Next index

'#############################################################################################
####
'Read Channel 2
   MainForm.ProgramStatus.Caption = "Reading channel 2 for file #" & fileCount + 1
   MainForm.Refresh

   If trace2.Load_File(files2(fileCount)) Then
      MainForm.MousePointer = vbDefault
      MsgBox "Error Loading File, Exiting CalcInjecter Sub", vbOKOnly, "File I/O Error"
      Exit Sub
   End If

'#############################################################################################
####
'Align channel 2 data
   MainForm.ProgramStatus.Caption = "Aligning Channel #2 for file #" & fileCount + 1
   MainForm.Refresh
```

```
    dumpPoint = triggerPoint - 144000
    If dumpPoint < 1 Then
        MsgBox "Dump Point at 100 cycles would result in a negative index", vbOKOnly, "Negaitiv Index"
        Exit Sub
    End If

    trace2.numberOfPoints = trace2.numberOfPoints - dumpPoint

    For index = 0 To trace2.numberOfPoints
        Call trace2.SetDataPoint(index, trace2.GetDataPoint(index + dumpPoint))
        total(index) = total(index) + trace2.GetDataPoint(index)
    Next index

'Align Chanal #4
MainForm.ProgramStatus.Caption = "Aligning Channel #4 for file file#" & fileCount + 1
MainForm.Refresh

    trace3.numberOfPoints = trace3.numberOfPoints - dumpPoint

    For index = 0 To trace3.numberOfPoints
        Call trace3.SetDataPoint(index, trace3.GetDataPoint(index + dumpPoint))
        total2(index) = total2(index) + trace3.GetDataPoint(index)
    Next index


Next fileCount

'Align Channel 3
MainForm.ProgramStatus.Caption = "Aligning Channel #3 for file series"
MainForm.Refresh

    dumpPoint = triggerPoint - 144000
    If dumpPoint < 1 Then
        MsgBox "Dump Point at 100 cycles would result in a negative index", vbOKOnly, "Negaitiv Index"
        Exit Sub
    End If

    trace3.numberOfPoints = trace3.numberOfPoints - dumpPoint

    For index = 0 To trace3.numberOfPoints
        Call trace3.SetDataPoint(index, trace3.GetDataPoint(index + dumpPoint))
    Next index

'###############################################################################################
'Output average fuel/air mixture
MainForm.ProgramStatus.Caption = "Outputting average Air/Fuel Mixture."
MainForm.Refresh
Open outputFile For Output As #1
'Open outputFile2 For Output As #2
xValue = 0
If MainForm.Condense.value = 0 Then
    For index = 0 To trace2.numberOfPoints
        total(index) = total(index) / fileCount
        total2(index) = total2(index) / fileCount
        Print #1, total(index)
```

```
        Print #2, total2(index)
    Next index
Else
    For index = 0 To trace2.numberOfPoints
        If j = 160 Then
            j = 0
            condensed(count) = condensed(count) / (160 * fileCount)
            iCondensed(count) = iCondensed(count) / 160
            Print #1, xValue & "," & condensed(count) & "," & iCondensed(count)
            'Print #2, xValue & "," & iCondensed(count)
            xValue = xValue + 0.111111111111
            count = count + 1
        Else
            condensed(count) = condensed(count) + total(index)
            iCondensed(count) = iCondensed(count) + total2(index)
            j = j + 1
        End If
   'Print #2, trace3.GetDataPoint(index)
   Next index
End If

Close #1
Close #2
'#############################################################################################
####
MainForm.MousePointer = vbDefault
MainForm.ProgramStatus.Caption = "Injector Calculations Finished"
MainForm.Refresh

                                                                                    End Sub
```

Appendix D

Igor-Pro Data Analysis Programs

Appendix D-1
Skip-Injection Hydrocarbon Mass Determination
Written By Me.

Program calculates the mass of fuel present during the skip injection event for single and three skip-injection events. Program works by finding the maximum pressure peak prior to the skip-injection event. The program then offsets a certain number of crank degrees and calculates the mass by averaging over the peak hydrocarbon spike, and applying appropriate conversion factors.

```
#pragma rtGlobals=1                    // Use modern global access method.
#include <Decimation>

// macro prompts the user for start and endpoint x axis values
// these values corral the misfire pressure for peak location determination

Macro setPoints(startpoint, endpoint, numCycles)
        Variable /G startGlobal
        Variable /G endGlobal
        Variable /G numGlobal
        Variable  startpoint
        Variable  endpoint
        Variable  numCycles
        Printf "Please enter startpoint: %g\r", startpoint
        Printf "Please enter endpoint: %g\r", endpoint
        Printf "Please enter # of cycles to average (1-3): %g\r", numCycles
        startGlobal         = startpoint
        endGlobal           = endpoint
        numGlobal           = numCycles
End

Function TrickyStuff( wave0, wave1, wave2 )
                        //, wave3)
        // global variables used for reading waves, corralling points, etc.

                WAVE wave0 = wave0
                WAVE wave1 = wave1
                WAVE wave2 = wave2
                //WAVE wave3 = wave3
                NVAR startGlobal        = root:startGlobal
                NVAR endGlobal                  = root:endGlobal
                NVAR numGlobal                  = root:numGlobal

        // local variables used to determine pressure location and peak pressure
                Variable peakPressure
                Variable pressLocation
                Variable offset             ; offset = 350  // there are approximately 200 degrees of offset
                Variable cycleOffset        ; cycleOffset = 720  // each cycle is 720 degrees
                Variable meanCrank          ; meanCrank = 350  // # of degrees averaged


        // creates the graph and formats to liking
                SetScale/P x 0,0.5,"", wave0, wave1, wave2
```

```
wave1 = wave1 / 1000
wave2 = wave2 * 3
wavestats wave1
wave1 = wave1 - V_min + 101.325
Display wave2
AppendToGraph/R wave1
ModifyGraph lsize(wave2)=1.0,rgb(wave2)=(0,0,65280)
ModifyGraph width=324,height=180
Label right "\\Z14Pressure (kPa)"
Label bottom "\\Z14Crank degrees"
Label left "\\Z14HC (ppm C)"
ModifyGraph fStyle(left)=1
ModifyGraph fStyle(bottom)=1
ModifyGraph fStyle(right)=1
ModifyGraph width=324,height=180
ModifyGraph gFont="Times New Roman"
ModifyGraph mirror(bottom)=2
ModifyGraph lstyle(wave2)=0,lstyle(wave1)=3
Legend/N=text0/J/S=1 "\\s(wave2) Fast FID HC\\Z12\r\\s(wave1) Pressure\\Z12"
SetAxis bottom 1000,6000
SetAxis left 0,60000
SetAxis right 0,3500
ModifyGraph axThick=0.75

// updates the graph prior to calling the macro
    doUpdate

// executes the macro to determine start and stop points
    Execute "setPoints()"

// calculates the peak pressure and location of peak pressure
    FindPeak /R=(startGlobal, endGlobal) /M = 1000 wave1
    peakPressure    = V_peakVal
    pressLocation   = V_peakLoc
    //print                         peakPressure
    //print                         pressLocation

// offsets to the approx. rising edge of HC spike, calculates mean value
    Variable count    // count is the loop counter
    Variable mult     // multiplier is used to increment the cycle calculations
    Variable mair     // mass of air per cycle at 3060 RPM, WOT, lbm/hr (obtained from calibration chart)
    Variable mair_cycle  // mass of air inducted per engine cycle, 3060 RPM, lbm/cycle. converted from mair
    Variable mf_HC  // mass fraction multiplier to be used converting mass air to mass fuel (see EES program and EXCEL equation)
    Variable load     // load used for mass airflow calculation (from calibration chart)
    Variable mean_HC        // mean [HC] value per cycle
    Variable mass_fuel      // mass of fuel per cycle, g/cycle
    Variable Lbm_g          // converts lbs to grams, used for conversion

// initializes the counters and limits
    count           = 0             // initialize the counter to 0
    Lbm_g           = 453.592       // Lbm to gram conversions
    load            = 100           // tests done at 100% load
```

```
	// initializes the calibration values
		// mass of airflow per hour, lbm/hr
			mair		= -0.001 * load ^ 2 + 0.3187 * load + 2.8633

		// mass of airflow per cycle, lbm/cycle
			mair_cycle	= mair * 2 / (3060 * 60 )

	do
		mean_HC =  mean( wave2, pressLocation + offset + (count * cycleOffset ) , pressLocation + offset + (count * cycleOffset+ meanCrank) )
		mf_HC  = 6.11E-13 * mean_HC ^ 2 + 4.70E-07 * mean_HC+ 8.99E-05
	// mass fraction conversion equation, EES file: INDOLENE
		//mf_HC = 6.46E-13 * mean_HC ^ 2 + 4.98E-07 * mean_HC+ 9.41E-05
	// mass fraction conversion equation, EES file: PROPANE
		mass_fuel = mair_cycle * mf_HC * Lbm_g  * 1000
		// read the above conversion
		count	+= 1
		//Printf "Cycle fuel mass is (mg): %g\r", mass_fuel
		//Printf "Cycle averaged PPM: %g\r", mean_HC
		Print mass_fuel
		//Print mean_HC
	while ( count < numGlobal )

End
```

Appendix D-2
Stop-Injection Hydrocarbon Mass Determination
Written By Me too.

Program calculates the mass of fuel per cycle after the cessation of fuel injection. Program works by finding the maximum pressure peak at the onset of the stop-injection event. The program then offsets a certain number of crank degrees and calculates the mass by averaging over the peak hydrocarbon spike, and applying appropriate conversion factors, similar to what was done in Appendix D-1.

```
#pragma rtGlobals=1                    // Use modern global access method.
#include <Decimation>

// ************************** STOPFIRE 500 CYCLE FUNCTION ***********************************

Function stopfire_500(HC40)

        WAVE HC40 = HC40        // global declaration of the HC wave
        SetScale/P x 0,0.5,"", HC40
        DeletePoints 0,325000, HC40
        //Execute "decimate(HC40, HC40, 50, 1)"
        HC40 = HC40 * 3
        //Display HC40

        wavestats HC40    // stats used to find the maximum HC spike- used to set starting point

        variable  count     // count is the loop counter variablelim is the loop limit
        variable  lim       // lim is the number of cycles to calculate [HC]
        variable  mult      // multiplier is used to increment the cycle calculations
        variable  mair      // mass of air per cycle at 3060 RPM, WOT, lbm/hr (obtained from calibration chart)
        variable  mair_cycle// mass of air inducted per engine cycle, 3060 RPM, lbm/cycle. converted from mair
        variable  mf_HC   // mass fraction multiplier to be used converting mass air to mass fuel (see EES program
and EXCEL equation)
        variable  load      // load used for mass airflow calculation (from calibration chart)
        variable mean_HC  // mean [HC] value per cycle
        variable mass_fuel  // mass of fuel per cycle, g/cycle
        variable Lbm_g    // converts lbs to grams, used for conversion

        //initializes the counters and limits
        count     = 0       // initialize the counter to 0. as opposed to 30534.
        mult      = 0       // initializes the multiplier to 0. god made me do it.
        lim       = 480     // calculates the mean [HC] for 450 cycles, lim is the limit variable
        Lbm_g     = 453.592// Lbm to gram conversions, correcting the Brits for 200 year+ of unit nonsense
        load      =  55     // tests done at 100% load. totally loaded. wow man, is that freedom rock...

        //initializes the calibration values
        mair      = -0.001 * load ^ 2 + 0.3187 * load + 2.8633      // mass of airflow per hour, lbm/hr
        mair_cycle= mair * 2 / (3060 * 60 )                         // mass of airflow per cycle, lbm/cycle
        mean_HC = mean (HC40, V_maxloc, V_maxloc - 640)     // calculates the first stopfire HC mass, ppm.
        mf_HC   = 6.11E-13 * mean_HC ^ 2 + 4.70E-07 * mean_HC+ 8.99E-05       // mass fraction conversion
        //mf_HC  = 6.46E-13 * mean_HC ^ 2 + 4.98E-07 * mean_HC+ 9.41E-05       // mass fraction conversion
        mass_fuel= mair_cycle * mf_HC * Lbm_g * 1000            // 1000 converts to mg/cycle
        print     mass_fuel
        print     mean_HC
        do
                count     += 1
                mult      += 1
```

```
                mean_HC =  mean( HC40, V_maxloc + count * 720 , V_maxloc + count * 720 - 640 )
                mf_HC    = 6.11E-13 * mean_HC ^ 2 + 4.70E-07 * mean_HC+ 8.99E-05          // mass fraction
conversion equation, EES file: INDOLENE
                // mf_HC = 6.46E-13 * mean_HC ^ 2 + 4.98E-07 * mean_HC+ 9.41E-05                    // mass
fraction conversion equation, EES file: PROPANE
                mass_fuel              = mair_cycle * mf_HC * Lbm_g           * 1000
                // read the above conversion. Tuesday nights at the 'Dice rule. Gonna miss it,  me Danny and Craig.
                // Print                mass_fuel
                        print                   mean_HC
        while ( count < lim )

End function
```

Appendix E

Engine Dimensions

Appendix E-1 Camshaft profile

Appendix E-1

Engine Camshaft Profile